UNIVERSITY OF CANTERBURY
Te Whare Wānanga o Waitaha
CHRISTCHURCH NEW ZEALAND

May 2010

The Characterisation and Development of a Passivated Inlet to Selected Ion Flow Tube Mass Spectrometry (SIFT-MS)

A thesis submitted in partial fulfilment of the requirements for the Degree of

Master of Science in Chemistry

in the

University of Canterbury
Christchurch, New Zealand

by

Christine J. Reed

Dedicated to my sister and friend,
Te Arohanui Pare Barney

Abstract

SIFT-MS is a relatively new trace gas analysis technique that has wide application. One particular attribute of the instrument is the ability to detect and quantify volatile organic compounds to the parts per trillion in real-time without the need for sample preparation. However the issue of maintaining accuracy at these low concentrations required attention as it was evident large or polar analytes were being lost by adsorption to the SIFT instrument's inlet system.

The purpose of this research was to evaluate the performance of a passivated inlet in lowering any adsorption in the inlet system compared to the current unpassivated inlet of the SIFT instrument. Volatile concentrations of vanillin ($C_8H_8O_3$ 152.15 g/mol), ammonia (NH_3 17.03 g/mol), and hydrogen sulfide (H_2S 34.08 g/mol) were measured. The results determined the passivated inlet provided a significantly better inlet response to these compounds. Consequently improved passivated inlets were installed on current models of SIFT-MS VOICE200®, and also the research laboratory VOICE100™ instrument.

Having established a more reliable sampling system for very low concentrations of analyte, attention was paid to SIFT-MS flavour analysis of two foods, cheese and chocolate. The volatile matrix of these foods is highly complex and the compounds of interest are typically difficult to measure. The key aroma compounds for analysis were based on reported literature and earlier SIFT-MS studies which provided a useful framework for the current food flavour research.

A significant finding from the SIFT-MS examination of Parmesan cheese is that differences in the relative concentration of some characteristic aroma compounds were a consequence of the milk type used in manufacture. Endogenous enzymes responsible for a multitude of reactions are mostly if not completely inactivated by the pasteurization temperature. A similar analysis approach was attempted for chocolate analysis. Here flavour

differences were not as clearly recognised as for the cheese samples. In chocolate there are a greater number of parameters that are involved in its manufacture. Nevertheless, some recognisable differences in chocolate could be attributed to cocoa bean type and flavour additions by the manufacturer.

TABLE OF CONTENTS

LIST OF FIGURES

LIST OF TABLES

Acknowledgements

I am thankful for the support and guidance of my supervisors Professor Murray McEwan and Dr. Daniel Milligan. In particular I appreciate their patience and kindness throughout some very trying times. Thank-you to the many who had a part in seeing me to the finish line, i.e. Dr. Vaughn Langford, Dr. Barry Prince, Dr. Greg Francis, Dr. Sunny Hu, Dr. Brett Davis, and all the helpful and friendly staff of SYFT Technologies. I think special mention should also be made of Professor Bryce Williamson. Please note if I have left anyone out, I'm sorry it is an unintentional oversight.

My gratitude goes to SYFT Technologies for funding two years of study, and the part-time contract given me over a year.

I wish to acknowledge my family and friends for generally putting up with whatever came up. Especially my boys, Adrian and Matthias who on more than one occasion kept me focussed, I love you both dearly.

CHAPTER ONE

Selected Ion Flow Tube Mass Spectrometry

The selected ion flow tube mass spectrometry (SIFT-MS) technique, including principles of operation and its application to trace gas analysis, is described in this chapter. The precursor technology to SIFT-MS is the selected ion flow tube (SIFT) instrument that is founded on the development of the flow tube reactor and has the aim of characterizing ion-molecule reactions. In contrast, SIFT-MS relies on knowledge of ion-molecule chemistry to report analyte concentrations. Subsequently the research and development of a commercial SIFT-MS instrument has afforded its wide application to trace gas analysis. Because of its rapid response time and sensitivity, the SIFT-MS technique is ideally suited to the measurement of low concentration volatile organic compounds in real time.

1.1 A Historical Review: Flowing Afterglow and the Selected Ion Flow Tube

1.1.1 Flowing Afterglow Technique

In the late 1960s Ferguson et al. devised a technique that allowed measurement of thermal energy gas-phase ion-molecule reactions (Ferguson et al. 1969). Known as the flowing afterglow (FA), the technique utilised a flow tube reactor in which fast flowing ion plasma could react with neutral gas-phase molecules at thermal energies. Downstream of the reaction region, a mass spectrometer is used to measure ion densities and product-ion masses of the ion-molecule reactions so that rate coefficients for the individual reactions can be determined. Some rapid

developments to the instrument followed, e.g. temperature variation of ion-molecule reactions (Adams et al. 1970, Böhme et al. 1969), and a significant number of kinetic measurements relevant to processes occurring in the Earth's atmosphere ensued greatly increasing our knowledge and understanding of the chemistry therein (Adams 1996, Graul & Squires 1988).

1.1.2 Selected Ion Flow Tube Technique

Despite its great success the FA technique suffered some serious limitations (Adams & Smith 1976), one of which was unwanted ion species in the flow tube. These unwanted ion species form from parent-ion gas, reactant-ion gas, and bath-gas interactions within the ion creation region of the flow tube. The problem is these ion species, including any concomitant electrons formed, simultaneously react with all reactants in the flow tube. Then competing reactions made it particularly difficult to determine accurate product-ion distributions and in some cases the result was erroneous rate coefficients and product ions.

In 1975 Adams and Smith made a modification to the FA technique which effectively removed the problem of unwanted ion species in the reactor (Adams & Smith 1976)**.** Built on the versatility of the FA instrument, the SIFT technique differs by generating ions in a remote ion source (see Figure 1). Reagent ions having a single mass-to-charge ratio are selected from this remote source and injected as a fast flowing ion swarm into the flow tube. This method of introducing a single reagent ion type greatly simplified the branching ratios of product-ions, such that accurate ion densities could be measured, and an analysis of complex ion-neutral reactions was made possible (Smith & Adams 1987).

Several laboratories around the world have used the SIFT technique to model previously unknown complex ion-molecule chemistry, such as reaction mechanisms occurring in the Earth's

ionosphere (Böhme 2000, Ferguson et al. 1979), extraterrestrial atmospheres (Anicich & McEwan 1997, Rowe & Parent 1995), and the interstellar medium (Petrie & Böhme 2003, Smith 1992). The SIFT technique is now a standard method to study thermalized positive and negative ion-molecule reactions relevant to complex ion-molecule chemistry.

1.1.2.1 Application of SIFT to Trace Gas Analysis: Selected Ion Flow Tube – Mass Spectrometry

Traditionally the SIFT instrument required routine removal of trace impurities from the air within the flow tube because they would react with reagent ions and form ionic species (Španěl & Smith 1996). From this observation Smith and Španěl proposed that if the rate coefficient and product ion(s) were known for a particular ion-molecule reaction, the concentration and identification of a trace gas analyte could be found providing the reagent ion used does not react with the major components of air (see §1.3.2). This relatively new technique of trace gas analysis became known as SIFT-MS. SIFT-MS analysis is sensitive to measuring very low concentrations (at the parts per trillion by volume/pptv level) of compounds in whole air, with no sample preparation in real-time.

The potential and subsequent development of SIFT-MS lay in its application to quantitative non-invasive on-line and real-time trace gas analysis. With that in mind, development and miniaturization of the SIFT instrument resulted in the first portable and commercial version of the SIFT-MS instrument VOICE100™ launched in March 2005 by Syft Technologies Ltd (SYFT) of Christchurch. One of the initial applications of the instrument was to detect and measure fumigant levels within transport containers shipped into seaports. Other applications areas include geochemical and environmental monitoring (Francis et al. 2007, Milligan et al.

2002), occupational hazards (Wilson et al. 2003), and medical diagnostics (Scotter et al. 2004). In 2007, SYFT released a lighter, more transportable and more sensitive SIFT-MS instrument, the VOICE200®. Both SIFT-MS instruments are used for the practical elements of this thesis in later chapters.

1.2 The SIFT Technique

1.2.1 The SIFT Instrument

In its general form, the SIFT instrument is comprised of three functional units: reagent-ion creation and selection; the flow tube reactor; and ion detection. These three units are represented by the line diagram of Figure 1 and an explanation of each unit is given below.

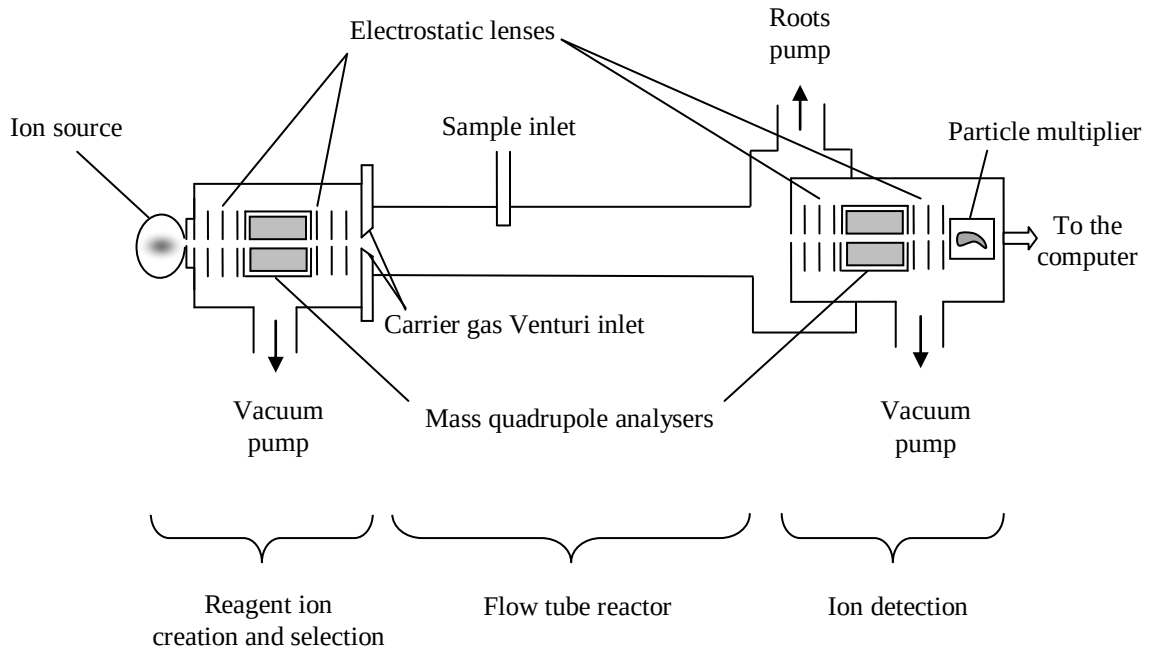

Figure 1: A schematic diagram of the SIFT instrument.

Reagent-ion creation and selection

The reagent-ion selection region contains an ion source, a quadrupole mass filter, and ion injection component in that order. A variety of ion sources are available depending on the experimental requirements (Smith & Španěl 1995). Microwave discharge (~ 2.5 GHz) of air is commonly used as a simple, effective and clean source of ionization producing primary reagent-ions H_3O^+, NO^+ and O_2^+. The ion source region operates at a pressure of ~0.4 Torr (Španěl et al. 2007). The created ion plasma is focused by electrostatic lenses into the upstream quadrupole mass filter. The quadrupole mass filter selects ions of a single mass-to-charge (*m*/*z*) ratio (Miller & Denton 1986). The upstream quadrupole operates at a pressure of ~10^{-5} Torr to minimise ion scattering and optimise quadrupole performance. The mass-selected reagent-ions are focused by electrostatic lenses to a Venturi injector which allows transmission of ions into the flow tube against a pressure gradient (Milligan et al. 2000, Vyacheslav et al. 1998).

The flow tube reactor

The flow tube reactor is typically 30 – 100 cm long and operates at a pressure of ~0.5 Torr. The flow tube is separated from the quadrupole mass filters so a high sample flow can be used. Reagent-ions are carried along the flow tube by a carrier gas (usually helium). Initial collisions between a reagent-ion and carrier gas atom lowers the energy of reagent-ions. The result is a thermal energy swarm with a Maxwell-Boltzmann distribution of translational energies. After a well-defined distance the turbulence decays and laminar flow of the carrier gas is established (Adams & Smith 1988). Ion-molecule reactions are initiated by the introduction of analyte sample to the reactor via a heated (typically 110°C) inlet tube (Chapter 2 details the SIFT-MS inlet). Chemical ionisation between reagent-ions and analyte occurs within a defined reaction time of a few milliseconds over a finite reaction length. A small sample of all the ions including

un-reacted reagent-ions, generated product-ions enter the downstream ion detection chamber through a pinhole sampling orifice in the downstream nose cone.

Ion detection

Once past the sampling orifice, reagent ions and product ions are focussed by electrostatic lenses into the downstream quadrupole mass analyser. The ion detection region operates at low pressure for the same reasons as the upstream quadrupole, in addition ion-molecule reactions effectively cease at this pressure. The flight time in the detection system is in the order of 100 μs. After mass selection, ions are again focussed by electrostatic lenses to a particle multiplier detector. The signals are pre-amplified then transmitted to a counter on the computer and recorded as counts per second. SIFT-MS software uses this data together with reaction kinetics and instrumental parameters to calculate absolute concentrations of target compounds (see §1.3.1.3).

1.2.2 Principles of SIFT

A generalised gas-phase ion-molecule reaction may be represented by:

$$A^+ + B \rightarrow C^+ + D \qquad (1)$$

The conditions are controlled so that the neutral concentration [B] is much greater than the reagent-ion A^+ density. Under those conditions pseudo first order kinetics applies and the rate coefficient *k* is determined by monitoring the semi-logarithmic decay of A^+ as a function of the flow rate of neutral reactant. By extrapolating the observed product-ion yields to zero flow, primary product-ion distributions are obtained (Smith & Adams 1987).

1.3 The SIFT-MS Technique of Trace Gas Analysis

1.3.1 Principles of SIFT-MS

The SIFT-MS technique begins with 'soft' chemical ionisation (CI) of the sample gas by mass-selected reagent ions. CI has the benefit of imparting charge to a reactant gas at relatively low energy, which reduces formation of fragmented products. A greatly simplified product ion spectrum results that is much easier to analyse. This is in contrast to the significant fragmentation that often results from 70eV electron impact ionisation used commonly in GC-MS methods (Hoffman & Stroobant 2007). Simple product ion spectra and rapid reaction of reagent ions with the analytes (within milliseconds) makes real-time measurement of rapidly changing compound concentrations possible.

1.3.1.1 Reagent Ions

H_3O^+ (19 m/z), NO^+ (30 m/z), and O_2^+ (32 m/z) have proved to be the best choices for most analyses although other ions can be used in special cases. These reagent ions are un-reactive with the major components of air, i.e. N_2, H_2O, CO_2, O_2, and Ar. Depending on the analyte and sample mixture one or multiple reagent ions can be used for the analysis adding to the specificity of the technique. Many of the ion-molecule reactions proceed by only one or two pathways with well defined reaction rates and branching ratios (Smith & Španěl 2005).

<u>H_3O^+ reactions</u>

Proton transfer is the dominant mode of reaction for H_3O^+. Here an H^+ ion is transferred to the analyte (A) by the reaction:

$$H_3O^+ + A \rightarrow A.H^+ + H_2O$$

Proton transfer reactions occur at 100% rate of collision efficiency for compounds with a proton affinity higher than that of water (691 kJ mol^{-1}).

Association is where the reagent ion attaches itself to the analyte and excess energy is carried away by a third body (M):

$$H_3O^+ + A + M \rightarrow A.H_3O^+ + M$$

In SIFT-MS the stabilizing third bodies (M) are the helium atoms of the carrier gas.

Water cluster formation of H_3O^+ by association always occurs with moist samples:

$$H_3O^+ + nH_2O + M \rightarrow H_3O^+.n(H_2O) + M \qquad (n = 1\text{-}3)$$

Water cluster ions are additional to the typically highest and primary H_3O^+ ion signal (*m/z* = 19). These water ion peaks (*m/z* 37 (n=1), 55 (n=2), and 73 (n=3)) must be measured as part of the H_3O^+ reagent ion signal for accurate calculation of concentrations. Moreover the relative amounts of these clusters depend on the moisture content of the sample and provide a measure of it.

<u>NO^+ reactions</u>

The reaction processes of NO^+ with organic molecules are more varied. *Hydride ion transfer* is one mode of reaction for NO^+ where an H^- ion is removed from the analyte by the reagent ion:

$$NO^+ + AH \rightarrow A^+ + HNO$$

This is generally the only NO^+ reaction process that occurs with aldehydes and ethers.

Association is a relatively common mode of reaction for NO^+ and occurs for polar organic molecules at thermal energies, especially carboxylic acids, esters and ketones:

$$NO^+ + A + M \rightarrow A.NO^+ + M$$

Charge transfer, where an electron is removed from the analyte leaving it positively charged, can only occur when the analyte has ionization energy less than 9.26eV. *Non-dissociative charge transfer* by NO^+ with organosulphur molecules and aromatic hydrocarbons produces analyte radical cations:

$$NO^+ + A \rightarrow A^{+\bullet} + NO^{\bullet}$$

O_2^+ reactions

The common mode of reaction for O_2^+ is electron transfer, also known as *charge transfer*:

$$O_2^+ + A \rightarrow A^+ + O_2$$

Charge transfer can occur at 0 – 100% of the rate of collisions between the reagent ion and a particular analyte.

Dissociative charge transfer is more common for O_2^+ than for NO^+, because O_2^+ has higher ionisation energy (12.07eV)

$$O_2^+ + A \rightarrow Fragment^+ + Neutral\ fragment(s) + O_2$$

1.3.1.2 Data Acquisition

There are two methods of data acquisition using a SIFT-MS instrument. The first is a mass scan mode (MS) which is excellent for primary investigations of unknown samples as all the

product-ions arising from all VOCs in the sample are detected. The second is selected ion monitoring mode (SIM) that provides rapid quantitative information about targeted VOCs in a sample. In SIM scans, selected *m/z* values are monitored. SIM scans are very useful for monitoring changes in compound concentration over time, or detecting differences in compound concentration between samples as the sample time for a particular ion is much greater than in a mass scan. In practise a combination of SIM and MS provides the maximum sample information by SIFT-MS.

SIM scan mode

A SIM scan measures an ion signal as counts per second (cps) for selected *m/z* data points in specified lengths of time (typically 25 ms each for reagent ions, 100 ms each for product ions). Each time reagent- and product-ions are counted (ion number density) the analyte concentration is calculated, providing a real-time response to any changes in concentration as time progresses. Several compounds can be simultaneously analysed in real time as the downstream mass spectrometer is rapidly switched between the reagent ions and the appropriate product-ions. Sensitivity and precision of the measurement increases as more scans are made and fewer *m/z* points scanned. For an accurate analysis the identification of several product-ions per compound is recommended so that, where possible, the effect of interfering compounds to the target compound's quantification can be reduced or eliminated. Therefore knowledge of the VOCs present in a sample is essential prior to conducting a SIM scan.

The results of a SIM scan can be displayed graphically in real-time on-line where the *x*-axis shows the time in seconds (s), and the *y*-axis as signal intensity in counts per second (cps), see Figure 2.

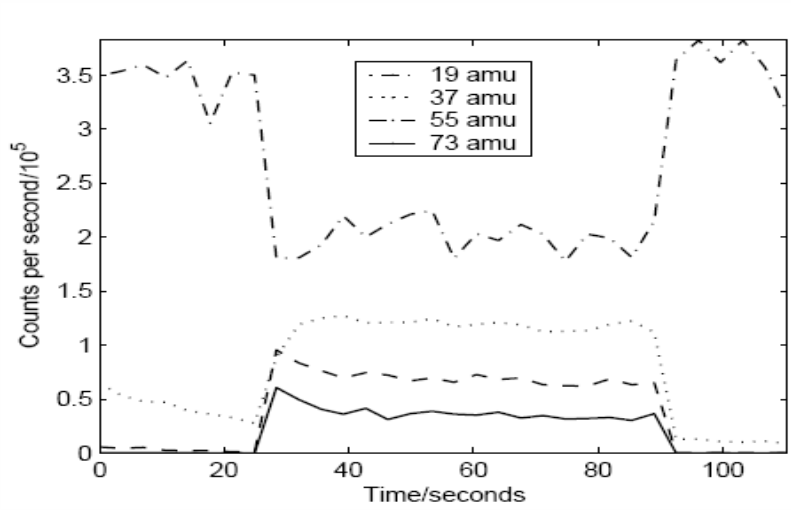

Figure 2: A SIFT-MS SIM scan showing H_3O^+ and the water clusters.

MS scan mode

To obtain a full MS all three reagent-ions are selected and in turn all product-ions between a specified *m/z* range (usually 10-250 amu) are measured by sweeping the downstream quadrupole over the range. As there are often many *m/z* values to be analysed, only a small amount of time (typically 10-20 ms) is spent counting each one which reduces sensitivity with respect to SIM. However when the compounds of a sample are unknown, or a large number of product ions are to be analysed, it is practical to run a full mass scan. A compound is identified by comparing observed product-ion masses to a database of reaction product masses for a particular reagent-ion. The analysis includes an understanding of water clusters and product ion fragmentation.

The results may also be displayed graphically where the *x*-axis shows the *m/z* ratio and the *y*-axis is the signal intensity in counts per second (cps).

1.3.1.3 SIFT-MS Calculation of Analyte Concentration

The conversion of measured ion number densities to a more meaningful analysis unit, parts per billion (ppb), is a multi-step calculation. Only a very brief presentation of the SIFT-MS quantitative method is related here, a rigorous account of the calculation method is provided by Smith and Španěl 2005, Španěl & Smith 1996.

For a gas mixture, an individual analyte can be quantified as the measured product-ion signals it forms are usually different to another reactant gas. The quantification of the reactant gas as follows:

Under all conditions [B] » A^+ and it follows from equation (1), the number of reagent ions and product-ions in the flow tube with respect to time is:

$$\frac{dA^+}{dt} = -D_{A^+}A^+ - k[B]A^+ \quad (2)$$

$$\frac{dC^+}{dt} = -D_{C^+}C^+ + k[B]C^+ \quad (3)$$

where A^+ is the ion density of the reagent-ion, C^+ is the ion density of the product-ion, *t* is the time, *k* is the rate coefficient, and [B] the analyte concentration. $D_A{}^+$ and $D_C{}^+$ are diffusion coefficients that account for the loss of product-ions by diffusion to the flow tube.

Integrating and evaluating equations (2) and (3) the ion densities of the reagent-ion and product-ion at any point in time *t*, becomes (Španěl & Smith 1996):

$$A^+{}_t = A^+{}_0 \exp\left(-k[B]t - D_{A^+}t\right) \quad (4)$$

$$C^+{}_t = C^+{}_0 \exp\left(k[B]t - D_{C^+}t\right) \quad (5)$$

where A^+_0 and C^+_0 are the reagent-ion and product-ion ion densities at t = 0 respectively.

In the case of SIFT-MS where perturbation of the reagent ion signal is kept small such that [B] is very close to zero, the analytical solution to simultaneous evaluation of equations (4) and (5) (Španěl & Smith 1996) can be simplified to give the concentration of an analyte [B]:

$$B_{ppbv} = \frac{[C^+]}{kt_r[A^+]}\,\gamma \qquad (6)$$

where *k* for the reaction is known, and t_r is the reaction time which is defined by flow tube parameters. $[A^+]$ and $[C^+]$ are measured as ion signal intensities.

The instrument calibration function γ is an integral part of the SIFT-MS calculation that: (1) accounts for differential diffusion of product-ions in the flow tube, (2) corrects for ion mass discrimination by the downstream quadrupole, and (3) converts the concentration of an analyte from molecules cm^{-3} to ppbv. Measured flow rates (Torr.L s^{-1}) of the carrier gas and inlet capillary gas are two important elements of γ. As long as the partial pressures of the carrier gas and sample gas are known, then the analyte concentration in a reactant gas sample can be evaluated.

The SIFT-MS instrument does not require calibration or an internal standard for calculation of an analyte concentration because the concentration can be calculated from the ratio of measured ion number densities, known experimental parameters, and known reaction rate coefficient. SIFT-MS analysis draws from a kinetic library of rate constants and product ion branching ratios. SYFT currently holds kinetic data for over 500 compounds made up of contributions by a number of research groups.

Accurate product ion branching ratios (BRs), are also required for SIFT-MS analysis because the concentration of an analyte is proportional to the amplitude of the product-ion signals which form (see §1.3.1.5). Accounting for product-ions, especially those arising from O_2^+ can be difficult at times because fragment ions are common and sometimes a number of different product ions occur. The suitability of a reagent-ion for a particular analyte can be determined at the time of setting up a SIFT-MS scan where information concerning product-ion BRs are recorded in the SYFT compound library.

1.3.1.4 SIFT-MS Measurement of Relative Rate Coefficients

When an exothermic proton transfer reaction from H_3O^+ occurs with unit efficiency a collision rate coefficient k_c can be calculated (Su & Chesnavich 1982). Empirical or 'relative rate' coefficients for non-proton transfer processes (such as association or electron transfer) may be determined by measuring H_3O^+, NO^+, and O_2^+ background signal intensities simultaneously. The method of 'relative rates' is followed for the analyte methional (104 *m/z*) below:

A Tedlar™ bag is filled with nitrogen and a MS measured to give a background signal for each reagent-ion. Then a neat sample of methional is placed in the Tedlar™ bag and filled with nitrogen such that an approximate half reduction (20 – 80%) of reagent-ion background signal is noted when a MS is measured. The two scans are superimposed for analysis (see Figure 2.3).

When the analyte concentration [B] is much greater than the reagent-ion density as is always the case, the analyte concentration is assumed constant and the reaction rate may be approximated to $k[B]I^+$.

In which case,

$$\frac{I^+}{I_0^+} = e^{k[B]t} \qquad (7)$$

$$\Rightarrow ln\left(\frac{[I^+]}{[I^+]_0}\right) = -k[B]t \qquad (8)$$

Where $[I^+]$ is the product-ion signal at 19, 30, or 32 *m/z* and $[I^+]_0$ is the reagent ion signal with zero flow of analyte [B]. $[I^+]$ and $[I^+]_0$ values are obtained from the above MS and t = 0.0038 s is the reaction time.

From Figure 3 the following analysis is made:

The H_3O^+ scan shows product ions at *m/z* 61, 105, 106, 107, and 165. The reaction of methional with the H_3O^+ ion results in a primary product ion at *m/z* 105 by proton transfer, and the C^{13} and S^{33} isotope peaks occur at *m/z* 106 and *m/z* 107. The peak at *m/z* 165 is a 2-phenylacetate impurity. The *m/z* 61 peak is unidentified but the signal intensity is relatively small. In this case (excluding the phenethylacetate impurity) the product-ion branching ratio (BR) is ~ 100% efficient for proton transfer.

The NO^+ scan shows product ions at *m/z* 104, 105, 106, 134, and 174. Methional reaction with the NO^+ ion results in a primary product ion at *m/z* 104 by charge transfer (and smaller signals at *m/z* 105 and *m/z* 106 from the C^{13} and S^{33} isotopes respectively), and *m/z* 134 is NO^+ association. The *m/z* 174 peak is unidentified but the signal intensity is relatively small and can be ignored. The product-ion BRs are assigned ~95% for charge transfer and ~5% for association.

The O_2^+ scan shows product ions at *m/z* 48, 76, 104, 105, and 106. Methional reaction with the O_2^+ ion results in primary product ion *m/z* 104 by charge transfer, and the isotope peaks at *m/z* 105 and *m/z* 106, *m/z* 76 is a fragment product from CO loss, and *m/z* 48 is unidentified. The product ion branching BRs are assigned ~60% for charge transfer, ~20% for the product ion at *m/z* 76, and ~20% for the unidentified product ion at *m/z* 48.

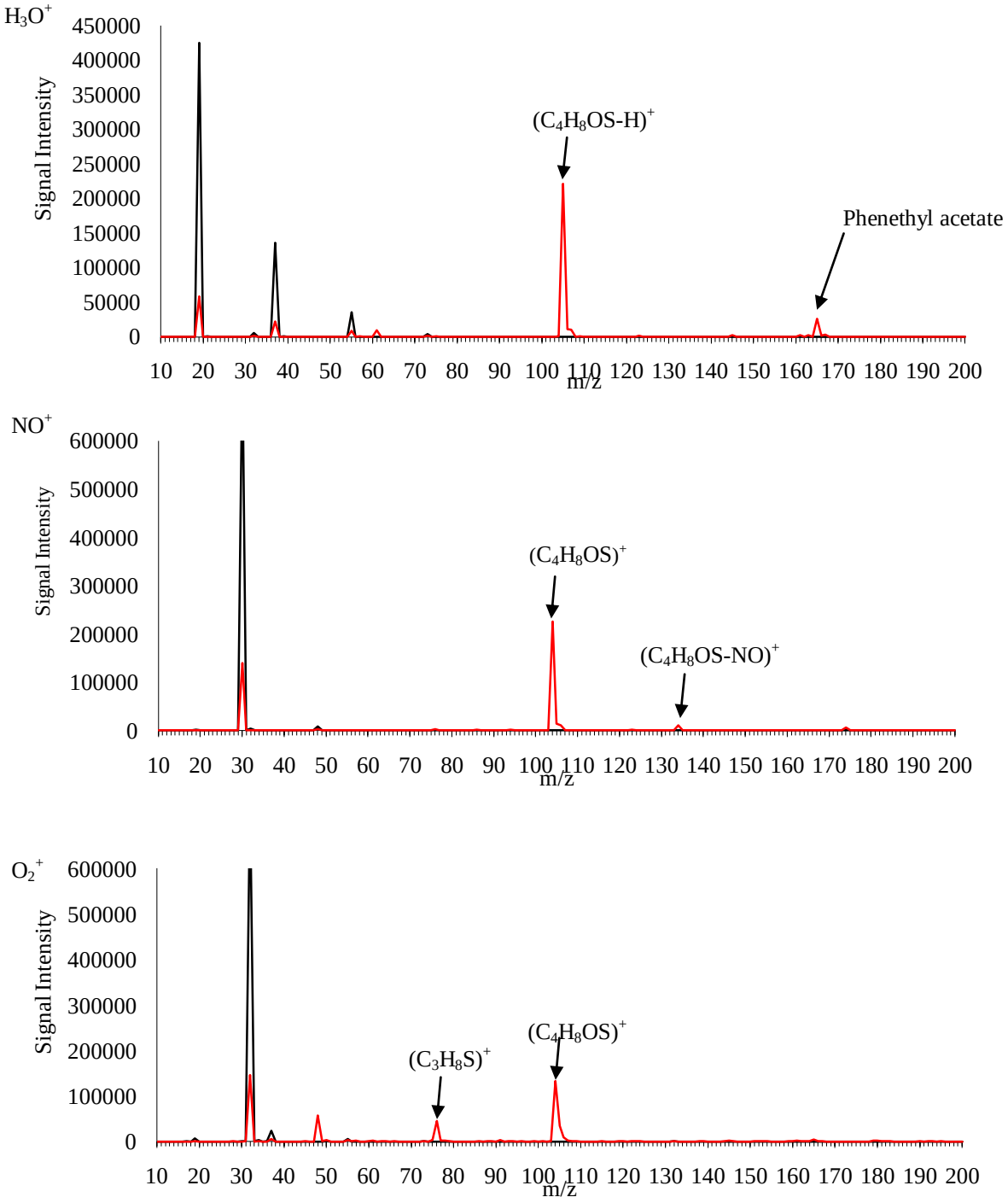

Figure 3: VOICE100™ H_3O^+, NO^+, and O_2^+ MS measurements of methional headspace (Background MS in black, methional MS in red).

	Methional, I^+	Background, I_0^+	$ln(I^+/ I_0^+)$	k[A]	Rate constant
H_3O^+	58,280	404,454	-1.937	509.8	2.00E-09*
NO^+	140,134	777,869	-1.714	451.0	1.77E-09ǂ
O_2^+	146,156	775,139	-1.668	439.0	1.72E-09ǂ

* Calculated H_3O^+ collision rate coefficient

ǂ "Relative rate" rate coefficient

Table 1: Data values obtained from VOICE100™ analysis of methional and relative rate coefficients.

1.3.1.5 Sampling Procedures

SIFT-MS analysis of ambient air is achieved by opening the sampling port to allow air to enter the flow tube via the calibrated capillary. Analysis of ambient air is simple because the sample input pressure remains at atmospheric pressure and the sample flow is unchanged.

SIFT-MS can be used to great effect to analyse headspace above liquids, solids, and *in vitro* cultures (Smith & Španěl 2005). Tedlar bags or glass vessels can also be used to collect samples and the sampling time may be extended until the sample is exhausted. A tedlar bag can be attached to the inlet port and the sample is drawn from the bag at the capillary flow rate. For a closed glass vessel, a needle connected to the sample port is used to pierce the septum and draw out sample gas. When sampling from a bag or glass vessel, the mean headspace concentration is recorded for a given sampling time.

Any fixed volume vessel must be sufficiently large so that pressure changes are negligible, as a reduced sample flow will result in lower measured signals and hence lower concentrations being reported. An alternative sampling method is simply to open the lid of the container and

offer the sample, or sample headspace, to the inlet port. This method, however, results in dilution of the headspace gases above the sample.

Breath is sampled without the need of pre-concentration by blowing through a tube directly at the inlet port. This method is preferred when possible because it avoids problems with trace gas condensation onto container surfaces.

1.4 Some SIFT-MS Applications

1.4.1 Medical Diagnostics and Disease Management

SIFT-MS provides a way of observing metabolic differences in humans because it is rapid, non invasive, and has sufficient sensitivity so that no pre-concentration of the samples are required (Španěl & Smith 1996). Moreover SIFT-MS does not require the removal of water vapour from a breath sample prior to analysis. The water cluster kinetics of both reagent- and product-ions is known and can be properly accounted for during compound concentration calculations (Smith & Španěl 2005). This unique feature of SIFT-MS allows the quantification of volatile trace compounds in the headspace of aqueous liquids such as urine, and blood which is valuable for clinical diagnosis (Wilson et al. 2002).

Metabolites are the result of biological processes that may produce detectable volatile compounds on exhaled breath. For example common breath components, ammonia, acetone, ethanol and isoprene concentrations are subject to diurnal (and nocturnal) variations following consumption of food, and during exercise (Senthilmohan et al. 2000). Some of these trace gases are elevated above “normal” concentrations when a person suffers from certain clinical conditions (Manolis 1983). In particular ammonia levels are greatly elevated above normal for patients suffering from end-stage renal failure, and studies have shown that breathe ammonia

concentrations fall during haemodialysis (Davies et al. 1997). These results support further research for an early detection of renal disease and optimizing the effectiveness of dialysis treatment.

SIFT-MS has made significant contributions to the real time detection of biomarkers in clinical areas (Senthilmohan et al. 2008, Carroll et al. 2005). SIM is ideal for quantifying known biomarkers, and MS have made it possible to identify previously unknown markers. Knowing compound fingerprints indicative of specific diseases and infections in real-time provides many clinical advantages. Cooperative studies are currently being carried out between Syft Technologies Ltd and renal, respiratory, intensive care, and surgical clinical research groups at several hospitals.

1.4.2 Geochemical Analysis of Petroleum Sulfides

Hydrogen sulfide (H_2S) and sulfur compounds are found in oil and natural gas in differing amounts. H_2S is highly toxic and, when the concentration is high (such as in sour gas) not only is the quality of petroleum lowered, it is a primary contributor to corrosion of production equipment (Agency for Toxic Substances and Disease, Simanzhenkov & Idem 2003). As refineries are typically large production areas linked by extensive piping the monitoring of corrosion areas is routine for safe operation and maintenance of equipment metals. An oil refinery will employ multiple processes to maximize the efficiency of operation and production.

The corrosion of metal wells and pipes has been found to be restricted to sulfide concentrations above minimum levels (Ghosh 2007). When minimal corrosion is likely, cheaper alloy metals are preferable, but when bad corrosion is expected more expensive but longer lasting alloy metals may be used. Early in production i.e. during drilling, SIFT-MS can

accurately determine the concentration of these corrosive compounds in real time, and a careful selection of longer lasting production materials can be included in planning for the refinery.

The world's energy demands are increasing and the number of sour wells is also likely to increase as the development of natural gas drilling is focused on deep gas formation. As wells containing higher concentrations of sulfur compounds become economic the potential increase of routine H_2S emission at oil and gas wells also increases, and there is therefore a need for preventative and workplace protection practices from hazardous H_2S concentrations. Based on these factors, a sensitive real time analytical technique such as SIFT-MS can provide a valuable tool for production engineers and for monitoring the safety of personnel.

1.4.3 Food and Flavour Development

In the area of food and flavour development it is necessary to consider a number of difficulties associated with analysis as they are incumbent on the technology used. First, the food matrix is usually comprised of a large number of chemical classes, and the most abundant volatile is water. Second aroma compounds of significance are usually present at very low concentrations. Finally, flavour changes as food is stored and some analysis methods require heating and these will cause chemical reactions to occur (Reineccius 2006).

SIFT-MS provides a valuable method of food headspace analysis (Xu & Barringer 2010a, 2010b). A recent SIFT-MS study identified methanol and ethanol as the volatiles that were in highest concentrations in olive oil and olive oil pomace headspace, contradictory to literature reports from chromatographic techniques. In addition the SIFT-MS Total Oxyradical Scavenging Capacity (TOSC) assay is used to measure antioxidants in food (Davis et al. 2005, Senthilmohan et al. 2009). Certain chromatographic techniques such as micro-extraction adsorb less polar

compounds preferentially, and a flame ionisation detector will cause the relative concentrations of small alcohols to appear less significant than larger alcohols. This result emphasises the advantages of SIFT-MS analysis to provide a non-preferential analysis of polar compounds.

Two chapters of my thesis present the ability of SIFT-MS to handle the requirements of food and flavour analysis. In Chapter 3, SIFT analysis looks at the relative importance of known aroma impact compounds between New Zealand and European cheeses, where the characteristic texture and flavor of cheese depends on the place of origin and manufacturing process. In Chapter 4, the focus turns to chocolate. The exact recipe and manufacturing processes of chocolate varieties is guarded by manufacturers whose chocolate is recognized for quality and taste. A SIFT-MS analysis of New Zealand and European milk and dark chocolates is presented. These chocolate analyses are then compared to a general flavour profile.

1.5 References

Adams, N. G. Gas Phase Ionic Reactions. *At. Mo. Opt. Phys. Handbook. pg 441*, Ed: G. W. F. Drake, Pub: AIP, Woodbury, New York, **1996**.

Adams, N. G.; Smith, D. Flowing afterglow and SIFT. *Techniques for the Study of Ion Molecule Reactions, Volume 20,* Ed. J.M. Farrar and W.H. Saunders, J. Wiley and Sons, **1988.**

Adams, N. G.; Smith, D. The selected ion flow tube (SIFT); A technique for studying ion-neutral reactions. *Int. J. Mass Spec. Ion Phys.*, **1976**, 21, 349-359.

Adams, N. G.; Böhme, D. K.; Dunkin, D. B.; Fehsenfeld, F. C. Temperature Dependences of the Rate Coefficients for the Reactions of Ar^+ with O_2, H_2, and D_2. *J. Chem. Phys.*, **1970**, 52, 4:1951-1955.

Anicich, V. G.; McEwan, M. J. Ion Molecule Chemistry in Titan's Atmosphere. *Planetary and Space Science*, **1997**, 45, 897 -921.

Böhme, D. K. Experimental studies of positive ion chemistry with flow-tube mass spectrometry: birth, evolution, and achievements in the 20th century. *Int. J. Mass. Spect.*, **2000**, 200, 97-136.

Böhme, D. K.; Dunkin, D. B.; Fehsenfeld, F. C.; Ferguson, E. E. Flowing Afterglow Studies of Associatin Reactions. *J. Chem. Phys.*, **1969**, 51, 3:863-872.

Carroll, W.; Lenney, W.; Wang, T.; Španěl P.; Alcock, A.; Smith D. Detection of Volatile Compounds Emitted by Pseudomonas aeruginosa Using Selected Ion Flow Tube Mass Spectrometry. *Ped. Pulm.*, **2005**, 39, 452-456.

Davies, S.; Španěl P.; Smith D. Quantitative Analysis of Ammonia on the Breath of Patients in End-Stage Renal Failure. *Kidney Int.*, **1997**, 52, 223-228.

Davis B. M.; Senthilmohan S. T.; Wilson P. F.; McEwan M. J. Major volatile compounds in head-space above olive oil analysed by selected ion flow tube mass spectrometry. *Rapid Comm. Mass Spect.*, **2005**, 19, 2272-2278.

Graul, S. T.; Squires, R. R. Advances in flow reactor techniques for the study of ion-neutral reactions. *Mass Spect. Reviews.*, **1988**, 7, 263-358.

Ferguson E. E., Fehsenfeld F. C., Schmeltekopf A. L. Flowing afterglow measurements of ion-neutral reactions. *Adv. At. Mol. Phys.*, **1969**, 5, 1-56.

Ferguson, E. E.; Fehsenfeld, F. C.; Albritton, D. L. *Gas Phase Ion Chemistry Volume 1*, Ed: M. T. Bowers, Pub: Academic Press, New York, **1979**.

Francis, G. J.; Wilson, P. F.; Milligan, D. B.; Langford, V. S.; McEwan, M. J. GeoVOC: A SIFT-MS method for the analysis of small linear hydrocarbons of relevance to oil exploration. *Int. J. M. Spect.*, **2007**, 268, 38-46.

Ghosh, D. P. Wet H_2S Cracking Problem in Oil Refinery Processes – Material Selection and Operation Control Issues. Paper presented at *Tri-Service Corrosion Conference*, Dec 3 – 7, Denver Colarado **2007**.

Hoffman, de E.; Stroobant, V. *Ion Sources.* Mass Spectrometry: principles and applications, Pub: John Wiley & Sons Ltd, **2007**.

Manolis, A. The diagnostic potential of breath analysis. *Clin. Chem.*, **1983**, 29, 1:5-15.

Miller, P. E.; Denton, M. B. The Quadrupole Mass Filter: Basic Operating Concepts. J. *Chem. Edu.*, **1986**, 63, 7:617-622.

Milligan, D. B.; Wilson, P. F.; Mautner M. N.; Freeman, C.G.; McEwan, M. J.; Clough, T. J.; Sherlock, R. R. Real-time, high resolution quantitative measurement of multiple soil gas emission: Selected ion flow tube mass spectrometry. *J. Environ. Qual.*, **2002**, 31, 515-524.

Milligan, D. B.; Fairley, D. A.; Freeman, C. G.; McEwan, M. J. A flowing afterglow selected ion flow tube (FA/SIFT) comparison of SIFT injector flanges and H_3^+ + N revisited. *Int. J. M. Spect.*, **2000**, 202, 351-361.

Narasimhan, L. R.; Goodman, W.; Patel, D. Kumar N. Correlation of breath ammonia with blood urea nitrogen and creatinine during hemodyalysis *Proc. Natl. Acad. Sci. U.S.A*, **2001**, 98, 8, 4617-4621.

Petrie, S.; Böhme, D. K. Mass spectrometry approaches to interstellar chemistry. *Top. Curr. Chem.*, **2003**, 225, 37-75.

"Public Health Statement for Hydrogen Sulfide" Agency for Toxic Substances and Disease. Available at http://www.atsdr.cdc.gov/toxprofiles/tp114-c1.pdf. Downloaded May 2010.

Reineccius G. *Flavor Chemistry and Technology (Second Edition)*. Pub:CRC Press Taylor and Francis Group, **2006**.

Rowe, B. R.; Parent, D. C. Techniques for the study of reaction kinetics at low temperatures: application to the atmospheric chemistry of Titan. *Plan. Space Sci.*, **1995**, 43, (1/2):105-114.

Scotter, J. M.; Langford, V. S.; Wilson, P. W.; McEwan, M. J.; Chambers, S. T. Real-time detection of common microbial volatile organic compounds from medically important fungi by Selected Ion Flow Tube-Mass Spectrometry (SIFT-MS). *J. Micro. Methods*, **2005**, 63, 127 – 134.

Senthilmohan, S. T.; Davis, B. M.; McEwan, M. J.; Improved peroxyl radical scavenging TOSC essay to quantify antioxidant capacity using SIFT-MS. *Redox Report*, **2009**, 14, 197 – 204.

Senthilmohan, S. T.; Kettle, A J.; McEwan, M. J.; Dummer, J.; Edwards, S. J.; Wilson, P. F.; Epton, M. J. Detection of monobromamine, monochloramine and dichloramine using selected ion flow tube mass spectrometry and their relevance as breath markers. *Rapid Commun. Mass Spect.*, **2008**, 22, 677-681.

Senthilmohan, S. T.; Milligan, D. B.; McEwan, M. J.; Freeman, C. G.; Wilson, P. F. Quantitative analysis of trace gases of breath during exercise using the new SIFT-MS technique. *Redox Report.*, **2000**, 5, 151-153.

Simanzhenkov, V.; Idem, R. *Crude Oil Chemistry*. Editor Marcel Dekkar, Inc. 221 - 259, **2003**.

Smith, D. The ion chemistry of interstellar clouds. *Chem. Rev.* 1992, 92, 1473-1485.

Smith D., Adams N. G. The selected ion flow tube (SIFT): Studies of ion-neutral reactions. *Adv. At. Mol. Phys.*, **1987**, 24, 1-49.

Smith, D.; Španěl, P. Selected ion flow tube mass spectrometry (SIFT-MS) for on-line trace gas analysis. *M. Spect. Rev.*, **2005**, 24, 661-700.

Smith, D.; Španěl, P. *Swarm Techniques.* Experimental Methods in Physical Sciences Vo.29A. Pub:Academic Press, Inc. **1995.**

Španěl, P.; Dryahina, K.; Smith D. Microwave plasma ion sources for selected ion flow tube mass spectrometry: Optimizing their performance and detection limits for trace gas analysis. *Int. J. M. Spect.*, **2007**, 267, 117–124.

Španěl P.; Smith D. Selected Ion Flow Tube – Mass Spectrometry: Detection and Real-time Monitoring of Flavours Relesed by Food Products. *Rapid Comm. M. Spect.*, **1999**, 13, 585-596.

Španěl P.; Smith D. Selected Ion Flow Tube: A Technique for Quantitative Trace Gas Analysis of Air and Breath. *Med. Biol. Eng. Comput.*, **1996**, 34, 409-419.

Su, T.; Chesnavich, W. J. Parameterization of the ion-molecule collision rate constant by trajectory calculations. *J. Chem. Phys.*, **1982**, 76, 5183–5185.

Vyachelslav, N. F.; Grabowski, J. J. Simplified injector flanges for the selected ion flow tube. *Int. J. M. Spect.*, **1998**, 177, 175-186.

Xu, Y.; Barringer, S. Comparison of Tomatillo and Tomato Volatile Compounds in the Headspace by Selected Ion Flow Tube Mass Spectrometry (SIFT-MS). *J. Food Science*, **2010**, 75, 3: C268 – C273.

Xu, Y.; Barringer, S. Comparison of Volatile Release in Tomatillo and Different Varieties of Tomato during Chewing. *J. Food Science*, **2010,** 75, 4:C352-C358(7).

Wilson, P. F.; Freeman, C. G.; McEwan, M. J.; Randall, A. A.; Shaw, F. M. SIFT-MS Measurement of VOC Distribution Coefficients in Human Blood Constituents and Urine. *Appl. Occ. Env. Hyg.*, **2003**, 18, 759-763.

Wilson, P. F.; Freeman, C. G.; McEwan, M. J.; Milligan, D. B.; Allardyce, R. A.; Shaw, G. M. *In situ* analysis of solvents on breath and blood: a selectied ion flow tube mass spectrometric study. *Rapid. Comm. M. Spect.*, **2002**, 16, 427-432.

Chapter 2

Comparison of a Passivated and Non-passivated SIFT-MS Inlet

Fundamental to the success of the SIFT-MS technique is accurate measurement of ion number densities (signal intensity) from the flow tube by which the concentration of an analyte compound in sampled gas can be calculated (Smith & Španěl 2005). An accurate measurement of analyte concentration in the sample requires a reliable transmission of the sample to the instrument. In §1.2 of Chapter 1 some important features of the SIFT instrument that allow for a quantitative analysis of ions in the flow tube are described. An additional element to the accuracy of the SIFT-MS technique that is often overlooked is the delivery of analyte sample via an inlet to the flow tube.

2.1 SIFT-MS Response to the Delivery of Analyte

The SIFT-MS technique provides a snapshot of all the volatile reactants present in a gas mixture. These volatile molecules largely have a mass less than 250 amu, of different shapes, volatilities, polarity, and transport properties (Eagleson 2004). Some of these properties i.e. analyte polarity and size promote adsorption to internal surface of the SIFT-MS inlet thus affecting delivery of analyte to the flow tube. Analyte molecules that have the tendency to stick to the inlet by adsorption are also referred to as “sticky” compounds and are problematic to SIFT-MS analysis.

To illustrate, consider the response curves of Figure 4. These curves represent the product ion signal intensity detected over time by the SIFT instrument. The maximum signal intensity reflects the actual concentration of analyte in the sample. For these theoretical inlets the volume of analyte drawn through the inlet and the detection time (the time between inlet opening and inlet closing) are the same.

- The first curve (——) illustrates the instrument's response to analyte delivered by an ideal sample inlet. When the inlet is opened the maximum signal intensity is measured indicating instantaneous delivery of the sample to the flow tube without loss of sample. When the inlet is closed the signal immediately falls to background intensity indicating instantaneous removal of the sample from the inlet and no apparent retention of analyte in the tubing.

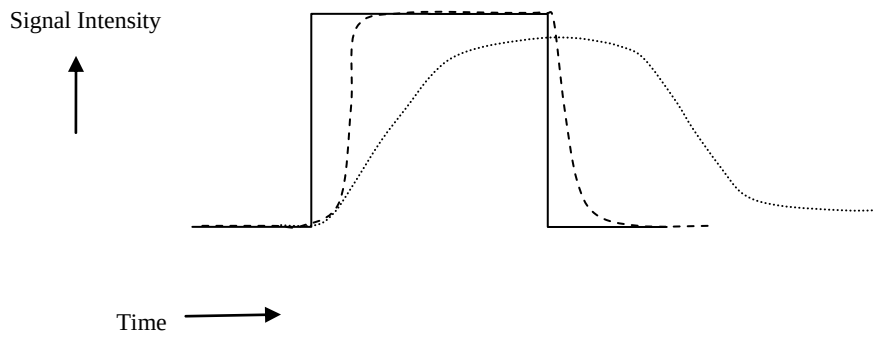

Figure 4: Response curves illustrating the detected product ion signal intensity as the inlet is open then shut for different theoretical inlets.

- The second curve (----) illustrates a somewhat exaggerated but typical response of the instrument to analyte delivered by the current SIFT-MS inlet. When the inlet is opened a gradual rise to maximum intensity is measured, and when the inlet is closed the signal intensity falls gradually.

Two causes account for this response: (i) a short time delay in response reflects the time to draw analyte through the length of the capillary when opened or closed, and is physically unavoidable, and (ii) analyte molecules adsorb to sites along the inlet as it is drawn through and the effect lessens as the inlet becomes saturated with analyte. One way of minimising adsorption of molecules and in turn the memory effect is to heat the inlet (see §2.2). A memory effect is where an amount of the previous analyte is retained in the inlet and carried over to the next sample analysis.

- The third curve (····) is a worst case scenario and clearly results in an unacceptable analysis. The problem of surface adsorption to the inlet is evident as signal intensity approaches but does not attain a maximum over the sampling time. For this analysis, the measurement of analyte concentration is not a true reflection of what is actually in the sample. In addition, note the extended time for signal intensity to fall-off after the inlet is closed. This indicates a memory effect that undermines the accuracy of an analysis as a relatively high amount of analyte concentration is already in the inlet.

We can see the success of SIFT-MS analysis is limited by the delivery of analyte to the flow tube. Loss of sample by adsorption to the inlet itself is concerning for SIFT-MS applications where the concentration is very low and/or real-time analysis is required, e.g. levels of ammonia on breath (Davies et al. 1997). A proposed improvement, and the subject of this chapter, is installing and characterising a prototype passivated inlet to the SYFT laboratory VOICE100™ research instrument. The performance of this inlet will be determined by comparing the measurements of selected analyte using a passivated inlet with the same measurements using an unpassivated inlet.

2.2 The SIFT-MS VOICE100™ Inlet

The sample inlet of the VOICE100™ is made up of uniformly heated stainless steel tubing. The tubing is usually heated to 110ºC to avoid cold spots in which condensation and/or adsorption of analyte will occur. To heat the inlet, a nichrome wire (powered by mains voltage with a variable resistor) covered in silicon rubber-insulation is wrapped evenly about its length. Fibre glass insulation is then wrapped about the inlet and held in place using fibreglass tape.

Analyte flow through the inlet is governed by a relatively short capillary (0.010″ internal diameter) that opens to a long connecting tube (0.25″ internal diameter) leading to the flow tube. The capillary and long tube join to a finger tube (0.125″ internal diameter) that protrudes downstream of the Venturi orifice and upstream of the sampling orifice of the flow tube. Analyte entry to the flow tube is through a circular aperture at the end of this finger tube. It must be noted the finger tube is stainless steel, but that should not affect the transfer of analyte to the flow tube because the flow tube it is at a pressure of ~0.5 Torr at which pressure molecules are not expected to undergo significant adsorption.

The VOICE100™ instrument is modular in design so to install a new inlet, the existing capillary and long tube is simply disconnected from the finger tube and a replacement attached (see Figure 5).

2.2.1 The Prototype Inlet

The passivated inlet has a deactivated silicon coating applied to the walls of the inner tube. Inlet deactivation has the benefits of low chemical reactivity, resistance to oils, solvent and water, and performance at temperatures of 200ºC. The passivated inlet is sheathed in copper tubing to prevent kinks occurring during handling. For an accurate analysis, any bends

or kinks in the inlet must be avoided because they constrict the flow of analyte throughout the tube.

The replacement unpassivated and passivated inlets are constructed similarly: A single capillary 80 cm long (~0.0625″ internal diameter) connects by a 90º elbow to the finger tube. This was deemed a practical length for breath analysis when a person would be seated to provide the sample. For the passivated inlet the elbow connector is also internally passivated, so the only difference between inlets is deactivated silica inside the tubing in the passivated inlet, and stainless steel in the unpassivated inlet.

The capillary and elbow are heated and insulated in the same manner as the original inlet. To ensure uniform heating of the inlet the temperature was measured at three points along the length of the tube. At the start and over the course of experiments, the air flow through the both inlets was measured at room temperature by a Digital Flow Control Meter HR™ ALLTECH. A significant reduction in air flow inferred a blockage that could be removed prior to measurements.

Analyte enters the flow tube facing the stream of reagent ions and carrier gas for which the end correction, ε is negative (Smith & Adams 1987). The end correction is a correction factor for the mixing effects of analyte entering the flow tube and is added to the reaction length l such that the effective reaction length is $(l + \varepsilon)$ and it is this length that is used in calculations.

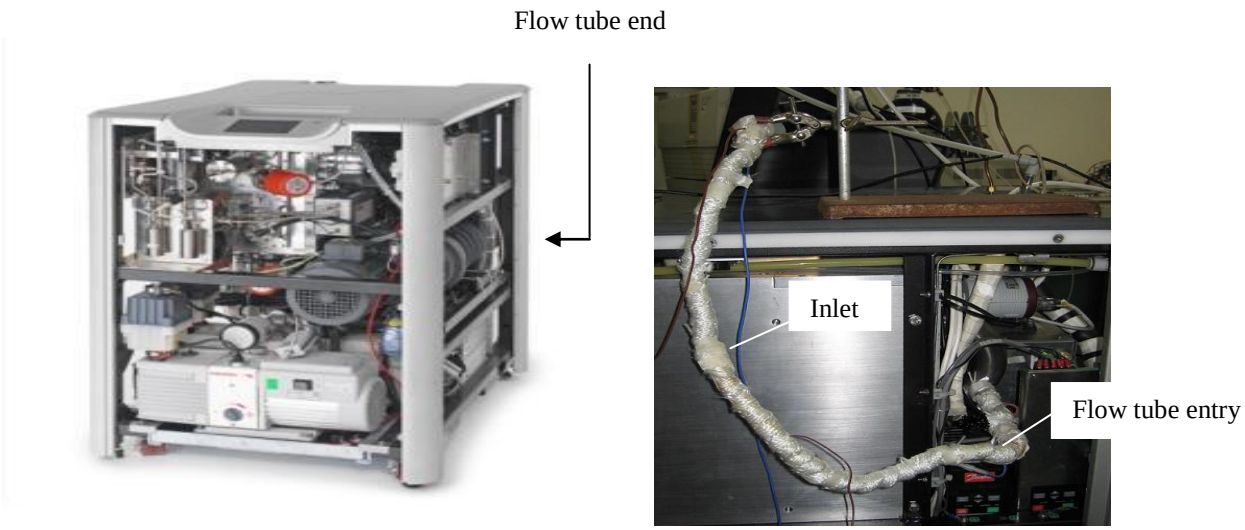

Figure 5: Photographs of the VOICE100™ instrument (left), and the prototype inlet installed directly to the flow tube (right).

2.3 Analytical Methods and Experiments

2.3.1 Analyte Samples

100 ml *solutions* of acetone and vanillin were prepared so the measured headspace concentration at room temperature was between 1 – 3 parts per million (ppm). This concentration range is typical of many SIFT-MS applications (Smith & Španěl 2005). Samples were placed in a 100 ml glass flask, and nitrogen gas (fixed flow of 250 sccm) was bubbled through the solution via a customised sintered tube to control the fluid flow (see Figure 6).

Measurement of the sample headspace began by placing the open end of the flask to the inlet portal (uncapped) and finished by removing the flask when the sampling time was complete. This gave the effect of inlet open and inlet shut (e.g. see Figure 9). Three replicate solutions were measured for each analyte. A selected ion mode (SIM) scan was used for the

analyses, and the concentration reported as the average of three replicate measurements. Referring to the response curve (----) of Figure 4, the maximum concentration obtained by a SIM scan within the sampling time was averaged.

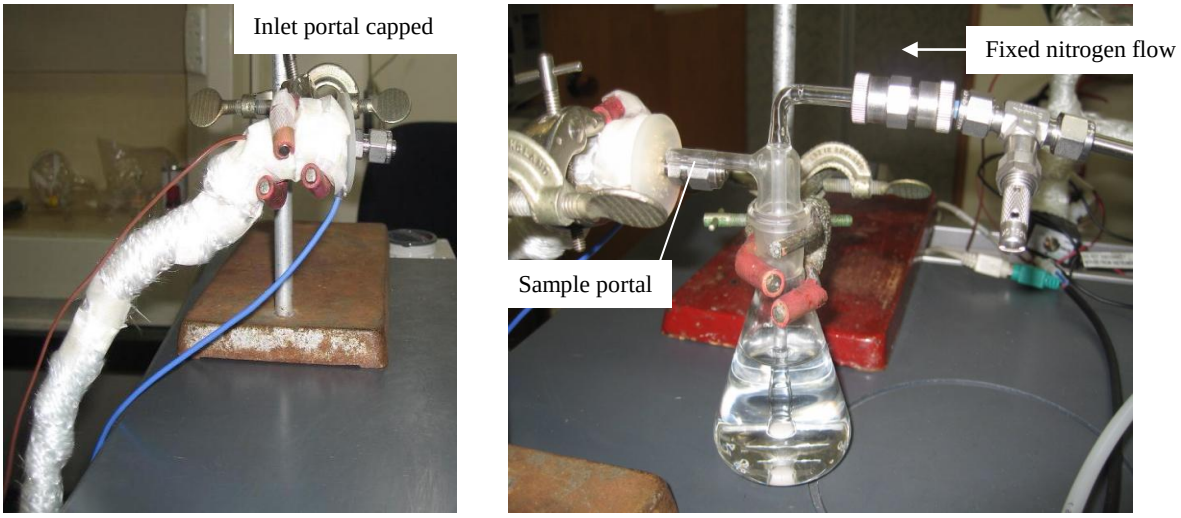

Figure 6: Photographs of the inlet portal (left) and the setup for measuring sample headspace (right).

Ammonia and H_2S samples were sourced by the *permeation tube method*. The permeation apparatus consists of a permeation tube contained in a highly accurate temperature controlled oven (Vici Metronics Inc.). A permeation tube is a length of Teflon™ pipe sealed at each end and filled with liquid or solid analyte. By placing the permeation tube in the oven and passing a measured flow of nitrogen over the tube, gas phase equilibrium is established and a constant stable gas phase concentration is created through permeation of the analyte through the Teflon™.

The compound permeation rate at a specific temperature is provided by the supplier (i.e**.** Kin-tek NH_3; 519 ng min^{-1} /30ºC, and Vici H_2S; 2725 ng min^{-1}/50ºC) from which the

concentration delivered is determined. The permeation apparatus creates a dynamic dilution at an accurate concentration by adjusting the flow of nitrogen over the tube, (typically ± 10%). Analyte is delivered to the inlet by connecting Teflon™ tubing from the permeation oven to the inlet portal. The amount of analyte sampled is determined by the inlet capillary flow rate and any excess flow of analyte is removed by a T-junction exhaust of Teflon™ tube placed prior to the inlet portal. A SIM scan was used for the analyses, and the concentration reported as the average of three replicate measurements.

2.3.2 Inlet Characterisation and Development Procedure

Both inlets were first characterised by adding acetone (CH_3COCH_3 58.08 g/mol) as an analyte. Acetone was chosen because it completely dissolves in water and is highly volatile. SIFT-MS headspace analysis of acetone is straightforward as it is volatile and does not adsorb strongly onto the surface of metals.

Both inlets were then compared by analysing other compounds: (i) ammonia (NH_3 17.03 g/mol), (ii) vanillin ($C_8H_8O_3$ 152.15 g/mol). These compounds are representative of those measured in different areas of SIFT-MS application, i.e. medical and diagnostic research (Diskin et al. 2003) and food and flavour research (Sharp 2009). They are also difficult compounds to measure as ammonia is a polar molecule and vanillin a relatively large molecule. The third compound (iii) hydrogen sulfide (H_2S 34.08 g/mol) is a compound of interest in the area of geochemical surveying.

Three inlet tests were performed: –

1) Linear response

The inlet is heated to 110°C, and serial dilutions of concentration are measured. Henry's law states that the liquid and gas phases are in equilibrium when the temperature is constant

(Eagleson 2004). The headspace concentration should therefore decrease on dilution of liquid concentration. Deviations from linearity would indicate a loss of sample concentration.

2) Temperature sensitivity

The inlet is heated to 60°, 110°, or 140°C, and two different concentrations of analyte measured. This test investigates any dependence of amount measured to the inlet temperature.

3) Response curve character

The inlet is heated to 60º, 110º, or 140ºC, and the analyte measured for a specific sampling time (see §2.3.1). The character of each response curve will indicate analyte lost by adsorption to the inlet.

2.4 SIFT-MS Product-ion Analysis

(i) Acetone reactions with SIFT-MS reagent ions result in the following primary product-ions:

$$CO(CH_3)_2 + H_3O^+ \longrightarrow (CO(CH_3)_2\text{-}H)^+ + H_2O \qquad m/z\ 59$$

$$CO(CH_3)_2 + NO^+ + M \longrightarrow (CO(CH_3)_2\text{-}NO)^+ + M \qquad m/z\ 88$$

$$CO(CH_3)_2 + O_2^+ \longrightarrow (CH_3CO\ CH_3)^+ + O_2 \qquad m/z\ 58$$

$$\longrightarrow (CH_3CO)^+ + CH_3O_2 \qquad m/z\ 43$$

The product-ion *m/z* 59 occurs by proton H^+ transfer from H_3O^+, *m/z* 88 via NO^+ association, *m/z* 58 by charge transfer from O_2^+, and *m/z* 43 via dissociative charge transfer and CH_3 removed. Hydration (+H_2O 18 g/mol) of the primary product-ion *m/z* 59 may result in a secondary product-ion at *m/z* 77.

$$CO(CH_3)_2.H^+ + H_2O + M \longrightarrow (CH_3CO\ CH_3).H^+ + H_2O + M \qquad m/z\ 77$$

(ii) Ammonia reactions with SIFT-MS reagent ions result in the following primary product-ions:

$$NH_3 + H_3O^+ \longrightarrow (NH_3\text{-}H)^+ + H_2O \qquad m/z\ 18$$
$$NH_3 + O_2^+ \longrightarrow NH_3^+ + O_2 \qquad m/z\ 17$$

The product-ion *m/z* 18 occurs by proton H^+ transfer from H_3O^+, and *m/z* 17 by charge transfer from O_2^+. Hydration of primary product-ions *m/z* 18 and *m/z* 17 may result in secondary product-ions at *m/z* 36 and *m/z* 35 respectively.

H_2O may also be removed from the secondary product-ion *m/z* 35 by a third body and subsequent protonation H^+ of this product ion produces another secondary product-ion at *m/z* 18. Finally hydration of this secondary product ion may result in another secondary product-ion *m/z* 36.

$$NH_3^+.H_2O + H_2O + M \longrightarrow NH_4^+ + H_2O + OH + M \qquad m/z\ 18$$
$$NH_4^+ + H_2O + M \longrightarrow NH_4^+.H_2O + M \qquad m/z\ 36$$

(iii) Vanillin reactions with SIFT-MS reagent ions result in the following primary product-ions:

$$C_8H_8O_3 + H_3O^+ \longrightarrow (C_8H_8O_3\text{-}H)^+ + H_2O \qquad m/z\ 153$$
$$C_8H_8O_3 + NO^+ \longrightarrow C_8H_8O_3^+ + NO \qquad m/z\ 152$$
$$C_8H_8O_3 + O_2^+ \longrightarrow C_8H_8O_3^+ + O_2 \qquad m/z\ 152$$

The product ion *m/z* 153 occurs by proton H^+ transfer from H_3O^+, *m/z* 152 by charge transfer from NO^+, and *m/z* 152 by charge transfer from O_2^+. Hydration of the primary product-ion *m/z* 153 may result in a secondary product-ion at *m/z* 171.

$$C_8H_8O_3.H^+ + H_2O + M \longrightarrow C_8H_8O_3.H^+.H_2O + M \qquad m/z\ 171$$

(iv) Hydrogen sulfide reactions with SIFT-MS reagent ions result in the following primary product-ions:

$$H_2S + H_3O^+ \longrightarrow (H_2S\text{-}H)^+ \qquad m/z\ 35$$

$$H_2S + O_2^+ \longrightarrow H_2S^+ \qquad m/z\ 34$$

The product ion *m/z* 35 occurs by proton H^+ transfer from H_3O^+ and the product ion *m/z* 34 by charge transfer from O_2^+.

2.5 Results and Discussion

2.5.1 Inlet Characterisation

The measured concentration of serial dilutions of acetone gave very good R^2 values for both inlets (see Figure 7). In addition a similar linear response was measured by each inlet within error suggesting minimal analyte adsorption as expected.

The acetone solutions made up for the temperature sensitivity tests are different for each inlet (see Table 2). To make a better comparison between the two inlets, the concentrations measured for each inlet at 60°C and 140°C were normalised to the corresponding 110°C concentration measured (see Figure 8).

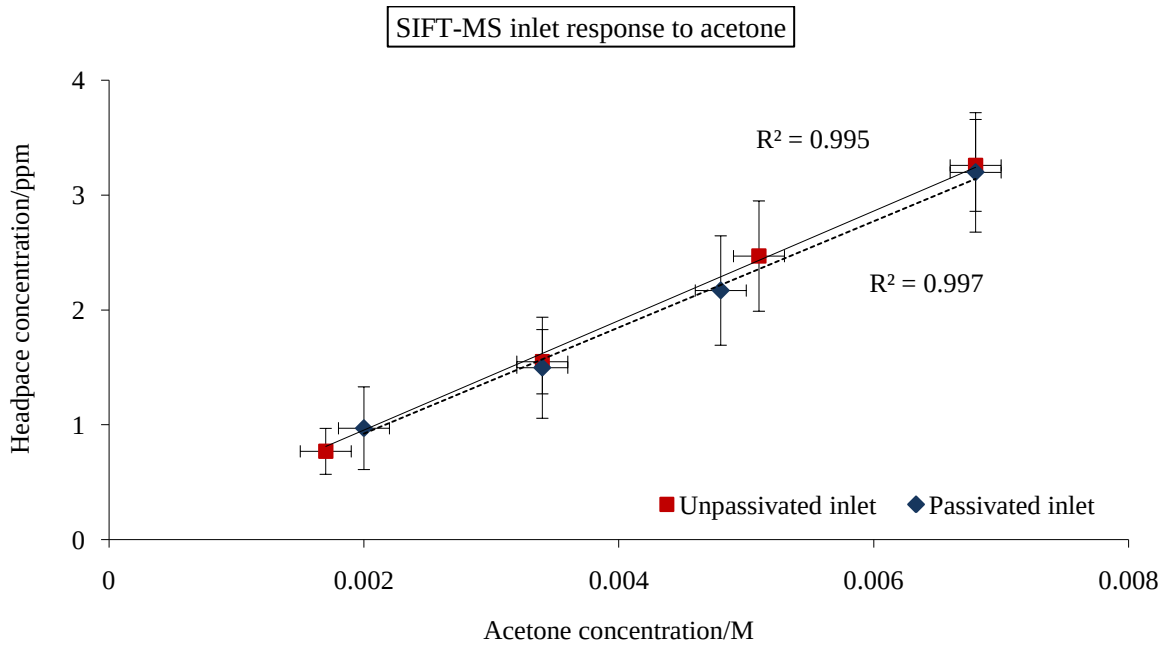

Figure 7: Response of unpassivated and passivated inlets at 110°C to acetone solutions. (Vertical error bars are ± 2 standard deviation (SD); horizontal error bars are ± 0.0002 ppm)

	Unpassivated inlet		Passivated inlet	
InletTemperature/°C	Solution Concentration		Solution Concentration	
	0.007 M	0.003 M	0.050 M	0.020 M
140	3.42 (0.13)	1.82 (0.11)	22.72 (1.91)	8.26 (1.20)
110	3.26 (0.10)	1.55 (0.07)	23.73 (0.85)	8.64 (0.45)
60	3.15 (0.13)	1.72 (0.09)	24.47 (0.96)	8.73 (0.78)

Table 2: Temperature sensitivity of SIFT-MS inlet to measure acetone concentration. (Average measured concentration (ppm) is given first, and 1SD in parentheses)

From Figure 8, the unpassivated inlet measured the 0.007 M acetone solution relatively efficiently except for 0.003 M solution where the actual concentration mixture was likely higher than thought. By comparison the passivated inlet measured acetone solution relatively efficiently at all temperatures.

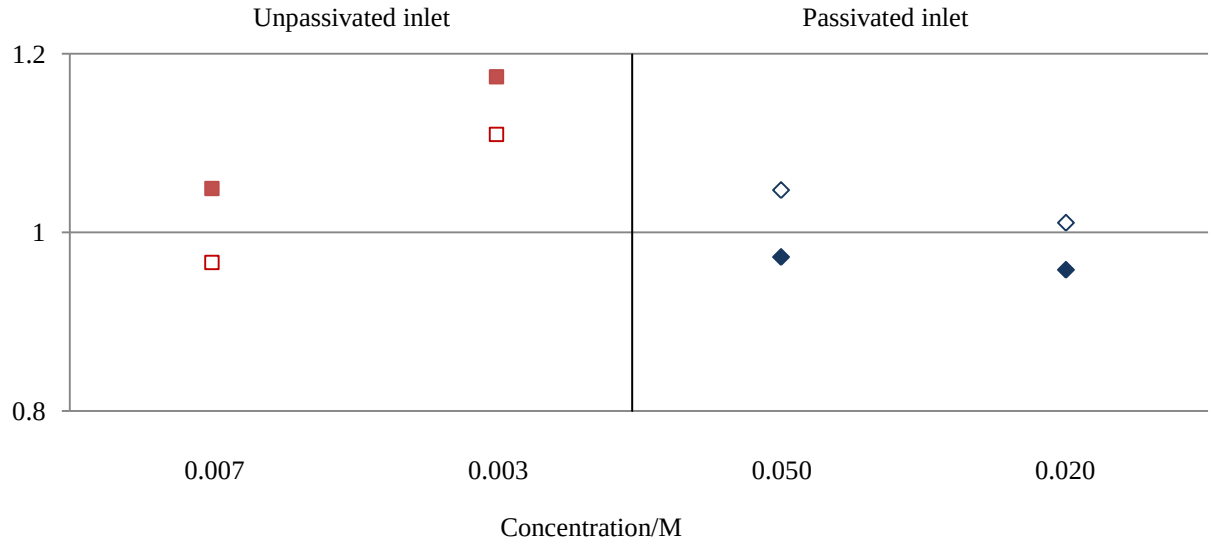

Figure 8: The concentration measured for 140ºC and 60°C inlets that are normalised to the respective 110°C inlet concentration (see Table 2). The filled data points are the normalised value for the inlet at 140° and, the unfilled data points are the normalised value for the inlet at 60°C.

The rise and fall response for both inlets at 140°, 110° and 60°C is shown in Figure 9. The sample is offered 35s after the start of the SIFT-MS SIM scan and removed 45s later.

The unpassivated inlet rise time is 1s at 140°, and ~2.5s at 110° and 60°C; and the fall time is 2s at 140°, and ~3s at 110° and 60°C. The passivated inlet rise time is 3s at 140°C, and about 2s at 110° and 60°C; and the fall time is 2s at all inlet temperatures. A rise time of 2s or less was expected for the high temperature passivated inlet. A longer rise time may be caused by the way the analyte sample is presented to the inlet portal. An obvious delay in response was noted when the solution was not positioned correctly.

The results show both inlets have a linear response to over this concentration range with relatively the same efficiency at all temperatures. Acetone is an analyte that has high volatility and is not particularly “sticky”. It is the behaviour of the next two analytes that provide a more demanding test of the effectiveness of the inlet system.

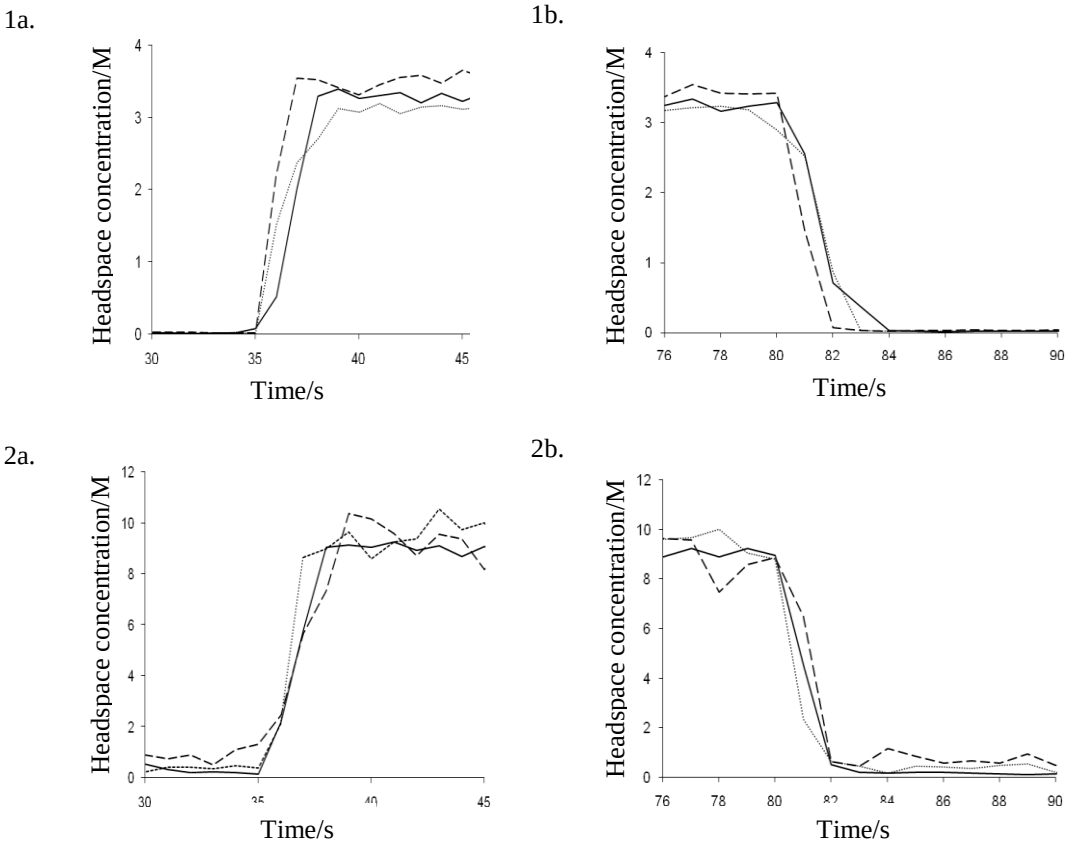

Figure 9: SIFT-MS analysis of acetone with the inlet at 140° (----), 110° (——), and 60°C (····). Graphs 1a and 1b are unpassivated inlet response curves. Graphs 2a and 2b are passivated inlet response curves.

2.5.2 Inlet Development

2.5.2.1 Ammonia

The response of the inlet system from serial dilutions of ammonia gave very good R^2 values for both inlets (see Figure 10).

From Table 3 we note the average ammonia concentration measured is less than the actual analyte concentration for both inlets underscoring the difficulty in measuring a "sticky" analyte like ammonia. We also note both inlets measured higher concentration as the inlet temperature increased. The unpassivated inlet provided just one concentration of

ammonia at an inlet temperature of 140°C within experimental uncertainty of the prepared concentration. On the other hand, the passivated inlet provided high and low ammonia concentrations within experimental uncertainty at inlet temperatures of 110°C and 140°C. This result confirms the rate of analyte adsorption on the walls of the inlet is less pronounced at higher inlet temperatures.

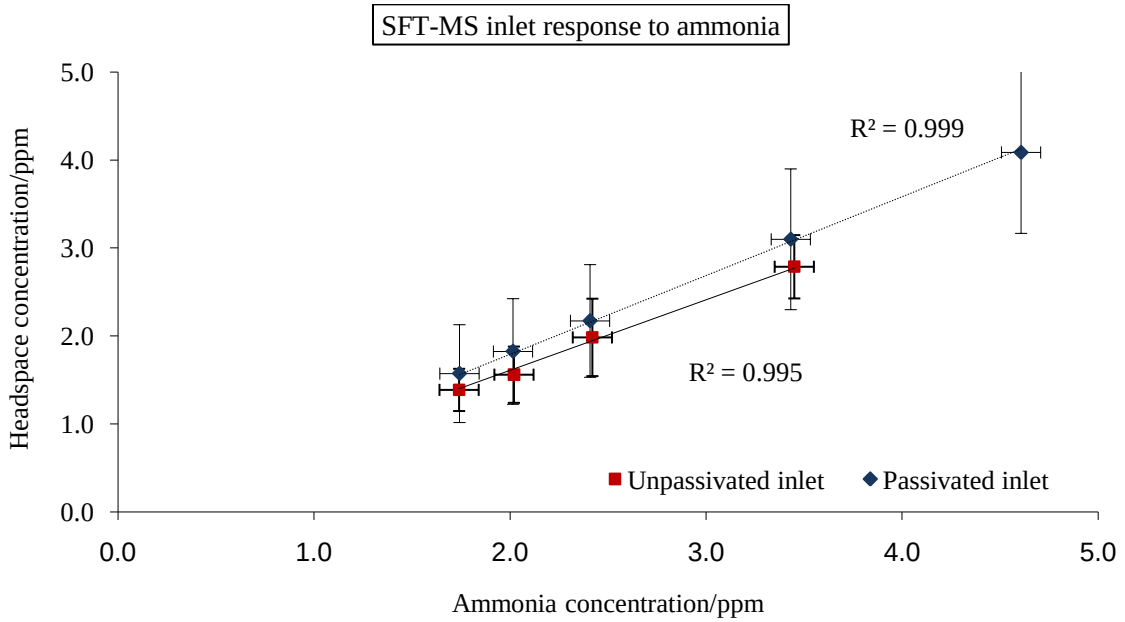

Figure 10: Response of unpassivated and passivated inlets at 110°C to ammonia solutions.(Vertical error bars are ± 2SD; horizontal error bars are ± 0.1ppm)

	Unpassivated inlet		Passivated inlet	
InletTemperature/°C	Prepared Concentration		Prepared Concentration	
	4.6 ppm	2.0 ppm	4.6 ppm	2.0 ppm
140	3.40 (0.17)	1.63 (0.96)	4.25 (0.26)	1.90 (0.17)
110	2.68 (0.52)	1.56 (0.11)	4.41 (0.19)	1.88 (0.88)
60	2.06 (0.09)	1.53 (0.08)	4.08 (0.23)	1.82 (0.15)

Table 3: Temperature sensitivity of SIFT-MS inlet to measure ammonia concentration. (Average measured concentration (ppm) is given first, and 2SD in parentheses)

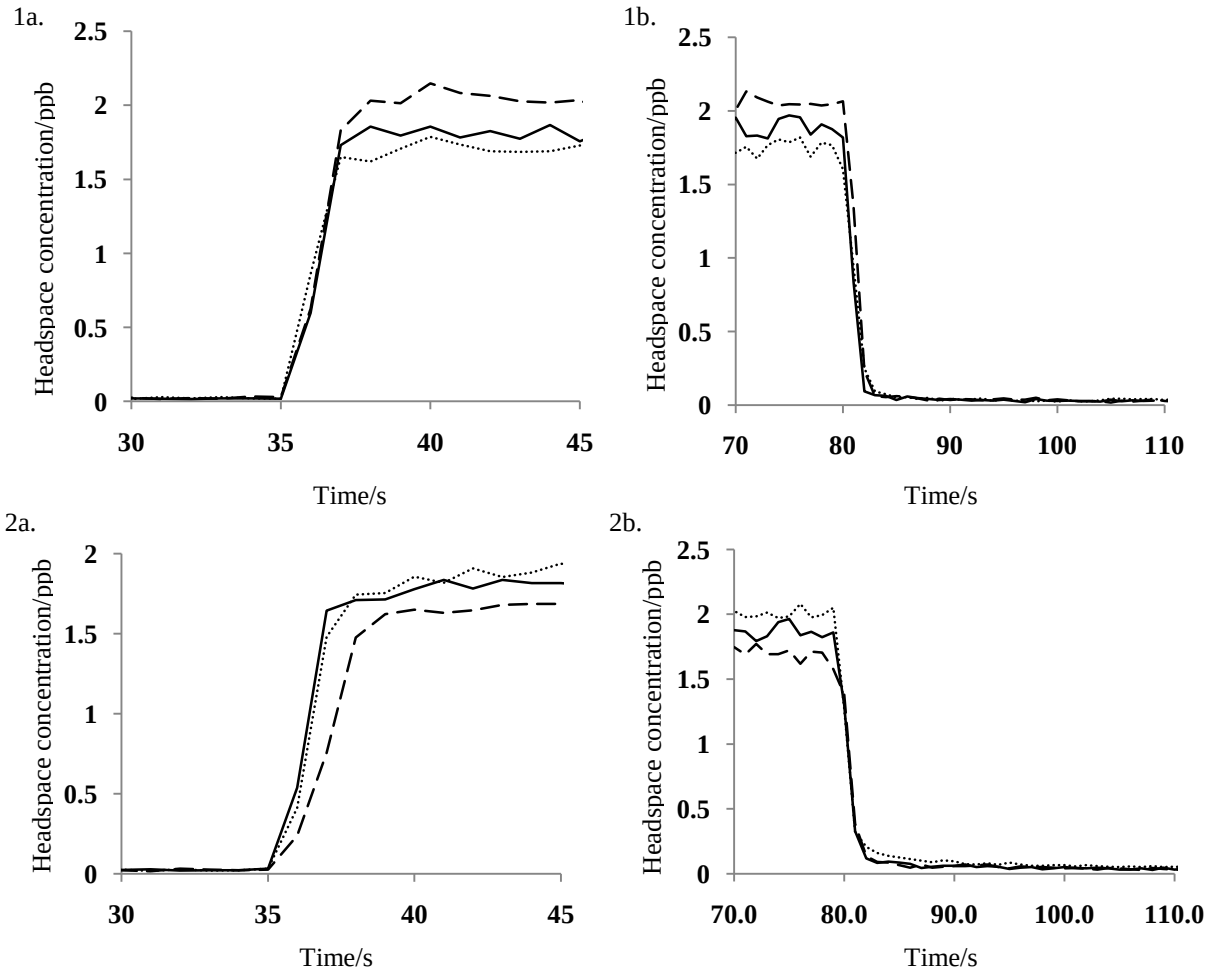

Figure 11: SIFT-MS analysis of 2.0 ppm ammonia solution at 140° (----), 110° (——), and 60°C (····) inlet temperatures. Graphs 1a, 1b are unpassivated inlet response curves, and, graphs 2a, 2b are passivated inlet response curves.

The rise and fall response for both inlets at 140°, 110° and 60°C is shown in Figure 11. The sample is offered 35s after the start of the SIFT-MS SIM scan and removed 45s later.

The unpassivated inlet rise time is ~1s at all inlet temperatures, and the passivated inlet rise time is 2s at 140°C; and 1s at 110° and 60°C. The 2s rise time for the inlet temerature at 140°C is an unexpected result and it may have resulted from a cold spot in the inlet.

In the first 3s after the sample was removed there was ~95% decrease in concentration, but it was another 20s until initial background concentration was reached for both inlets. This demonstrates the problem of analysing ammonia on breath as: (i) some carryover of

ammonia concentration occurs in the inlet between breaths, and (ii) 20s can be a long time to wait between exhalations. In the present case, it seemed most of the ammonia was about the portal of the inlet as a heat gun applied between measurements purged the residual analyte quickly. That would suggest a higher inlet temperature could be beneficial.

The results have shown both inlets have a good linear response over this concentration range. However loss of analyte by adsorption to the inlet is observably worse for the unpassivated inlet at 60°C inlet temperature. Both inlets measured a higher concentration when the inlet temperature was higher, but only the passivated inlet provides the ammonia concentration accurately within experimental uncertainty. On introduction of the sample the response was the same for both inlets and apparently not temperature dependent. The memory effect is evident however for both inlets on withdrawal of sample suggesting a higher inlet temperature would be useful to purge residual ammonia between measurements.

2.5.2.2 Vanillin

Vanillin required more preparation for analysis as vanillin crystals are only sparingly soluble in water. The solutions were heated in a sonic vibrator until they dissolved. Moreover only a relatively small amount of vanillin crystals could be dissolved to make up solutions because saturation was evident for greater amounts. As a consequence measured vanillin concentrations were also very small with the concentrations measured to 0.1ppm. However, despite these difficulties the inlet tests provided some good results.

The response of the passivated inlet system from serial dilutions of vanillin gave a better R^2 value than the unpassivated inlet (see Figure 12). This result indicates loss of more of the vanillin sample to the unpassivated inlet. Incidentally the vanillin solutions were measured from low to high concentration to minimise the residual amount of analyte in the inlet

between measurements. However it is evident there was residual background of analyte as the response curves do not pass through (0,0).

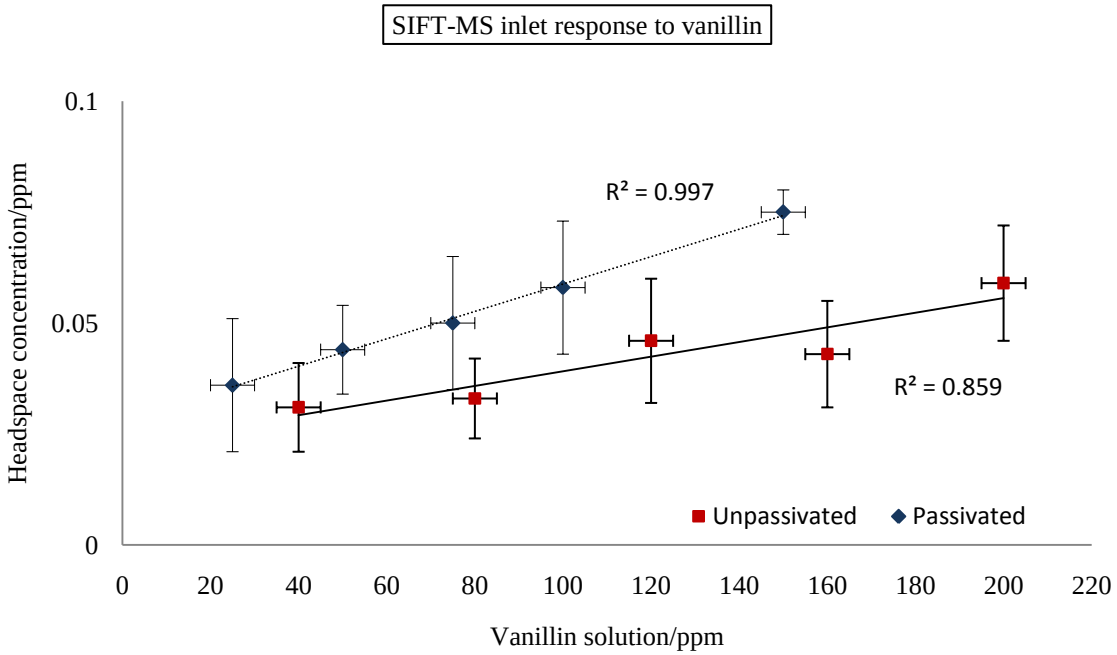

Figure 12: Response of unpassivated and passivated inlets at 110°C to vanillin solutions. (Vertical error bars are ± 2SD; horizontal error bars are ± 5ppm)

	Unpassivated inlet		Passivated inlet	
InletTemperature /°C	Nominal Concentration 100 ppm	50 ppm	Nominal Concentration 100 ppm	50 ppm
140	0.063 (0.017)	0.044 (0.012)	0.060 (0.032)	0.043 (0.019)
110	0.043 (0.011)	0.036 (0.012)	0.058 (0.015)	0.044 (0.010)
60	0.048 (0.014)	0.028 (0.012)	0.053 (0.058)	0.037 (0.044)

Table 4: Temperature sensitivity of SIFT-MS inlet to measure vanillin concentration. (Average measured concentration (ppm) is given first, and 2SD in parentheses)

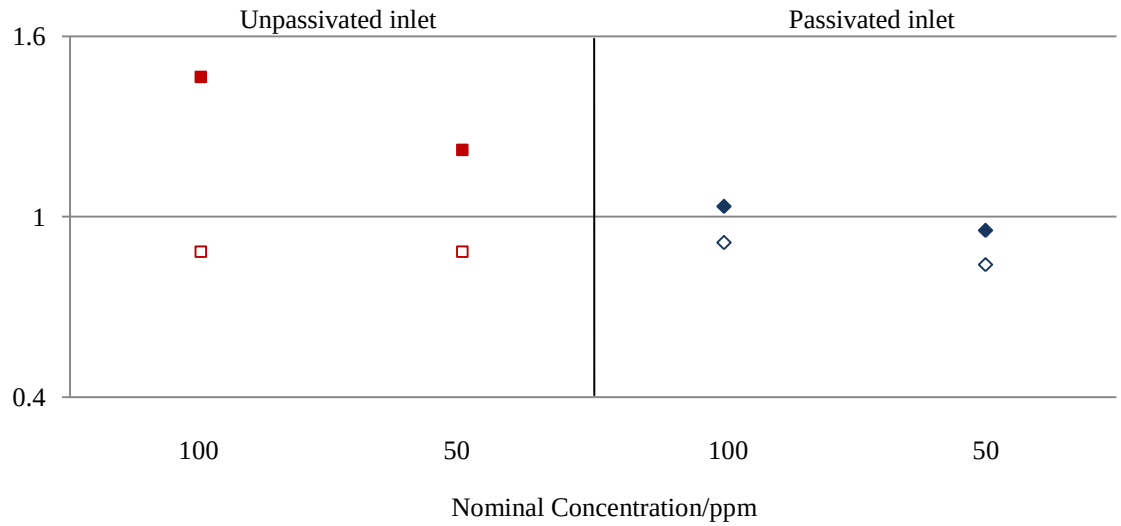

Figure 13: The concentration measured for 140ºC and 60°C inlets that are normalised to the respective 110°C inlet concentration (Table 4). The filled data points are the normalised value for the inlet at 140° and, the unfilled data points are the normalised value for the inlet at 60°C.

From Figure 13 and Table 4, we note both inlets measured higher concentration as the inlet temperature increased. We also note the unpassivated inlet measured relatively low concentrations compared to the passivated inlet at 140ºC and 60°C, and a concentration value similar to the passivated inlet at 140ºC. On the other hand the passivated inlet measured vanillin relatively efficiently at all temperatures is therefore the more efficient of the two inlets.

The difficulty in interpreting these results are the very large standard deviation. These are large because the measured signals were at times not much higher than background signals and correspondingly noisy, an unavoidable consequence of low analyte volatility and low concentration solutions.

Another problem that was noticed during the analysis of vanillin solutions was the inconsistent measurements for the same concentration solutions between days. This

inconsistency was attributed to a variation in the position of the product ion peak at 152 *m/z*. The downstream scan-line calibration on a VOICE100™ instrument ensures ions of a certain *m/z* value are recorded by the control software at their correct *m/z* value. This problem in mass position was solved by using the O_2^+ reagent ion 32 and 152 *m/z* with vanillin present for calibration of the downstream scan-line. Measured concentrations were more consistent after that.

Figure 14 shows the SIFT-MS response to vanillin for both inlets at 140° and 110°. The 60^{o}C response curves were poor in this case, taking most of the sampling time to reach an apparent maximum and very noisy so they are not presented.

The vanillin solution was sampled 35s and 30s after the start of the SIFT-MS SIM scan with the unpassivated and passivated inlets respectively. Then 55s and 75s later the vanillin solution was removed from the unpassivated and passivated inlets respectively. A heat gun was again applied to purge the inlet between measurements. We note no difference in the rise and fall time of the curves for inlet temperature. The rise time of the unpassivated inlet is ~5s and the fall time ~15s whereas, the rise time of the passivated inlet is 20s and the fall time ~40s.

The results have shown both inlets have a good linear response though not with the same efficiency. Loss of analyte is noted for the unpassivated inlet with increasing solution concentration. An inlet temperature of 140^{o}C is favoured for a more sensitive concentration measurement by both inlets and is now well established.

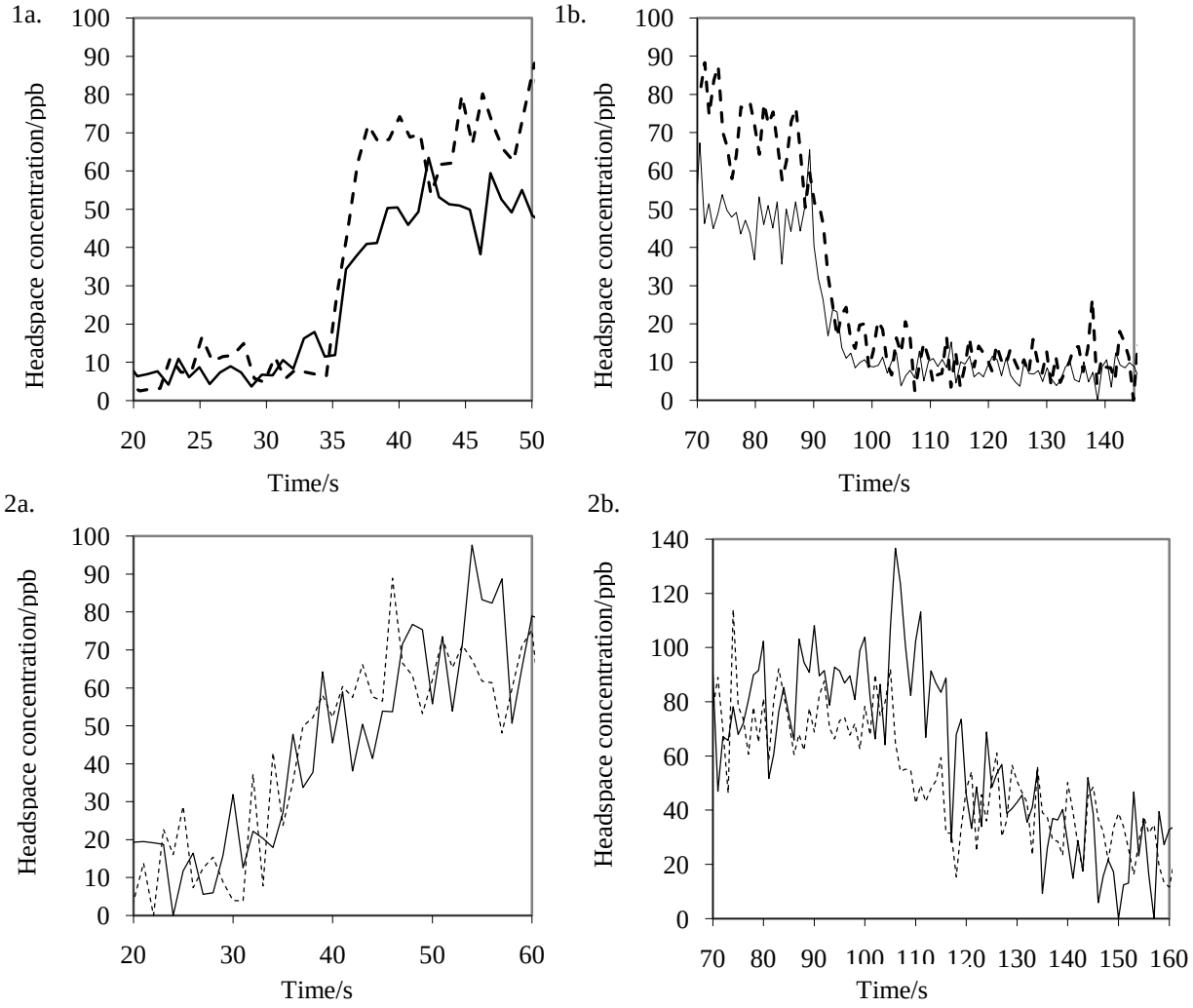

Figure 14: SIFT-MS analysis of 100 ppm vanillin solution at 140° (----) and 110° (—) inlet temperatures. Graphs 1a, 1b are unpassivated inlet response curves, and, graphs 2a, 2b are passivated inlet response curves.

2.5.2.3 Hydrogen sulfide

When the H_2S concentration in crude oil is high, it is very corrosive to steel pipes and different methods of reducing this effect are employed. H_2S is lost as sulphuric acid on unpassivated steel catalytic sites at high temperatures (Craig et al. 2006). Here the effect of high inlet temperature on the sampling probe for H_2S analysis by SIFT-MS was investigated.

The response of the passivated inlet system from serial dilutions of H_2S gave a slightly better R^2 value than the unpassivated inlet at 110°C (see Figure 15). The result indicates some loss of analyte by adsorption to the unpassivated inlet.

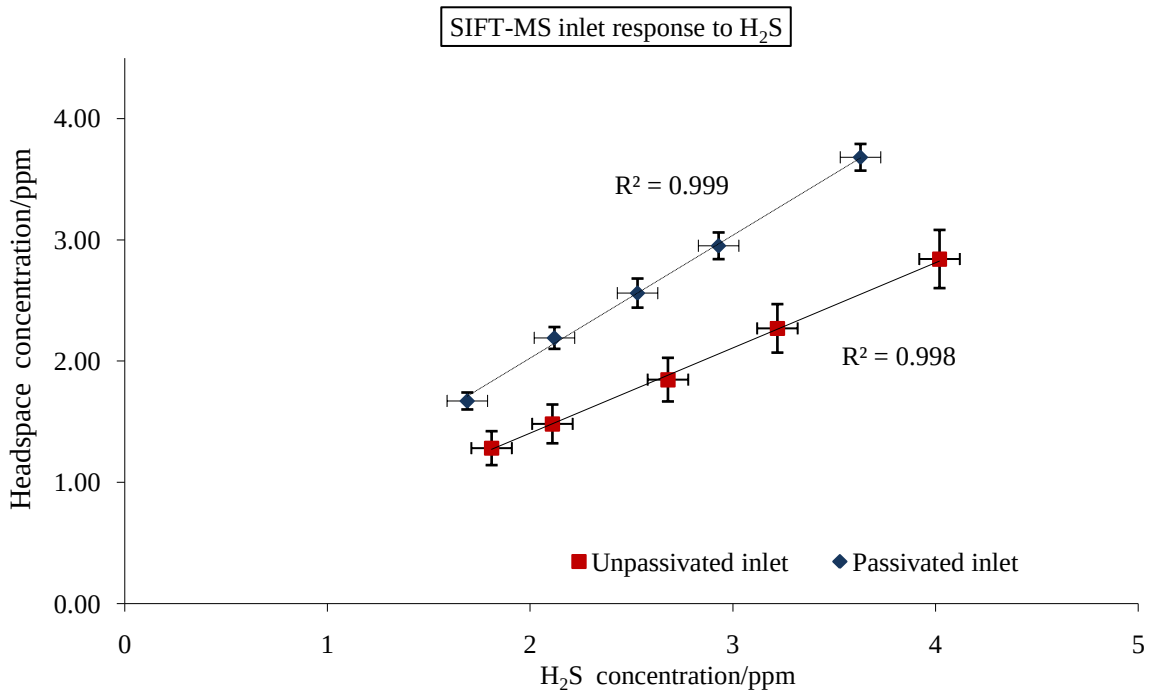

Figure 15: Response of unpassivated and passivated inlets at 110°C to H_2S solutions. (Vertical error bars are ± 2SD; horizontal error bars are ± 0.4ppm)

From Table 5 at temperatures higher than 60°C we see the loss of H_2S to the unpassivated inlet as the measured concentration is reduced. However for the passivated inlet the concentrations measured are all within experimental uncertainty at all temperatures.

The results indicate greater sensitivity of the passivated inlet to H_2S concentration than the unpassivated inlet. Another important result was the effect of high inlet temperature on H_2S analysis was not evident for the passivated inlet but observed for the unpassivated inlet.

This would suggest the suitability of a passivated inlet, even at high temperature, for geochemical surveys by the SIFT-MS technique.

	Unpassivated inlet	Passivated inlet
InletTemperature /°C	Prepared Concentration 4.0 ppm ± 0.4ppm	Prepared Concentration 4.0 ppm ± 0.4ppm
140	2.8 (0.4)	3.7 (0.4)
110	2.8 (0.2)	4.0 (0.4)
60	3.7 (0.4)	3.7 (0.4)

Table 5: Temperature sensitivity of SIFT-MS inlet to measure 4.0ppm H_2S concentration (average measured concentration (ppm) is given first, and 2SD in parentheses).

2.6 Conclusion

The need for an alternative inlet for SIFT-MS analysis arose because of the problem of loss of sample by adsorption to the walls of the inlet tubing. From the onset it was believed a passivated inlet would minimise this problem so a comparison was made between the unpassivated and passivated inlets.

Firstly acetone was used as a relatively non-"sticky" compound to establish the linear response, temperature sensitivity, and response curve character of the inlets. Both inlets were seen to transport acetone reliably at all inlet temperatures, and delivered the same amount of acetone to the instrument at 110°C. In addition both inlets responded in the same manner on introduction and removal of the analyte sample.

Based on this analysis, the character of the passivated inlet was developed using three important "sticky" compounds: ammonia, vanillin, and H_2S.

The main points gathered from the analyses were:

- The passivated inlet tranfers analyte as reliably as an unpassivated inlet.
- Analyte adsorption is reduced for the passivated inlet and observed as higher concentration measuements for most analyses.
- The passivated inlet can perform more efficiently than the unpassivated inlet at temperature greater than 110ºC.
- For accurate transfer of "difficult" analytes and those of lower volatility the presence of a completely passivated inlet is necessary.

In the writing of this thesis, these principles have been utilised on the new high performance inlet for the new generation SIFT-MS instrument VOICE200® launched in 2007.

2.7 References

Craig, B. D.; Lane, R. A.; Rose, D. H. Corrosion Prevention and Control: A Program Management Guide for Selecting Materials. Advanced Materials, Manufacturing, and Testing Information Analysis Center, September **2006**.

Davies, S.; Španěl P.; Smith D. Quantitative Analysis of Ammonia on the Breath of Patients in End-Stage Renal Failure. *Kidney Int.*, **1997**, 52, 223-228.

Diskin, A. M.; Španěl, P.; Smith, D. Time variation of ammonia, acetone, isoprene and ethanol in breath: a quantitative SIFT-MS study over 30 days. *Physiol. Meas.*, **2003**, 24, 1:107 – 119.

Eagleson, M. *Concise Encyclopedia Chemistry*. Translated and revised, de Gruyter **2004**.

Sharp, M. D. Analysis of Vanilla Compounds in Vanilla Extracts and Model Vanilla Ice Cream Mixes Using Novel Technology. Thesis for Master of Science, Ohio State University **2009.**

Smith, D.; Španěl, P. Selected ion flow tube mass spectrometry (SIFT-MS) for on-line trace gas analysis. *M. Spect. Rev.*, **2005**, 24, 661-700.

Smith D., Adams N. G. The selected ion flow tube (SIFT): Studies of ion-neutral reactions. *Adv. At. Mol. Phys.*, **1987**, 24, 1-49.

CHAPTER THREE

SIFT-MS Analysis of Cheese

In this chapter a comparison of Italian Parmigiano-Reggiano and Grana Padano cheeses and some New Zealand Parmesan cheeses is made using SIFT-MS analysis of cheese headspace. This analysis is based on the relative abundance and concentration of aroma compounds (also known as odour active compounds) that are reportedly characteristic of the cheese flavour. In view of the number of challenges associated with aroma analysis (Reineccius 2006) a preliminary SIFT-MS analysis of Cheddar and Blue cheeses is also presented.

3.1 Introduction

Of the thousands of cheese varieties produced throughout the world, most select cheeses are European manufactured (Fox & McSweeney 2004). Furthermore significant value is given to cheese attributed with originality and quality. For example, in Italy banks accept wheels of Parmigiano-Reggiano (commonly referred to as Parmesan) as collateral, depositing them in large climate controlled warehouses while they age.

Within Europe, Parmesan cheese is a protected designation of origin (PDO) product of Italy. This designation serves to promote and protect the quality of the cheese requiring adherence by cheese manufacturers to strict manufacturing protocol and, animal nutrition guidelines (European Policy for Quality Agricultural Products 1997).

Outside of Europe many Parmesan cheeses are produced although their reputation is shadowed by comparison to the Italian original. Nevertheless these cheese varieties are a

valuable commodity for countries of manufacture including New Zealand, Australia and the USA.

3.2 The Manufacture of Cheese and Cheese Flavour Development

Cheese flavour is defined by the balance of aroma compounds rather than their absence or presence (Frank et al. 2006). The complexity of cheese headspace is formidable as more than 600 volatiles have been identified in the headspace of cheese but only a fraction of these are responsible for flavour (Curioni & Bosset 2002). Moreover the volatiles evolved by the cheese reflect their presence in bulk cheese from which differences between varieties of a cheese may be explained (Zehentbauer & Reineccius 2002).

3.2.1 Cheese Manufacture

The manufacture of cheese arose from its quality of preserving the nutrients of milk which coincidentally tasted good. Essentially cheese-making consists of:

1. Curd formation, where casein the major protein of milk is coagulated by acid and/or rennin trapping milk fat. This allows the production of a product in which milk solids are reduced to a concentrated form.
2. The curd is treated and loss of whey (the whey is the serum or liquid part of the milk that remains after curd separation) advances. The manner in which curd is treated is specific to a cheese variety.
3. Finally there occurs a period of storage, during which the cheese ripens and flavour develops.

Generally the main processing steps are as follows:

- Depending on cheese variety the milk may be prepared by pasteurization, standardization, or skimming of fat before cheese-making. The milk is then heated and a starter culture usually lactic acid bacteria (LAB) added. As the concentration of lactic acid increases, milk pH lowers to about 5.2 (cheese pH < 5). For all hard cheeses rennin is added at this acidity, and curd is rapidly produced.
- The curd is cut into uniform pieces, salted and stirred. Cutting of the curd increases surface area and shortens the distance for whey to escape. Salt increases curd firmness and also controls microbial activity. The curd is then drained after which it is heated to a high temperature expelling more whey. At this phase the moisture content of the final cheese is controlled affecting the texture of the cheese. Generally the higher the scalding temperature, the drier and harder is the curd (Parmesan is heated to a temperature of 54-58°C).
- The curd is mechanically pressed to force out any residual whey, and the cheese molded to give its final shape. The molded cheese is then dry-salted or placed in a brine bath. This process slows down or stops acid production, a requirement for proper curd ripening.
- The mold is removed from the brine and, for hard cheeses, left to mature or ripen in temperature and humidity controlled rooms.

The final cheese variety and its flavour will depend on the type of milk used, the manner of producing the curd and the organisms involved in the ripening.

3.2.2 Metabolic Processes of Cheese Flavour

Cheese flavour develops throughout ripening where chemical and/or biochemical reactions proceed simultaneously to bring about the formation of a large number of different molecules. It should be noted here a food's flavour may be defined in the simplest sense by taste and aroma (Reineccius 2006). Among the volatile molecules produced, those which are

odour active and have a high flavour dilution value are known as aroma compounds (Belitz, Grosch & Schieberle 2004).

The aroma compounds of cheese are obtained via degradation of the major constituents of milk, i.e. lactose, protein and fat, and mediated by enzymes from the micro-organisms in the starter and non-starter bacteria of the milk itself, or by an additional culture. The primary degradation pathways are glycolysis, proteolysis, and lipolysis.

3.2.2.1 Glycolysis

The homo-fermentation of milk lactose to lactic acid is known as glycolysis. It is an essential primary reaction in cheese manufacture where lowering of milk pH affects curd formation and inhibits the growth of undesired bacteria. Although most (96 - 98%) milk lactose is drained off with the whey, residual lactose in fresh curd is metabolized to produce some important background flavour compounds during the early stages of ripening (Robinson 2002).

3.2.2.2 Proteolysis

Proteolysis of casein by proteinases and peptidases yield small peptides that are degraded further to yield amino acids. The sources of proteolytic enzymes are from the milk itself, starter and non-starter bacteria, and secondary microorganisms. Small peptides and amino acids contribute directly to flavour, but they are more important as precursors to a multitude of flavour compounds (Sousa et al. 2001). The extent of proteolysis is controlled by cheese pH, moisture, salt/moisture levels, temperature, and the duration of ripening.

3.2.2.3 Lipolysis

Lipolysis occurs as indigenous lipases of milk or microbial lipases and esterases breakdown milk triglycerides (which constitute more than 98% of milk fat) resulting in free

fatty acids (Robinson 2002). It is well established that milk fat is essential for the development of correct flavour in cheese during ripening (Collins et al 2003). Moulds produce the largest amount of lipase such that extensive lipolysis is desirable in overall flavour development of soft cheeses such as Blue cheese and Camembert (Molimard & Spinnler 1996).

3.2.3 Cheese Aroma Compounds

Few cheese aroma compounds are obtained from milk lactose and most are derived from milk casein and fat (Fox & McSweeney 2004). Glycolysis generates organic acids, alcohols, aldehydes, and dicarbonyls. Proteolysis generates peptides and amino acids that are converted to Strecker aldehydes, amines, pyrazines, sulfur-containing compounds and alcohols. Lipolysis produces free fatty acids that are converted to aldehydes, ketones, lactones, and esters.

For this analysis selected aroma compounds are placed in six major groups: aldehydes, esters, ketones, volatile fatty acids, sulfur-containing compounds, pyrazines and alcohols together.

3.2.3.1 Aldehydes

Most aldehydes are formed by Strecker degradation of amino acids, and some straight-chain aldehydes may also result from auto-oxidation of saturated FAs. The Strecker reaction occurs between an α-dicarbonyl compound and an amino acid to yield CO_2, an aldehyde and a ketone. This reaction is simple and can occur without enzymatic catalysis during ripening (Curioni & Bosset 2002). Aldehydes do not accumulate to high concentrations in cheese because they are rapidly transformed to alcohols or to the corresponding acids (McSweeney & Sousa 2000).

Straight-chain aldehydes (*n*-butanal, *n*-pentanal, *n*-hexanal, etc) are important precursors to acids (Barbieri et al. 1994) and characterized by '*green, grass-like*' odour (Collins et al. 2004). Branched-chain aldehydes (2-, 3-methylbutanal and 2-, 3-methylpropanal) are characterized by '*malty, green*' odour that for 3-methylbutanal becomes '*fruity*' at low concentration. Acetaldehyde may be produced by the breakdown of threonine and is characterized by a '*pungent*' odour, also known as an aroma note (Molimard & Spinnler 1996).

Aromatic aldehydes (particularly phenylacetaldehyde) have also been identified as potent odorants in some cheese types. Phenylacetaldehyde is associated with a pleasant '*floral, rose-like*' odour of Camembert cheese (Yvon & Rijnen 2001).

3.2.3.2 Esters

Esters are common to cheese and can be synthesized by two enzymatic mechanisms: esterification and alcoholysis. Esterification of fatty acids and alcohols by LAB esterases is generally regarded as the mechanism of ester formation in which ethanol is the major alcohol. Ester synthesis via alcoholysis is essentially a transferase reaction in which fatty acyl groups from acylglycerols and acyl-coenzyme A derivatives are directly transferred to alcohols, and is the major mechanism of ester biosynthesis by dairy LAB and yeasts.

Ethyl esters of short-chain fatty acids (ethyl butanoate, ethyl pentanoate, ethyl hexanoate, and ethyl octanoate) are characterized by *'fruity'* odour that can be regarded either as a defect or as an attribute depending on the cheese variety.

3.2.3.3 Ketones

2,3 Butanedione (diacetyl) is generated mainly from lactose and citrate metabolism, the amount of which is dependent on LAB activity during fermentation. 2,3 Butanedione has a desirable *'buttery, nut-like'* odour that contributes positively to aroma of many cheese types

(Curioni & Bosset 2002). In fresh cheese curd, 2,3 butanedione is present in high concentrations but as cheese ages most of it undergoes chemical reactions to generate other compounds contributing to the desirable aroma of matured cheese (Qian et al. 2002).

Methyl ketones (MeKs) are formed from saturated fatty acids via β-oxidation or decarboxylation of β-keto acids (Collins et al. 2003, Kinsella and Hwang 1976). The rate of generation is affected by temperature, pH, the physiological state of mould in mould-ripened cheese, and the concentration of fatty acids. As a cheese ages the concentration of MeKs increases (Thierry et al. 1999) but may also be reduced to secondary alcohols.

2-Heptanone has a strong '*Blue cheese'* odour and for higher molecular weight MeKs a '*floral'* odour predominates. 2-Octanone, 2-nonanone, 2-decanone, 2-undecanone are described as having '*fruity*', '*floral*' and '*musty*' odours. MeKs are responsible for the unique flavour of Blue cheese especially 2-heptanone and 2-nonanone (Jolly & Kosikowski 1975, Dartley & Kinsella 1971).

3.2.3.4 Volatile Fatty Acids (VFAs)

VFAs are mostly formed throughout cheese ripening by enzymatic hydrolysis of triglycerides or by the breakdown of amino acids. Short- to medium-chain VFAs (C4:0–C12:0) have low perception thresholds and among mixtures of VFAs additive effects are recognised (Collins et al. 2003). VFAs also serve as precursors to MeKs, alcohols, lactones and esters.

Straight-chain VFAs have distinctive odours: ethanoic (acetic) acid '*sour*', butanoic acid '*rancid*', hexanoic acid '*pungent*', octanoic acid '*musty*'. Ethanoic acid originates mostly from the early degradation of lactose by homo-fermentative LAB (Moio & Addeo 1998). Long-chain FAs (>12 carbon atoms) are considered to play a minor role in cheese flavour due to their high perception thresholds (Molimard & Spinnler, 1996).

VFAs are desirable to the overall flavour development in certain cheeses, such as hard Italian cheese and Blue cheese. In most cheese varieties, however, even moderate levels of VFAs are considered rancid and undesirable. Cheese pH influences the flavour impact of VFAs, for example at pH ~5.2 a considerable portion of VFAs are present as salts which are non-volatile (Singh et al. 2003, McSweeney & Sousa 2000).

3.2.3.5 Sulfur Containing Compounds

Sulfur compounds (SCs) originate most commonly via degradation of the sulfur amino acid methionine ($C_5H_{11}NO_2S$) by bacteria and yeasts. SCs are essential to the '*strong garlic, sulfury*' aroma of cheese, and participate in the uniqueness and quality of a cheese depending on their identity and concentration (Kubickova & Grosch 1998).

Methional is the principal product of Strecker degradation of methionine (Engels et al. 2000, Yvon & Rijnen 2001) and contributes positively to cheese in low concentrations (Curioni & Bosset 2002). Methional may be reduced to methionol (CH_3-S-$(CH2)_3$-OH), or it may degrade to methanethiol.

Methanethiol (CH_3SH) is a first step degradation product of methionine that is readily oxidized to form dimethyldisulfide (DMDS) (CH_3-S-S-CH_3), and dimethyltrisulfide (DMTS) (CH_3-S-S-S-CH_3). The occurrence of these compounds is modulated by the concentration of methanethiol and the reductive potential of the cheese (Landaud et al. 2008). Dimethylsulfide (DMS) (CH_3-S-CH_3) is a metabolite of propionic acid bacteria acting on methionine. McSweeney & Sousa 2000 suggested it could also be produced directly from methanethiol. Hydrogen sulfide (H_2S) is the primary degradation product of cystein and readily oxidizes to form thioesters (Belitz & Grosch & Schieberle 2004).

3.2.3.6 Alkyl-pyrazines and Alcohols

On heating of milk, alkyl-pyrazines may form via the Maillard reaction (Griffith & Hammond 1989), but in cheese they are mainly produced via the condensation of nitrogen-containing amino acids during ageing (Reineccius 2006). Alkylpyrazines (see Figure 3.1) are potent odourants due to their very low odour threshold values and characterized by '*savoury*', '*roasted*', and '*nut-like*' odours (Belitz, Grosch & Schieberle 2004). In cheese they are typically trace flavor components, with low volatility, and it is difficult to gauge their relative importance to other aroma compounds.

Alcohols can form in cheese via enzymatic reduction of MeKs or Strecker aldehydes that form in the degradation of milk fat and milk protein respectively (Engels et al. 1997). Secondary alcohols resulting from lipolysis, typically make a minor contribution to aroma unless present in relatively high concentration (ppm), or if they are unsaturated. Of the secondary alcohols, 2-heptanol, which is characterized by '*floral*' odour, has been identified as a key odorant of various cheeses (Curioni & Bosset 2002, Engels et al. 1997).

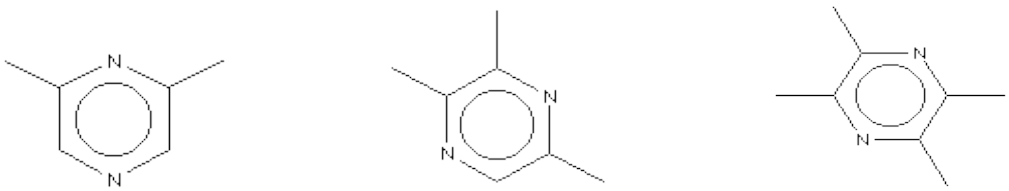

2,6-Dimethylpyrazine Trimethylpyrazine Tetramethylpyrazine

Figure 16: Nitrogen-containing heterocyclic compounds.

3.3 SIFT-MS analysis of cheese

3.3.1 Experimental Method and Analysis

Ten cheeses from a local supermarket were analyzed: 4 brands of New Zealand (NZ) Parmesan, 2 brands of Italian (IT) Parmesan i.e. Grana Padano (GP) and Parmigiano

Reggiano (PR), a single brand of NZ mild, tasty and vintage Cheddar, and a Danish Blue cheese. The cheeses were purchased as: 200g blocks of NZ Parmesan, and 195g wedges of IT Parmesan. The cheeses were all stored in their original packaging and refrigerated at ~4°C throughout analysis.

3.3.1.1 Experimental Method

The preparation and analysis of samples here is the same for all cheeses: Three replicate 5g samples of grated cheese where placed in clean 1L Schott glass bottles and sealed with a rubber septum. Cheese was either crumbled or grated on the broad edge of blocks and long edge of wedges. To encourage a good presence of volatiles in the headspace, every bottle was positioned on its side with the crumb or grate covering the bottom. All cheese samples (including three blank bottles) were incubated at 37°C (Sanyo MIR 262 incubator) for at least half an hour then removed moments before SIFT-MS headspace analysis.

3.3.1.2 Experimental Analysis

A Syft Technologies Ltd VOICE200® was used to perform a SIFT-MS selected ion mode (SIM) scan of all blank samples and cheese headspace samples. Odour active compounds were selected for analysis based on literature for Cheddar, Blue, and Parmesan cheeses. A hot passivated needle attached to the instrument inlet was used to pierce the rubber septum of the Schott bottle and withdraw a headspace sample for testing (see Figure 17).

At the onset of analysis three blank replicates were measured followed by the headspace of each of the cheese samples. An additional SIM scan of background air was performed between cheese varieties to minimize any carryover of concentration. A SIM scan took 2 minutes to complete, and following that a 1½ minute full mass scan (MS) 15 – 250 *m/z* was

run for each bottle. The concentration of analyte compounds in the sample headspace was calculated as the average of three scans minus the average of three blank scans.

Figure 17: Experimental analysis of cheese headspace by a VOICE200® instrument.

3.3.2 Cheddar Cheese

In NZ, mild, sharp/tasty, and extra sharp/vintage corresponding to 6, 12 and 18+ months of ripening, respectively, are the common varieties of Cheddar cheese. A SIFT-MS examination was carried out to see whether a difference in concentration of selected aroma compounds in the cheese headspace could be related to flavour differences between mild, tasty, and vintage Cheddars from a NZ manufacturer.

3.3.2.1 SIFT-MS Results and Discussion – Cheddar cheese aroma

Of the compounds measured (see Figure 18) some appeared to be more important to the aroma of tasty/vintage Cheddar: acetic acid, butanoic acid, 2-heptanone, 1-octen-3-one, methanethiol, DMTS, ethyl butanoate and ethyl hexanoate (Frank et al. 2006, Curioni &

Bosset 2002). Other compounds also important to the aroma of vintage Cheddar are: DMS, DMDS, and methional. The typical odours associated with these compounds suggest an increase in *'rancid' 'sulfury/eggy'* and *'fruity'* aroma as Cheddar matures (Muir et al. 1996). In particular vintage Cheddar is characterized by a strong SC contribution to its aroma.

An investigation of methylpyrazines was also made and in agreement with other studies, relatively low amounts were measured in the cheese samples (Frank et al. 2004, 2006). Avsar et al 2004 suggests their contribution to Cheddar aroma is greater when other compounds with stronger odour contributions do not predominate. This would suggest mild Cheddar aroma is characterized by a '*roasted*' and '*nut-like*' odour contribution that lessens as Cheddar ages.

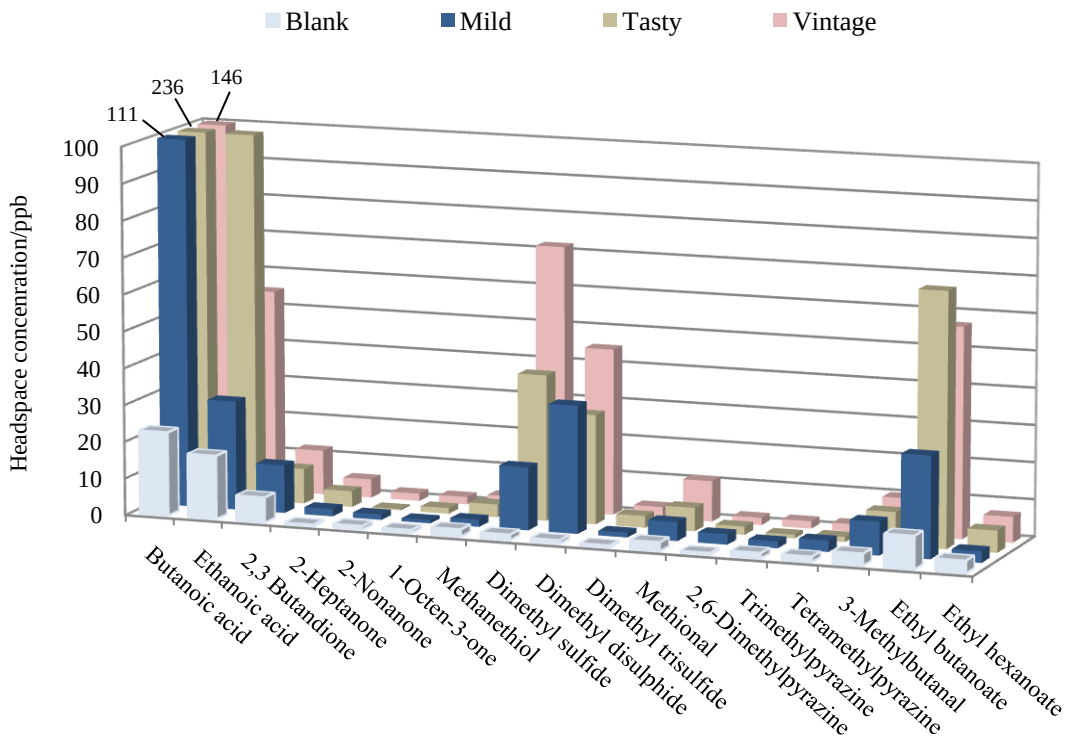

Figure 18: SIFT-MS analysis of selected aroma compounds in NZ Cheddar cheese headspace.

3.3.3 Blue Cheese

In the manufacture of cheese certain processes are performed to produce compounds peculiar to the cheese flavour. For example Blue cheese is mould ripened, whereby the curd is inoculated by *Penicillum roqueforti* and a smelly blue-green or blue-gray mould distinctive to the cheese forms throughout ripening. *P. roqueforti* possesses considerable lipolytic activity producing many VFAs that are degraded to form high concentrations of MeKs (Robinson 2002, Collins et al 2003). Compounds from this group and ethyl esters are characteristic of this cheese (Qian et al. 2002a, Molimard & Spinnler 1996).

2-Heptanone and 2-nonanone are recognised as the two most important compounds contributing to Blue cheese aroma (Frank et al 2004, Qian et al 2002a, Curioni & Bosset 2002). By comparison even-numbered chains 2-pentanone, 2-hexanone and 2-undecanone make a relatively smaller contribution to the aroma (Qian et al. 2002a., Collins et al. 2003, Molimard & Spinnler 1996).

3.3.3.1 SIFT-MS Results and Discussion – Blue cheese aroma

A SIFT-MS examination was carried out to see whether typical Blue cheese character is evident by comparing the concentrations of selected MeK compounds with vintage Cheddar cheese. In Cheddar cheese MeKs are thought to play a limited role in flavour but elevated levels are expected with cheese maturation time (see §3.3.2.1).

Comparatively elevated amounts of 2-heptanone, 2-nonanone, 2-hexanone and 2-undecanone was measured in Blue cheese headspace as expected (see Figure 19). A high amount of 2-butanone was also measured in Blue cheese headspace but this compound is not considered important to Blue cheese flavour (Fox & McSweeney 2004, McSweeney & Sousa 2000). 1-Octen-3-one has previously been associated with the important '*musty*' odor of Cheddar and Camembert cheeses (Curioni & Bosset 2002, Molimard & Spinnler 1996) and from the analysis it is apparent more of this compound is in Cheddar headspace.

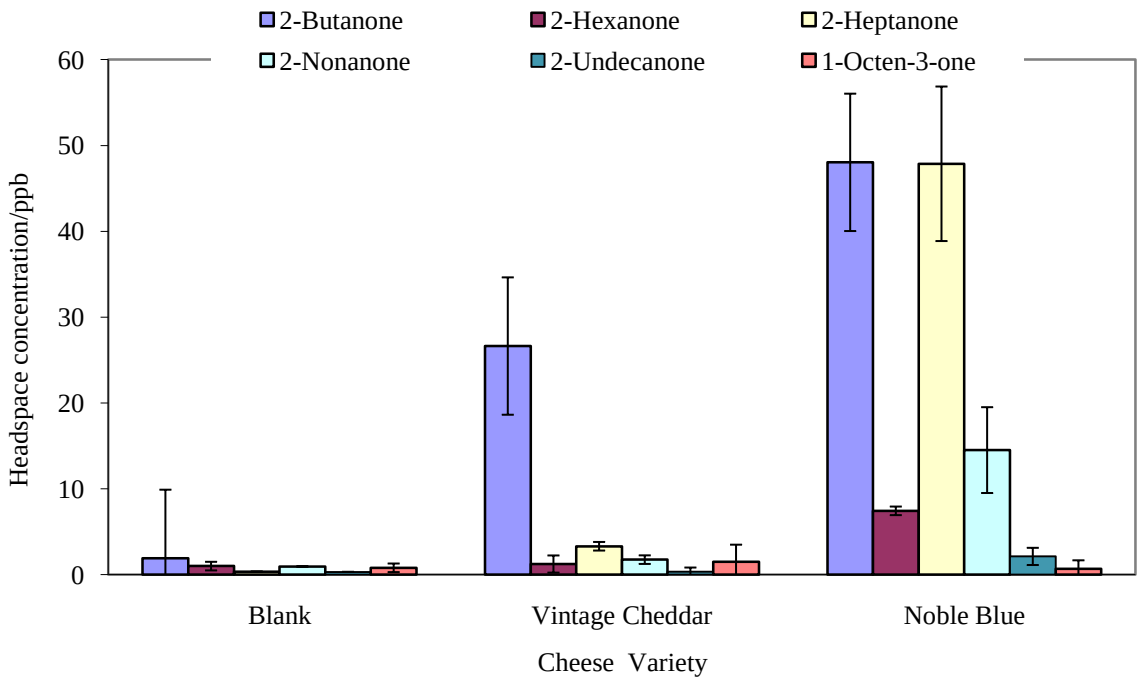

Figure 19: SIFT-MS analysis of selected methyl ketones in NZ Vintage Cheddar and Danish Blue Noble cheese headspace (The error bars are 1 standard deviation (SD) of the average concentration).

3.3.4 Parmesan Cheese

Parmesan flavour peculiar to different regions of Italy are recognised. The best of IT Parmesan is Parmigiano-Reggiano (PR) produced in the southern lowlands of the Po valley and the northern Appennines of Italy (Bellisia et al. 2003). Grana Padano (GP) is also well known among IT Parmesan that is produced in a different region of northern Italy. Both cheeses are made from raw bovine milk and manufactured according to PDO regulation allowing a high level of uniformity in the quality of cheese (Careri et al. 1996) but GP is matured for 12 months rather than 24 months for PR.

3.3.4.1 SIFT-MS Results and Discussion – Parmesan cheese aroma

3.3.4.1.1 Volatile fatty acid (VFA) profile

VFAs (C4:0 – C12:0) are significant contributors to the aroma of hard IT cheese. Qian & Reineccius 2002 attributed the *'cheesy, lipolysed'* character of Parmesan aroma to butanoic, ethanoic, hexanoic, octanoic and decanoic acids. The following discussion relates to Table 6 and Figure 20.

Butanoic, Hexanoic and Ethanoic acids

Of the VFAs measured, butanoic acid and ethanoic were present in high concentration contributing to the characteristic flavour of Parmesan.

For IT Parmesan, butanoic acid and hexanoic acid concentration for PR is twice that for GP contributing more to flavour. The selective release of predominantly C4:0 then C6:0 by enzymes (endogenous or starter bacteria) during lipolysis has been reviewed (Collins et al. 2003). In addition to enzyme activity, cow breed and nutrition and/or seasonal and regional variation has a direct influence to butanoic acid concentration in milk (Barbieri et al. 1994).

For NZ Parmesan, butanoic acid concentration for NZ-1 and NZ-2 headspace is twice that for NZ-3 and NZ-4, while hexanoic acid concentration varied. The activity of endogenous milk enzymes in these cheeses is reduced because of inactivation by milk pasteurization (Collins et al. 2003). Therefore rennet paste, starter and non-starter bacteria have the greater influence on the concentration of these compounds for NZ Parmesan and provide a likely explanation for their variation in concentration.

Ethanoic acid concentration is twice as high in IT Parmesan headspace compared to the NZ Parmesan. This difference may be explained by microorganisms, in particular the starter bacteria strain and manufacturing processes which affect the rate of ethanoic acid generation by lactose metabolism (Collins et al. 2003, McSweeney & Sousa 2000, Grappin et al. 1999, De Felice et al. 2001, Moio & Addeo 1998).

	PR		GP		NZ-1		NZ-2		NZ-3		NZ-4	
Butanoic acid	9320	*(235)*	3278	*(1264)*	9611	*(1208)*	11671	*(1694)*	4930	*(619)*	5471	*(1468)*
Ethanoic acid	3935	*(512)*	4032	*(172)*	1664	*(532)*	2307	*(104)*	1727	*(534)*	1733	*(835)*
Hexanoic acid	260	*(43)*	120	*(42)*	71	*(30)*	370	*(50)*	150	*(30)*	54	*(18)*
Octanoic acid	82	*(9)*	48	*(20)*	51	*(2)*	65	*(18)*	63	*(4)*	48	*(4)*
Decanoic acid	17	*(2)*	9	*(4)*	12	*(1)*	15	*(1)*	14	*(2)*	9	*(2)*

Table 6: Average concentration (ppb) of selected VFAs measured in IT and NZ Parmesan cheese headspace (The numbers in parenthesis are 1SD of the average concentration).

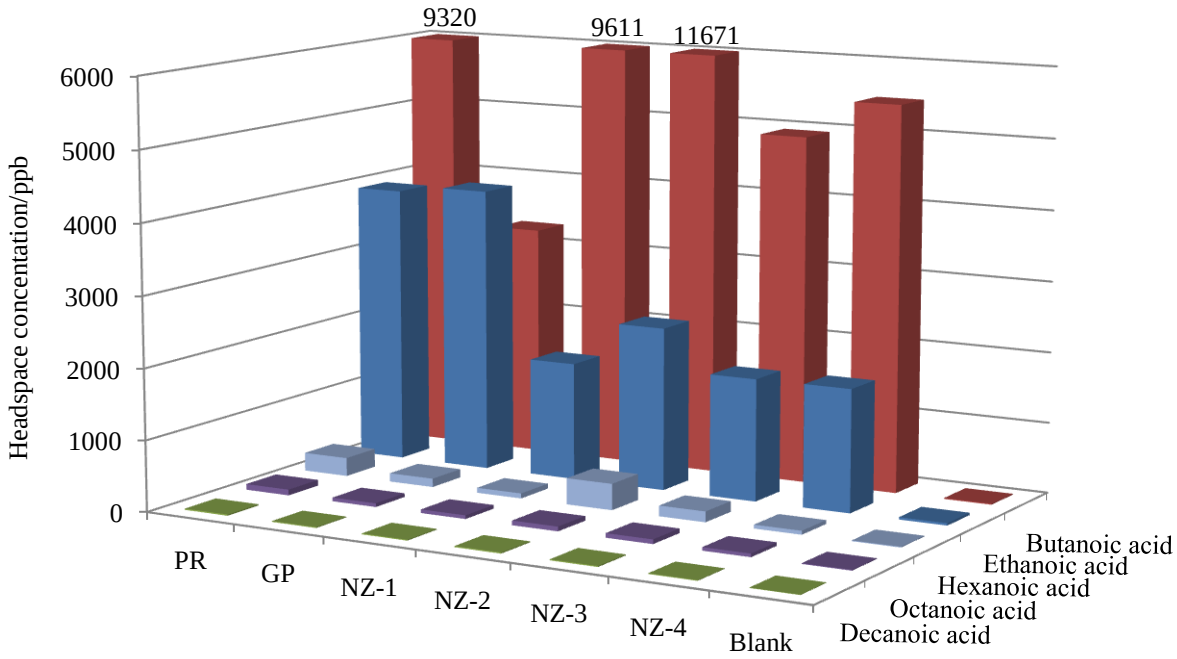

Figure 20: SIFT-MS analysis of selected VFA compounds in IT and NZ Parmesan cheese headspace.

Octanoic and Decanoic acids

Although octanoic and decanoic acids are low in concentration they likely contribute to Parmesan aroma by an additive effect (see §3.2.3.4).

3.3.4.1.2 Sulfur compound (SC) profile

Methional is a potent odourant of IT Parmesan and is thought to provide the '*eggy, cheesy*' aroma note of PR by a flavour interaction with DMTS (Frank et al. 2004, Qian & Reineccius 2003a, 2003b, 2003c). Methanethiol and DMDS are associated with desirable cheese flavour and are thought to contribute the '*cabbage, onion*' aroma of Parmesan (Landaud et al. 2008, Singh et al. 2003, Barbieri et al. 1994). Methionol, DMS, and H_2S are other potentially important sulfur-containing compounds that have been measured in Parmesan headspace (Landaud et al. 2008, Qian & Reineccius 2003a, 2003b, 2003c, Barbieri et al. 1994). The following analysis relates to Table 7 and Figure 21.

	PR		GP		NZ-1		NZ-2		NZ-3		NZ-4	
Methional	152	*(8)*	85	*(16)*	73	*(6)*	81	*(4)*	87	*(6)*	83	*(12)*
Methionol	233	*(25)*	53	*(11)*	22	*(6)*	74	*(4)*	34	*(7)*	36	*(7)*
Dimethyldisulfide	196	*(18)*	72	*(20)*	16	*(5)*	85	*(10)*	28	*(2)*	11	*(2)*
Dimethylsulfide	122	*(3)*	46	*(7)*	42	*(3)*	91	*(2)*	31	*(11)*	22	*(1)*
Dimethyltrisulfide	15	*(3)*	11	*(1)*	15	*(1)*	16	*(3)*	14	*(2)*	9	*(1)*
Methanethiol	19	*(1)*	10	*(1)*	3	*(1)*	11	*(2)*	6	*(1)*	3	*(0)*
Hydrogen Sulfide	8	*(1)*	1	*(0)*	2	*(0)*	2	*(0)*	2	*(0)*	1	*(0)*

Table 7: Average concentration (ppb) of selected SCs measured in IT and NZ Parmesan cheese headspace (The numbers in parenthesis are 1SD of the average concentration).

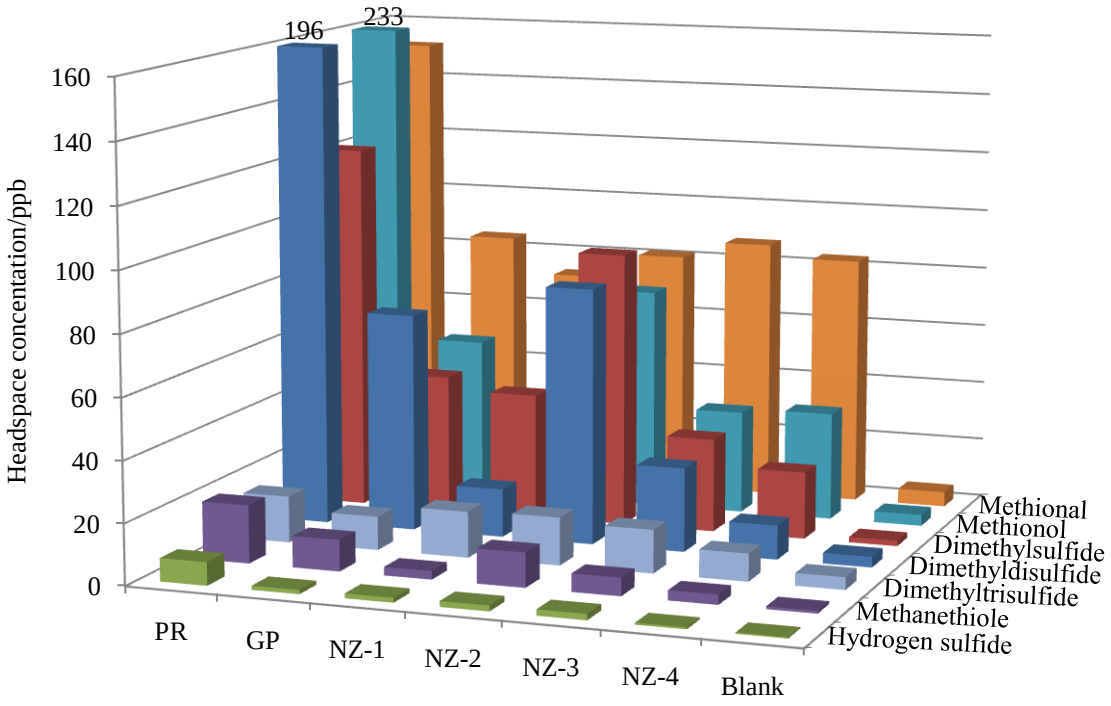

Figure 21: SIFT-MS analysis of selected SCs in IT and NZ Parmesan headspace.

Methional and methionol

Methional concentration is twice as high and methionol concentration is a lot higher for PR contributing more to the flavour than the other cheeses. The extent of methional reduction to methionol is very different among cheeses. This biochemical reaction is dependent on both dehydrogenase activity and the reductive potential of the cheese (Singh et al. 2003, McSweeney & Sousa 2000). It appears the reductive potential of PR favours the formation of methionol.

Methanethiol, DMDS and DMTS

Methanethiol is highly reactive and as expected its concentration is relatively low in all samples. It is apparent methanethiol readily converts to DMDS rather than DMTS (Belitz et al. 2004). The greater amount of DMDS in PR headspace is apparently related to the higher concentration of methanethiol and the reductive potential of the cheese (see §3.2.3.5).

DMS

DMS likely has an important role in the flavour of Parmesan cheese because it has a low odour threshold value and the concentration is relatively high (Belitz et al. 2004). The concentration of DMS varies throughout ripening and a low concentration of DMS has been related to the milk grass season (Dimos et al.1996), providing some reason for differences in concentration among cheeses.

Hydrogen sulphide (H_2S)

H_2S is highly reactive and as expected the concentration is relatively low in all samples (Landaud et al. 2008). H_2S likely has a limited role in the flavour of Parmesan cheese because even though its odour threshold value is low (Belitz et al. 2004) its concentration is very low in comparison with the other SCs.

3.3.4.1.3 Aldehyde profile

Acetaldehyde, 2-methylpropanal, 3-methylbutanal, and phenylacetaldehyde represent important aldehydes found in Parmesan aroma in particular acetaldehyde is thought to provide a '*sharp, pungent*' aroma note (Qian & Reineccius 2003a 2003c, Barbieri et al. 1994). Another report concluded acetaldehyde, 2-methylpropanal, 2-methylbutanal and 3-methylbutanal were most likely responsible for the '*green, malty*' aroma of PR (Qian & Reineccius 2003b). The following analysis relates to Table 8 and Figure 21.

	PR		GP		NZ-1		NZ-2		NZ-3		NZ-4	
Acetaldeyde	2018	*(201)*	1534	*(778)*	2045	*(406)*	11150	*(572)*	3950	*(674)*	1224	*(135)*
3-Methylbutanal	308	*(54)*	357	*(43)*	107	*(1)*	226	*(14)*	670	*(39)*	335	*(81)*
Phenylacetaldehyde	134	*(20)*	43	*(14)*	41	*(7)*	72	*(7)*	68	*(10)*	79	*(11)*

Table 8: Average concentration (ppb) of selected aldehydes measured in IT and NZ Parmesan cheese headspace (The numbers in parenthesis are 1SD of the average concentration). 3-Methylbutanal and 2-methylbutanal are reported together

Acetaldehyde

Acetaldehyde makes a relatively large contribution to Parmesan aroma, where a significant amount was measured for NZ-2 Parmesan that may account for a rancid end note on tasting. With regard to acetaldehyde derived from LAB activity, differences in concentration can result according to season of production (Barbieri et al. 1994).

3-Methylbutanal

The concentration of 3-methylbutanal varied widely among cheeses. The likely reason for differences in amount is proteolytic enzymes provided by rennet paste and secondary microorganisms, and the manufacturing processes which influence their activity (Grappin et al. 1999, Dunn & Lindsay 1985).

Phenylacetaldehyde

Low concentrations of phenylacetaldehyde were measured in Parmesan aroma and the amount varied between cheeses. Higher concentrations of phenylacetaldehyde may be related to elevated amounts of phenylalanine which is dependent on the rate of proteolysis and the rate of protease activity (Dunn & Lindsay, 1985). Proteolysis is strongly influenced by the salt/moisture index of the cheese (Belitz et al. 2004) and determined by manufacturing conditions.

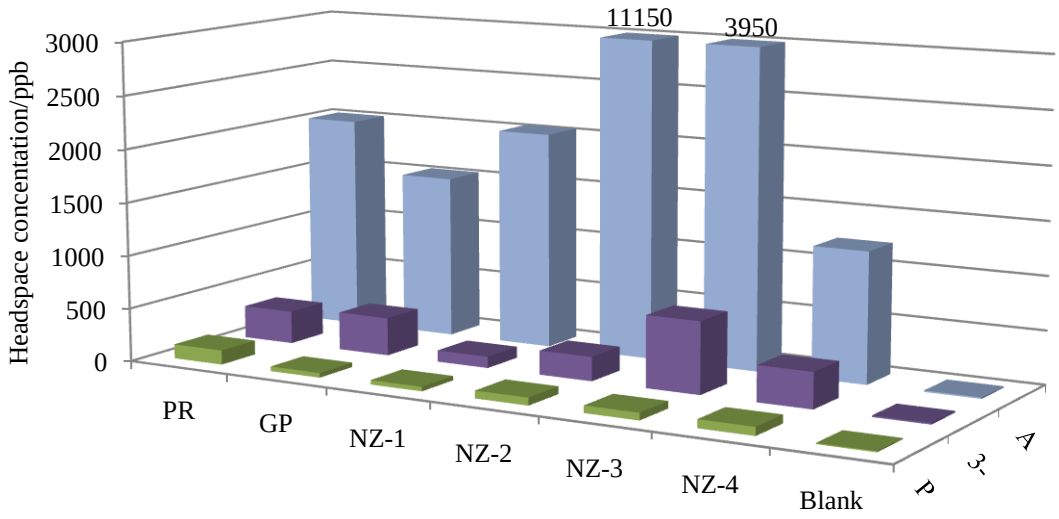

Figure 22: SIFT-MS analysis of selected aldehydes in IT and NZ Parmesan cheese headspace. 3-Methylbutanal and 2-methybutanal are reported together.

3.3.4.1.4 Ester profile

Fruitiness is generally an attribute of IT Parmesan (Liu et al. 2004, Barbieri et al. 1994), where the flavour interaction of ethyl butanoate, ethyl hexanoate and ethyl octanoate is thought to provide the characteristic '*fruity*' aroma note of PR (Qian & Reiniccus 2003a, 2003b, 2003c). Ethyl butanoate and ethyl hexanoate are reported as potent odourants and these compounds also contribute to the '*fruity*' aroma note of GP (Frank et al. 2004, Moio & Addeo 1998). The following analysis relates to Table 9 and Figure 23.

Ethyl butanoate, ethyl hexanoate and ethyl octanoate

Ethyl butanoate dominates the ester contribution to Parmesan aroma, especially in PR and NZ-2 headspace. It is apparent the formation of ethyl butanoate is favoured by esterase and lipase enzymes supplied by starter LAB and rennet paste. The likely reason for differences in amount of this compound is the strain of microorganism, and the manufacturing processes which influence their activity (Liu et al 2003).

Comparing the concentration and odour threshold value of ethyl hexanoate and ethyl octanoate (Belitz et al. 2004), it appears these compounds likely add to the flavour of Parmesan by contributing to ethyl butanoate aroma.

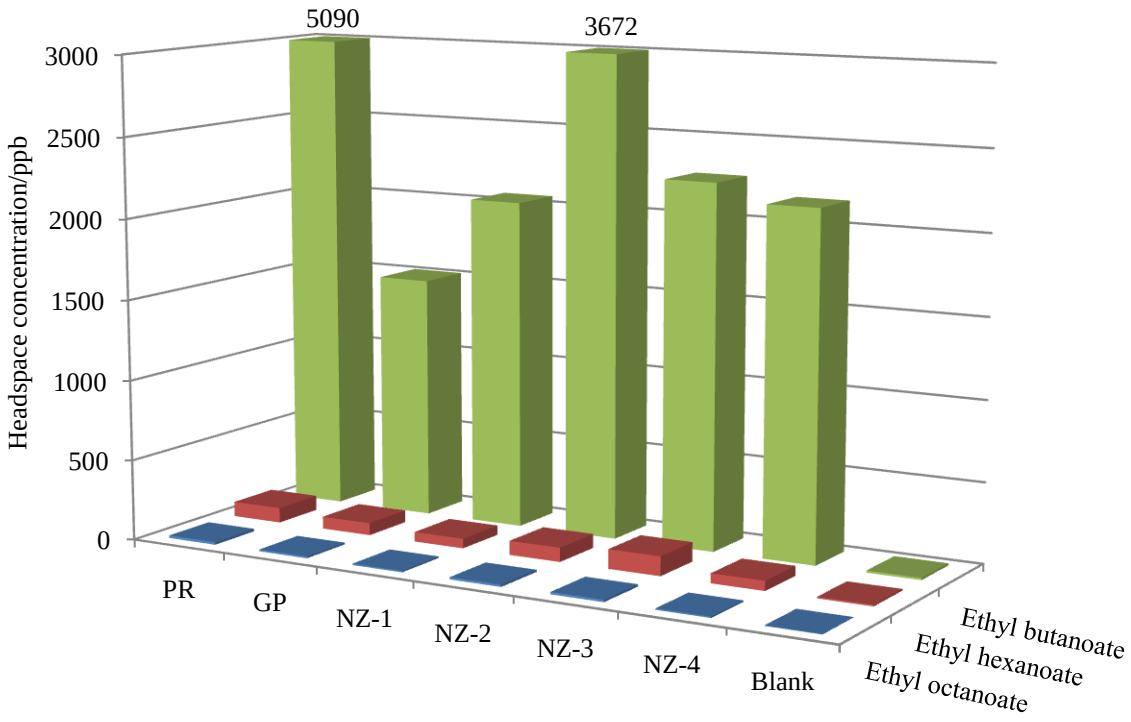

Figure 23: SIFT-MS analysis of selected esters in IT and NZ Parmesan cheese headspace.

	PR		GP		NZ-1		NZ-2		NZ-3		NZ-4	
Ethyl butanoate	5002	*(1276)*	1510	*(172)*	2053	*(178)*	3685	*(744)*	2261	*(302)*	2154	*(640)*
Ethyl hexanoate	93	*(8)*	76	*(39)*	60	*(3)*	88	*(18)*	120	*(15)*	61	*(23)*
Ethyl octanoate	16	*(2)*	11	*(3)*	9	*(1)*	14	*(1)*	14	*(3)*	8	(2)

Table 9: Average concentration (ppb) of selected esters measured in IT and NZ Parmesan cheese headspace (The numbers in parenthesis are 1SD of the average concentration).

3.3.4.1.5 Ketone profile

Ketones represent the second largest class of cheese volatiles in GP and are reportedly similar to the amounts measured in PR aroma (Moio & Addeo 1998, Barbieri et al. 1994). The major representatives of 2-alkanones with odd number carbons are: 2-pentanone, 2-heptanone, 2-nonanone and 2-undecanone. The major representatives with even number carbons are: 2-hexanone, 2-octanone and 2-decanone. However of these compounds, 2-heptanone contributing a '*fruity, blue cheese*' aroma note and 2-nonanone contributing a '*fruity, floral*' aroma note are thought important to the characteristic aroma of Parmesan (Qian et al. 2003a, 2003c). The following analysis relates to Table 10 and Figure 24.

	PR		GP		NZ-1		NZ-2		NZ-3		NZ-4	
2,3 Butanedione	144	*(17)*	136	*(22)*	88	*(6)*	98	*(5)*	201	*(6)*	166	*(24)*
2-Heptanone	240	*(29)*	255	*(204)*	62	*(2)*	84	*(14)*	70	*(9)*	46	*(9)*
2-Nonanone	67	*(15)*	113	*(104)*	14	*(1)*	13	*(2)*	15	*(2)*	11	*(1)*
2-Hexanone	67	*(7)*	42	*(22)*	15	*(2)*	18	*(4)*	23	*(3)*	16	*(3)*

Table 10: Average concentration (ppb) of selected ketones measured in IT and NZ Parmesan cheese headspace (The numbers in parenthesis are 1SD of the average concentration).

2,3 Butanedione (Diacetyl)

There is no significant difference in the amount of 2,3 butanedione measured between IT Parmesan, but the difference is 2-fold between NZ Parmesan. With regard to 2,3 butanedione derived from LAB activity, significant differences in concentrations can result according to different production zones (Barbieri et al. 1994).

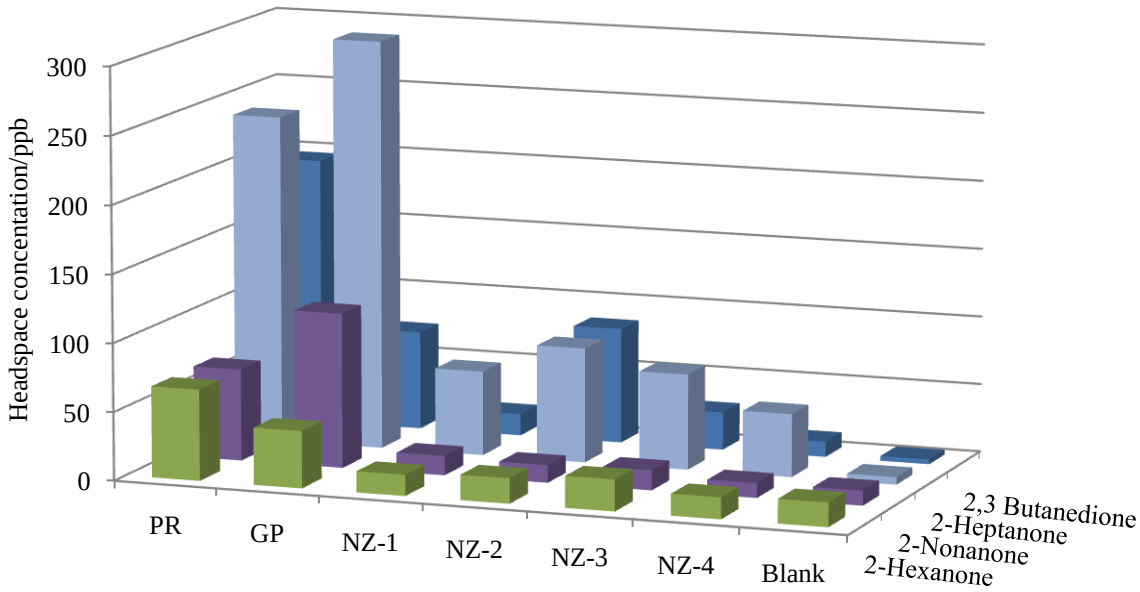

Figure 24: SIFT-MS analysis of selected MKs in IT and NZ Parmesan cheese headspace.

MeKs

NZ Parmesan lacks the MeK content that is apparent in IT cheese samples, and the result of milk pasteurization. Clearly endogenous lipoprotein lipase of raw milk accounts for the difference in MeK concentration between IT and NZ Parmesan (Collins et al. 2003).

3.3.4.1.6 Alkylpyrazine and Alcohol profile

Dimethylpyrazine and trimethylpyrazine are thought responsible for the '*baked-nutty*' aroma note of PR and GP (Qian & Reineccius 2003c, Moio & Addeo 1998, Barbieri et al. 1994). Qian & Reineccius 2003b also suggested dimethylpyrazine is a potent odourant of PR. Frank et al. 2004 repoted tri- and tetramethylpyrazine present in hard cheese samples, and strong '*savoury*', '*musty potato*' like aroma notes, respectively. The following analysis relates to Table 11.

3-Methylbutanol and 2-heptanol, among other alcohols represent a large class of volatile compounds in the headspace of GP (Moio & Addeo 1998, Barbieri et al. 1994). The studies

of Qian & Reineccius 2003a, Qian & Reineccius 2003c concluded most alcohols were not important to PR, although 2-heptanol might contribute a '*fruity*' note and 3-methylbutanol a '*green*' note. The following analysis relates to Table 11.

	PR		GP		NZ-1		NZ-2		NZ-3		NZ-4	
Tetramethylpyrazine	181	(15)	41	(10)	16	(1)	73	(11)	46	(7)	20	(3)
Dimethylpyrazine	132	(8)	60	(10)	50	(2)	80	(10)	46	(8)	31	(5)
Trimethylpyrazine	38	(7)	17	(4)	13	(2)	30	(8)	19	(4)	17	(2)
3-Methylbutanol	1689	(135)	436	(291)	191	(7)	166	(17)	235	(5)	250	(42)
2-Heptanol	195	(14)	96	(73)	18	(0)	54	(8)	40	(5)	24	(4)

Table 11: Average concentration (ppb) of selected alkylpyrazines and alcohols measured in IT and NZ Parmesan cheese headspace (The numbers in parenthesis are 1SD of the average concentration).

Alkylpyrazines

Clearly alkylpyrazines, tetramethylpyrazine and dimethylpyrazine are characteristic of PR aroma. Acetoin is the most likely precursor of tetramethylpyrazine and the amount of acetoin produced in cheese is affected by the cheese starter culture. In addition manufacturing conditions such as pH and temperature throughout ripening may affect which pyrazines are formed and therefore the extent to which they are produced (Rizzi 1988).

Alcohols

Alcohol compound concentration increases throughout ripening (12 and 24+ months) and may explain the higher alcohol concentration in PR headspace compared to the other cheeses (Thierry et al. 1999). In addition strong reducing conditions favour the formation of alcohols (Engels et al. 1997). Clearly the reductive potential of PR is favourable for the reduction of 3-methylbutanal to 3-methylbutanol (see §3.2.4.3). The enzymatic reduction of

2-heptanone to 2-heptanol also appears important to PR aroma (Molimard & Spinnler 1996), and to a lesser extent GP.

3.4 Conclusion

NZ is a leader in the global dairy industry. Cheese manufacture within this country caters more for the domestic market producing high volumes of Cheddar. NZ also produces a wide variety of specialty cheeses, including Parmesans. However NZ Parmesans often do not provide a good representation of the aroma of the genuine Italian parmesans, such as PR and GP.

Conventional aroma analysis techniques such as gas chromatography mass spectrometry – olfactometry and aroma extraction dilution analysis have identified and quantified many of the important odourants in cheese. However these techniques have a number of drawbacks, i.e. the analysis can be calibration dependent, time consuming and labour intensive. For food flavour research and development the rapid analysis of headspace aroma as it evolves is desirable, e.g. characterizing the typical aroma of good cheese flavour. Here the SIFT-MS technique was successfully applied to measure relative concentration of aroma compounds in a finite sample of cheese headspace in real time.

Observable differences in VFAs, SCs, and ester concentration were noted applying the SIFT-MS technique to aroma analysis of Cheddar cheese varieties. These differences can be related to the ageing of the cheese (Frank et al. 2006), where elevated amounts of SCs are characteristic of vintage Cheddar.

The concentrations of selected MeKs were compared for Blue cheese and vintage Cheddar cheese. Elevated concentrations of 2-heptanone and 2-nonanone were measured in Blue cheese headspace. This is an expected result for Blue cheese because of the particular manner in which the cheese is produced.

An examination of key aroma compounds in the headspace of Parmesan cheeses revealed the raw milk of the IT varieties and the pasteurized milk of the NZ varieties as a significant reason for the differences between them (Robinson 2002). In addition to this observation other reasons given for differences are starter culture, manufacturing processes, and regional conditions that influence the quality of milk.

3.5 References

Avsar, Y. K.; Karagul-Yuceer, Y.; Drake, M. A.; Singh, T. K.; Yoon, Y.; Cadwalladar, K. R. Characterization of Nutty Flavor in Cheddar Cheese. *J. Dairy Sci.*, **2004**, 87, 1999-2010.

Barbieri, G.; Bolzoni, L.; Careri, M.; Mangia, A.; Parolari, G.; Spagnoli, S.; Virgili, R. Study of the Volatile Fraction of Parmesan Cheese. *J. Agric. Food Chem.*, **1994**, 42, 1170-1176.

Bellisia, F.; Pinetti, A.; Pagnoni, U. M.; Rinaldi, R. Volatile components of Grana Parmigiano-Reggiano type hard cheese. **2003**, *Food Chemistry*, 83, 55-61.

Belitz, H. –D.; Grosch, W.; Schieberle, P. *Food Chemistry (3rd Revised Edition)*, Translation by Burghagen, B. B., Springer-Verlag Berlin Heidelberg, **2004**.

Careri, M.; Spagnoli, S.; Panari, G.; Zonnoni, M.; Barbieri, G. Chemical Parameters of the Non-volatile Fraction of Ripened Parmigiano-Reggiano Cheese. *Int. Dairy J.*, **1996**, 6, 147-155.

Collins, Y. F.; McSweeney, P. L. H.; Wilkinson, M. G. Lipolysis and free fatty acid catabolism in cheese: a review of current knowledge. *Int. Dairy J.*, **2003**, 13, 841-866.

Curioni, P. M. G.; Bosset, J. O. Key odorants in various cheese types determined by gas chromatography-olfactometry. *Int. Dairy J.*, **2002**, 12, 959-984.

Dartley, C. K.; Kinsella, J. E. Rate of Formation of Methyl Ketones during Blue Cheese Ripening. *J. Agr. Food. Chem.*, **1971**, 19, 4:771-774.

Dimos, A.; Urbach, G. E.;Mille, A. J. Changes in Flavour and Volatiles of Full-fat and Reduced fat Cheddar Cheeses During Maturation. *Int. Dairy Journal*., **1996**, 6, 981-995.

Dunn, H. C.; Lindsay, R. C.; Evaluation of the Role of Microbial Strecker-Derive Aroma Compounds in Unclean-type Flavors of Cheddar Cheese. *J. Dairy Sci.*, **1985**, 68, 2859-2874.

Engels, W. J. M.; Alting, A. C.; Arntz, M. M. T. G.; Gruppen, H.; Voragen, A. G. J.; Smit, G.; Visser, S. Partial purification and characterization of two aminotransferases from *Lactococcus lactis* subsp. *cremoris* B78 involved in the catabolism of methionine and branched-chain amino acids. *Int. Dairy J.*, **2000**, 10, 443-452.

Engels, W. J. M.; Dekker R.; de Jong, C.; Neeter, R.; Visser, S. A Comparative Study of Volatile Compounds in the Water-soluble Fraction of Various Types of Ripened Cheese. *Int. Dairy J.*, **1997**, 7, 255-263.

de Felice, M.; Gomes, T.; De Leonardis, T. Addition of animal and microbiallipases to curd. Effects on free fatty acid composition during ripening. **2001**, *Lait*, 71, 637-643.

European Policy for Quality Agricultural Products. http://ec.europa.eu/agriculture/index_en.htm (accessed Dec 16, 2009).

Fox, P. F.; McSweeney, P. L. H. Cheese: An overview. In *Cheese Chemistry, Physics and Microbiology Volume 1 General Aspects (Third Edition)*, P. F. Fox, P. L. H. McSweeney, T. M. Cogan, T. P. Guinee., Elsevier Academic Press, **2004**, 1-19.

Frank, D.; O'Riordan, P.; Zabaras, D.; Varelis, P. Cheddar cheese volatile profiling using dynamic headspace and gas chromatography-mass spectrometry olfactometry. *Aus. J. Dairy Tech.*, **2006**, 61, 2:105-107.

Frank, D. C.; Owen, C. M.; Patterson, J. Solid phase microextraction (SPME) combined with gas-chromatography and olfactometry-mass spectrometry for characterization of cheese aroma compounds. *Lebensm-Wiss. U-Technol.*, **2004**, 37, 139-154.

Grappin, R.; Beuvier, E; Pouton, Y.; Pochet, S. Advances in the microbiology and biochemistry of Swiss-type cheeses. *Lait*, **1999**, 79, 3-22.

Griffith, R.; Hammond, E. G. Generation of Swiss Cheese Flavor Components by the Reaction of Amino Acids with Carbonyl Compounds. *J. Dairy Sci.*, **1989**, 72, 604-613.

Jolly, R. C.; Kosikowski, F. V. Flavor Development in Pasteurized Milk Blue Cheese by Animal and Microbial Lipase Preparations. *J. Dairy Sci.*, **1975**, 58, 6:846-852.

Kinsella, J. E.; Hwang, D. H. Biosynthesis of Flavors by *Penicillium Roqueforti*. *Biotechnol. & Bioeng.*, **1976**, 18, 7:927–938.

Kubícková, J.; Grosch, W. Quantification of Potent Odorants in Camembert Cheese and Calculation of their Odour Activity Values. *Int. Dairy J.*, **1998**, 8, 17-23.

Landaud, S; Helnick, S; Bonnarme, P. Formation of volatile sulphur compounds and metabolism of methionine and other sulphur compounds in fermented food. *Appl. Microbiol. Biotechnol.*, **2008**, 77, 1191-1205.

Liu, S.-Q.; Holland, R.; Crow, V.L. Esters and their biosynthesis in fermented dairy products: a review. *Int. Dairy J.*, **2004**, 14, 923–945.

McSweeney, P. L. H.; Sousa, M. J. Biochemical pathways for the production of flavour compounds in cheeses during ripening: A review. *Lait*, **2000**, 80, 293-324.

Moio, L.; Addeo, F. Grana Padano cheese aroma. *J. Dairy Res.*, **1998**, 65, 317-333.

Molimard, P.; Spinnler, H. E. Review: Compounds involved in the flavour of surface mould-ripened cheeses: Origins and properties. *J. of Dairy Sc.*, **1996**, 79, 169–184.

Muir, D. D.; Hunter, E. A.; Banks, J. M.; Horne, D. S. Sensory properties of Cheddar cheese: changes during maturation. *Food Research Int.*, **1996**, 28, 6:561-568.

Qian, M.; Nelson, C.; Bloomer S. Evaluation of Fat-Derived Aroma Compounds in Blue Cheese by Dynamic Headspace GC/Olfactometry–MS. *JOACS,* **2002a**, 79, 7:663-667.

Qian, M.; Reineccius, G. A. Identification of Aroma Compounds in Parmigiano-Reggiano Cheese by Gas Chromotography/Olfactometry. **2002**. *J. Dairy Science*. 85, 1362-1369.

Qian, M.; Reineccius, G. A. Quantification of Aroma Compounds in Parmigiano-Reggiano Cheese by a Dynamic Headspace Gas Chromatography-Mass Spectrometry Technique and Calculation of Odor Activity Value. *J. Dairy. Sci.*, **2003a**, 86, 770-776.

Qian, M.; Reineccius, G. A. Potent aroma compounds in Parmigiano Reggiano cheese studied using a dynamic headspace (purge-trap) method. *Flavour Fragr. J.*, **2003b**, 18, 252-259.

Qian, M.; Reineccius, G. A. Static Headspace and Aroa Extract Dilution Analysis of Parmigiano Reggiano Cheese. *J.Food. Sci.*, **2003c**, 68, 3:794-798.

Reineccius, G. *Flavour Chemistry and Technology (Second Edition)*, Taylor & Francis Group, **2006**.

Rizzi, G. P. Formation of Pyrazines from Acyloin Precursors in Mild Conditions. *J. Agric. Food Chem.*, **1988**, 36, 2:349-352.

Robinson, K. *Dairy Microbiology Handbook (Third Edition)*, Wylie Interscience, **2002**.

Singh, T.K.; Drake, M.A.; Cadwallader, K.R. Flavor of Cheddar Cheese: A Chemical and Sensory Perspective. *Comp. Rev. Food Sci. Food Safety*, **2003**, 2, 139-162.

Sousa, M. J.; Ardo, Y.; McSweeney, P. L. H. Advances in the study of proteolysis during cheese ripening. *Int. Dairy J.*, **2001**, 11, 327-345.

Thierry, A.; Maillard, M. -B.; Le Quéré, J. -L. Dynamic headspace analysis of Emmental aqueous phase as a method to quantify changes in volatile flavour compounds during ripening. *Int. Dairy J.*, **1999**, 9, 453-463.

Yvon, M.; Rijnen, L. Cheese flavour formation by amino acid catabolism. *Int. Dairy J.*, **2001**, 11, 185-201.

Zehentbauer, Z.; G.A. Reineccius, G. A. Determination of key aroma components of Cheddar cheese using dynamic headspace dilution assay. *Flavour Fragr. J.* **2002**, 17, 300-305.

CHAPTER FOUR

SIFT-MS Analysis of Chocolate

4.1 Introduction

Chocolate is a desirable food but until the 19th Century it was a luxury item that was widely inaccessible. However in 1828, C. van Houten a Dutch chocolate maker established an inexpensive method of pulverizing and de-fatting roasted cocoa beans from which the unique flavour of chocolate is derived. Some 50 years later further developments to chocolate making occurred greatly affected the acceptability of chocolate as we know it today. First in 1876 Daniel Peter, a Swiss chocolate maker made the world's first milk chocolate by successfully adding condensed milk to cocoa, suppressing the bitter taste of cocoa beans resulting in the chocolate becoming more palatable. Then in 1880 Rodolphe Lindt, another Swiss chocolate maker, developed the process of conching and created a smoother, less bitter, and easier to mould chocolate (Beckett 2000).

The distinguishing characteristics of quality chocolate with good flavour intensity and texture have been attributed to the quality of raw ingredients and the care taken during chocolate manufacture (Jackson 1999). However producers of quality chocolate protect their products individual characteristics and value by guarding exact recipes and the manufacturing methods they employ. This makes the task of defining chocolate flavour difficult. The aroma component of food is important to our perception of flavour and comparatively easy to analyse. More than 500 volatile compounds in the headspace of chocolate have already been identified by flavour chemists (Afoakwa et al. 2008).

The SIFT-MS technique is applied here for the first time to flavour analysis of milk chocolate (MC) and dark chocolate (DC) of European and New Zealand origin. The analysis involves measurement of selected aroma compounds that have been identified as characteristic of chocolate flavour (see §4.3.4). Apparent differences in the relative concentration of these compounds and their probable relationship to chocolate ingredients and the manufacturing process will also be examined. In addition, the analyses will be used to develop a general aroma character for MC and DC.

4.2 Manufacture of Chocolate

A pleasant eating MC is formulated by combining cocoa liquor, sugar, cocoa butter, milk solids or milk powder, emulsifiers and flavour compounds. DC contains a higher percentage of cocoa solids than MC, and as it is generally made without a milk ingredient the flavour is much stronger (Schnermann & Schieberle 1997, Haylock & Dodds 1999). To obtain cocoa liquor the roasted cacao nib (roasted coco beans separated from their husks) is crushed and some of the cocoa butter removed. Further disintegration of cocoa particles results in a homogenous mobile paste, called cocoa liquor (see §4.2.1).

To produce a flavoursome, structurally homogenous and stable chocolate product that melts in the mouth, a traditional set of processing steps is followed (Reineccius 2006, Belitz et al. 2004).

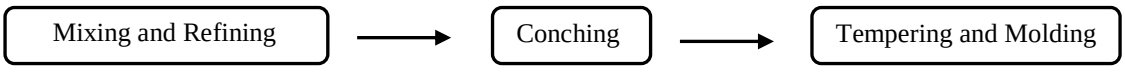

Figure 25: Primary processing steps of chocolate production. See the sections 4.2.1, 4.2.2 and 4.2.3 for an explanation of these processing steps.

4.2.1 Mixing and Refining

Cleaned roasted cocao nibs are first crushed to a homogenous, coarse chocolate paste. Fine-grinding or refining of the chocolate paste, either continuously or with batch mixers, disintegrates particle sizes to < 30 µm. This process is carried out in a mill fitted with multiple, water-cooled rollers normally using a combination of two- and five-roll refiners (Figure 26).

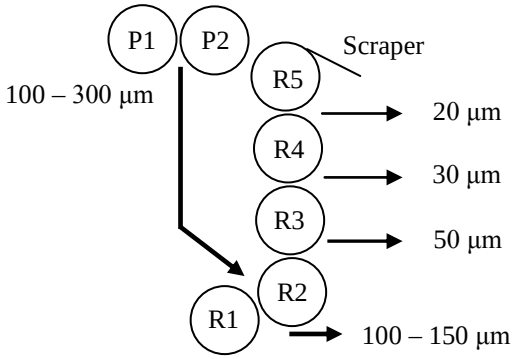

Figure 26: Schematic diagram of a five-roll refiner (P1 and P2 show the previous two-roll refiner).

The purpose of particle size (PS) reduction is to reduce the coarseness of chocolate in the mouth and to lower chocolate viscosity. Eating chocolates have a PS generally less than 30 µm and give a longer residence time in the mouth with the result that flavour persists longer than coarse chocolate (Mongia 1997, Afoakwa et al. 2009). Traditional continental European chocolate has been described as having a fineness of 15 – 22 µm (Ziegler & Hogg 1999).

4.2.2 Conching

The smoothness of fine eating chocolate requires the refined cocoa mass to be conched. Conching is a three stage process: dry-phase, pastry-phase, and liquid-phase, during which the chocolate mass is mixed, ground and kneaded in a conche machine from 4 – 24 hrs at temperatures of 49 - 85°C depending on chocolate ingredients (Afoakwa et al. 2007).

Conching is also the last opportunity for the chocolate manufacturer to develop the flavour of the final product. Cocoa mass (the crushed cocoa bean with some of the cocoa butter removed from the mixing and refining step) contains acidic (mainly acetic acid) and bitter residues from cocoa bean fermentation. During conching much of these undesirable flavours are removed and flavour additions are made (Afoakwa et al 2008, Hoskin 1994). The three most common flavour additions to the cocoa mass are vanilla, salt, and nut paste (see §4.3.1.3).

4.2.2.1 Dry-phase conching

A small amount of cocoa butter (~ 1%) is added to the cocoa mass and mixed at 65ºC for MC or 75ºC for DC (Belitz et al. 2004). At this stage a loss, of moisture occurs and the mass becomes crumbly. In addition to moisture loss volatile acids are removed and aeration is very important to enable these to escape (Beckett 1999).

4.2.2.2 Pastry-phase conching

In this second phase of the conching process cocoa butter is added and stirred for homogenisation of the cocoa mass. The purpose of this stage is to smear fat (23 – 28% cocoa butter and milk fat when present) around sugar particles (and non-fat milk solids when present) thus improving rheology. Here chocolate rheology relates to how solid particles (sugar, cocoa, and milk solids if present) respond to shear forces of mixing (Chevally 1999). The mixing time occurs at controlled temperatures, and will depend on the initial cocoa intensity and the desired product taste (Bolenz et al. 2003).

4.2.2.3 Liquid-phase conching

Two to three hours before the end of the conching process lecithin (a surfactant) and flavour additions are made to thin chocolate prior to tempering. High speed stirring mixes

these additions into the chocolate mass. A very precise and controlled amount of lecithin is added as it is very effective in reducing chocolate viscosity (Nebesny & Żyżelewicz 2005).

4.2.3 Tempering and Moulding

Before chocolate can be satisfactorily processed from liquid to solid, it must be tempered. This process is important for the stable form, glossy appearance, and "snap" of chocolate. (Beckett 2000) Carefully timed cooling of the molten chocolate and stirring induces cocoa butter crystallization that has a melting temperature of 34 - 35ºC. Finally the temperature is raised to ~ 30ºC to melt out unstable crystals and the chocolate is poured into moulds. When the air bubbles have been removed, the chocolate is slowly cooled to a solid (Talbot 1999).

4.3 Flavour of Chocolate

In this section the origin of chocolate flavour compounds are discussed. Good cocoa flavour has low intensity bitter and sour qualities derived from reduced polyphenol and acid content during roasting (Camu et al. 2008). Flavour qualities such as '*cocoa/chocolate-like*' and '*sweet honey/caramel-like*' rate highly, whereas a moderate '*roast*' intensity and some '*floral/fruity*', '*smoky*' qualities are recognised (Frauendorfor & Schieberle 2008). In the manufacture of chocolate these various flavour notes can be developed (made more or less intense) such that different chocolate makers produce recognizable chocolate flavour.

It is understood that cocoa and chocolate flavour is strongly influenced by: (i) the cocoa bean (bean species and farming origin), (ii) post-harvest processing (cocoa bean fermentation, drying, and roasting), and (iii) manufacturing processes (conching and flavour additives) (Afoakwa et al. 2008). These major developments in chocolate flavour production are outlined in Figure 27, and discussed in sections 4.3.1, 4.3.2 and 4.3.3.

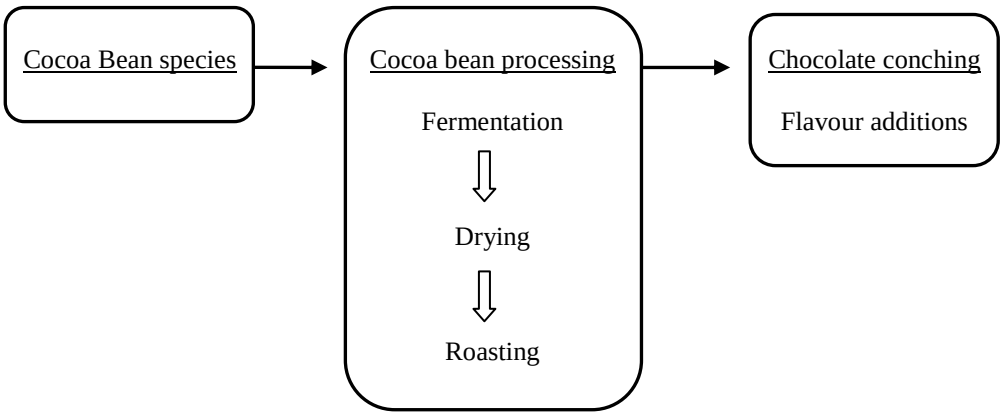

Figure 27: Major developments in the production of chocolate flavour.

4.3.1 Cocoa Bean Species

Cacao beans are harvested from the flower of the *Theobroma cacao* tree that grows within a suitable environment 20º either side of the equator. There are three primary commercial varieties of bean cultivated: (1) Forastero beans are characteristically strong in cocoa flavour but bitter. This bean however accounts for the bulk of world cocoa bean production as the plant species is high-yielding and disease resistant. (2) Criolla beans are flavoursome, highly aromatic and of fine-grade quality but the plant species is low-yielding and prone to disease. (3) Trinitario beans (a hybridization of the Criolla and Forestero species) are of fine-grade quality from a high-yielding hardy plant. (Belitz et al. 2004, Jackson 1999).

The main cocoa bean growing areas are West Africa, South East Asia and South America (World Cocoa Foundation Market Update 2009). Beans from different origins are known to have distinct flavour characteristics such as '*acidic*, *fruity*, or *spicy*' (Afoakwa et al. 2008, Jackson 1999). These differences in flavour are ascribed to bean variety and hence its composition, location of growth, and local farming conditions (Rohsius et al. 2006, Perego et al. 2004, Luna et al. 2002, Reineccius et al. 1972). Chocolate manufacturers select beans

according to the desired product flavour and cost, where typically a blend of fine-grade bean quality is used in lesser quantity with a bulk-grade bean and both are selected to make specific contributions to the overall flavour profile.

4.3.2 Cocoa Bean Processing

4.3.2.1 Fermentation

Fermentation facilitates separation of the bean from the surrounding pulp and shell. Various volatile components are generated (alcohols, esters, and fatty acids) throughout this process and may enter the bean as flavour constituents or act as flavour precursors. Fermentation also reduces the bitterness of the cocoa bean as stringent alkaloids and phenolic compounds diffuse out of the bean and are oxidized to form insoluble compounds (Belitz et al. 2004, Schwan & Wheals 2004).

A most important result of the fermentation process is the development of necessary aromatic precursors. Diffusion of metabolites, mainly ethanol and acetic acid, into the bean causes deactivation of the bean, and the conditions (pH and temperature) are set for complex biochemical reactions to occur. These reactions include acid bacteria hydrolysis of stored proteins, glucose and fructose to generate peptides, amino acids and reducing sugars i.e. flavour precursors. The occurrence and concentration of the many flavour precursors are dependent on enzymatic reactions and yeasts (Schwan & Wheals 2004, Dimick & Hoskin 1999).

4.3.2.2 Drying

Following fermentation, cocoa beans are washed and dried to contain less than 8% moisture content thus reducing mould contamination and subsequent off-flavours (Dimick & Hoskin 1999). Although sun-drying is the traditional method, mechanical drying methods may also be used such as air-blowing or oven-drying. Good drying practices assist the cocoa

beans to develop flavour quality, a good brown colour and lowers astringency and bitterness (Dimick & Hoskin 1999).

Drying assists flavour development as amino acids, reducing sugars and peptides formed during fermentation begin non-enzymatic Maillard reactions - the main process by which flavour precursors are developed into cocoa flavour. In addition oxidation of polyphenols gives rise to new flavour components, and some excess acids (lactic and acetic acids) may volatize out of the bean (Schwan & Wheals 2004).

4.3.2.3 Roasting

Additional bean processing may involve the cleaning and sorting of the beans by size to avoid over- or under-roasting. Generally roasting is a two step process, first the beans are dried to 3% moisture followed by rapid heating to the roast temperature in the range of 120 - 150°C (Heemskerk 1999). Prior to roasting, beans may taste astringent, bitter, and acidy (Sanagi et al. 1997). Roasting contributes to further oxidation of phenolic compounds and the removal of acetic acid, volatile esters and other undesirable aroma components (Belitz et al. 2004, Dimick & Hoskin 1999).

The Maillard or non-enzymatic browning reaction is one of the most important and complex reactions to occur during the roasting process. The main reaction is Strecker degradation of free amino acid and reducing sugar precursors to form aroma compounds (Reineccius 2006, Dimick & Hoskin 1999). A high concentration of these precursors is responsible for the formation of heterocyclic N and O compounds such as pyrazines and furanones, together with aldehydes which are essential to chocolate flavour (Dimick & Hoskin 1999). After roasting, cocoa beans possess the typical intense aroma of cocoa (Frauendorfer & Schieberle 2008, Bonvehí 2005).

4.3.3 Manufacturing Processes

4.3.3.1 Conching and Flavour Additions

An analysis of headspace volatiles suggests chemical changes occur during conching but unfortunately these chemical changes are not well known and there is conflicting opinion on the reactions that occur. Counet et al. (2002) and Schnermann & Schieberle (1997) noted an increase of some aroma compounds at high temperatures applied during conching, although Hoskin & Dimick (1983) suggest conching temperatures are below thermal thresholds for Maillard reactions. Bolenz et al. (2003) concluded in the case of MC, flavour development in the conch is not as important as previously assumed. They argue that raw materials of high quality also play a very important role for milk chocolate flavour.

Evidently essential Strecker degradation aroma compounds present prior to conching may be partially lost through evaporation and/or chemical reactions after conching, thus affecting the intensity of certain flavours (Belitz et al. 2004). Studies that compare the flavour difference of conched and unconched chocolate, describe conched chocolate as “mellow” compared to unconched chocolate (Dimick & Hoskin 1999).

The addition of milk and other additives such as vanillin enhances the desired chocolate flavour (Afoakwa et al. 2007). Artificial vanilla flavour, vanillin, is commonly used to create creamy notes to chocolate flavour. Salt is the second most common addition that accents clean flavour notes to chocolate.

4.3.4 Chocolate Odourants

The volatile matrix of cocoa and chocolate is composed of more than 500 compounds (Reineccius 2006). Flavour analyses have already identified important contributors to chocolate flavour and it is generally accepted that the cocoa fraction obtained from the cocoa mass has a predominant impact on chocolate flavour. Table 12 lists aroma compounds that

have frequently been associated with cocoa, MC, and DC (Afoakwa et al. 2008, Bonvehí 2005, Reineccius 2006, Belitz et al. 2004, Counet et al. 2002, Schieberle & Pfner 1999, Schnermann & Schieberle 1997).

Here, the selection of compounds for analysis was based on flavour dilution and odour activity values provided in the literature and their relative occurrence. The odour activity value is a measure of the importance of a compound to aroma defined by the concentration of the compound divided by the odour threshold value (Belitz et al. 2004). Aroma compounds with very low odour threshold values are deemed odour impact compounds due to their overall sensory value.

Cocoa	Milk Chocolate	Dark Chocolate
2-Phenylethanol	Sotolon	Furaneol
Maltol	Vanilla	2-Methylpropanal
Linalool	2-Methylpropanal	2,3-Methylbutanal
Sotolon	3-Methylbutanal	Phenylacetaldehyde
Furaneol	Phenyacetaldehyde	(E)-2-nonenal
2,3-Methylbutanal	(*E*)-2-nonenal	(E)-2-octenal
Phenylacetaldehyde	(E)-2-octenal	(E)-2-heptenal
(E)-2-nonenal	2-Methyl-3-(methyldithio)furan	Methylpyrazine
(E)-2-octenal	2,3-Butanedione	C4-alkylpyrazines
Hexanal	1-Octen-3-one	2-Isopropyl-3-methoxypyrazine
Ethyl-2-methylbutanoate	2,3-Diethyl-5-methylpyrazine	2,3-Dimethylpyrazine[a]
2-Phenylethyl acetate	C4-alkylpyrazines[a]	Trimethylpyrazine
2-Methyl-3-(methyldithio)furan	2,3-Methylbutanoic	DMDS[b]
2,3-Diethyl-5-methylpyrazine	Dimethyltrisulfide	2-Acetylpyrrole
C4-alkylpyrazines[a]	DMTS[b]	Acetaldehyde
2-Isopropyl-3-methoxypyrazine		
Trimethylpyrazine		
2,3-Methylbutanoic acid		
2-Methylpropionic acid		
Acetic acid		

DMDS/DMTS[b]

[a] C4-alkylpyrazines includes tetramethylpyrazine, 3(or 5)-dimethyl-3(or 2)-ethylpyrazine, and 2-ethyl -3,5(or 6)-dimethylpyrazine.

[b] DMDS = dimethyldisulfide, DMTS = dimethyltrisulfide.

Table 12: Important odourants of cocoa, milk chocolate, and dark chocolate.

4.3.4.1 Pyrazines

Pyrazines are nitrogenous heterocyclic compounds characterized by low molecular weight and high volatility (Belitz et al. 2004). Excluding tetramethylpyrazine (TMP) which is biosynthesized during cocoa fermentation, pyrazines are products of Maillard reactions during cocoa bean roasting and, associated with pleasant aromas of chocolate (Reineccius 2006).

Alkyl pyrazines that have similar odour may be additive in intensity (Frauendorfer & Schieberle 2008, Counet et al 2002). In particular Perego et al. (2004) found high concentrations of trimethylpyrazine and TMP linked to strong '*cocoa-chocolate*' aroma. Schnermann & Schieberle (1997) found 2-isopropyl-3-methoxypyrazine made a significant contribution to cocoa and bitter chocolate suggesting it is a characteristic aroma compound of DC.

4.3.4.2 Aldehydes

Strecker aldehydes are products of Maillard reactions (Reineccius 2006) generated by cocoa bean roasting. Three important aldehydes that have been identified as potent odorants that make strong contributions to chocolate aroma are 2- and 3-methylbutanal and 2-methylpropanal (Counet et al. 2002, Smit et al. 2008). These three aldehydes are thought to

play an important role in balancing chocolate flavour (Afoakwa et al. 2008). Frauendorfer & Schieberle (2008) also identified phenylacetaldehyde as an aroma impact compound of roasted cocoa beans.

Unsaturated aldehydes may form as oxidation products of linoleic and linolenic acids in cocoa butter when bean moisture content is high (Dimick & Hoskin 1999). Their occurrence and concentration is influenced by bean fermentation reaction conditions (pH and temperature), roasting time and temperature. (E)-2-Alkenals have very low flavour threshold values but are highly volatile, so although relatively low concentrations of these compounds are expected they make potent aroma contributions (Reineccius 2006, Belitz et al. 2004).

4.3.4.3 Pyrones and Furanones

Pyrones and furanones are oxygen-containing heterocyclic compounds formed by the Maillard reaction. Maltol (3-hydroxy-2-methyl-4H-pyran-4-one) has a '*caramel-like*' odour that enhances the sweet taste of food, and is able to mask bitter flavour (Reineccius 2006). According to Belitz et al. (2004) furaneol (4-hydroxy-2,5-dimethyl-3(2H)-furanone), sotolon (3-hydroxy-4,5-dimethyl-2(5H)-furanone) and abhexone (3-hydroxy-5-ethyl-4-methyl-2(5H)-furanone) also have '*caramel-like*' odours. They all share a planar enol-oxo-configuration. Schnermann & Schieberle (1997) identified furaneol as a key odorant of MC. 2-Acetylpyrrole is a nitrogen-containing heterocyclic compound formed via the Maillard reaction that has a '*caramel-like*' odour.

4.3.4.4 Volatile fatty acids

Volatile fatty acids (VFAs) are formed during cocoa bean fermentation and they may also occur via deamination of amino acids (Reineccius 2006). Acetic and butanoic acids have been identified as important odorants of cocoa although high concentrations would have a

negative effect on cocoa aromatic quality (Schwan & Wheals 2004). Branched chain VFAs such as 3- and 2-methylbutanoic acid, have been identified as key odorants of MC (Schnermann & Schieberle 1997).

Much of the excess acetic acid and other organic acids formed in fermentation are removed by drying and roasting of cocoa beans, and later in conching for chocolate. Therefore careful processing determines the final amounts of these acids in chocolate.

4.3.4.5 Sulfur containing compounds

Sulfur compounds are not characteristic of chocolate aroma however mixtures of sulfur compounds with aldehydes were found to give chocolate-like odours (Lopez & Quesnel 1974). Typically sulfur compounds have very low odour thresholds (Belitz et al. 2004) and have distinctive aroma character so small quantities of these compounds can affect the food's aroma (Hoskin & Dimick 1984).

Sulfur-containing aroma compounds are generated by Maillard reactions during bean roasting (Frauendorfer & Schieberle 2008). Methional is a Strecker aldehyde, derived from methionine, and is a well known precursor of sulfides such as DMDS and DMTS after radical- or light-initiated degradation to methanethiol (Counet et al. 2002). Schnermann and Schieberle (1997) identified DMTS as a key component of MC.

Another important sulphur compound identified in chocolate is 2-methyl-3-(methyldithio)furan. A proposed formation route for this compound is via the reaction of 2-methyl-3-furanthiol (formed by thermal degradation of thiamine) with methanethiol (Maarse 1991) that likely occurs during fermentation (Afoakwa et al. 2008).

4.3.4.6 Alcohols and Ketones

Counet et al. (2002) identified 2-phenylethanol as contributing to the typical *flowery* note of DC and linalool (3,7-dimethyl-1,6-octadien-3-ol), a terpenoid alcohol, as also contributing

to the characteristic *floral* note of chocolate. 2-Phenylethanol can be formed from either carbohydrate or amino acid metabolism by yeast during fermentation, or an alternative formation pathway involves reduction of the corresponding aldehyde and/or ketone (Vandamme 2003, Belitz et al 2004).

2,3-Butanedione (diacetyl) has been identified as a high impact odorant and 1-octen-3-one as an important odorant of MC (Schnermann & Schieberle 1997). Both compounds are products of milk fat oxidation and citrate metabolism. In addition 1-octen-3-one may be generated during conching (Counet et al. 2002), and 2,3-butanedione will form during plant biosynthesis of valine and leucine.

4.3.4.7 Esters and Vanillin

During bean fermentation, lipid metabolism by yeast provides a large number of acids and alcohols that may undergo esterification yielding a variety of esters (Frauendorfer & Schieberle 2008, Reineccius 2006). These esters may act as odorants and flavour precursors. As flavour precursors, natural variation and local differences in the fermentation processes which affect ester formation can be related to differences in chocolate flavour (Camu et al. 2008). Variation in the ester concentration has also been reported as resulting from the conching process (Counet et al. 2002). All the esters selected for analysis here have a *fruity* aroma note hence they likely make an additive aroma contribution to chocolate.

Natural vanilla or vanillin is a common flavour addition to enhance the creamy '*vanilla*' notes of chocolate (Jackson 1999).

4.4 SIFT-MS Analysis and Discussion

4.4.1 Experimental Method and Analysis

Commercial blocks of MC and DC were purchased from a local supermarket for analysis. These were two brands of New Zealand chocolate for both MC and DC (NZ-1 and NZ-2) and one brand of Swiss chocolate for both MC and DC. The ingredients label of each block reads:

NZ-1 MC (27% cocoa, 27% milk solids): Cocoa mass, cocoa butter, milk solids, full cream milk, sugar, emulsifiers.

NZ-2 MC (33% cocoa solids, 30% milk solids): Milk chocolate (sugar and cocoa solids), milk powder, emulsifier (soya lecithin), flavour.

Swiss MC (30% cocoa solids): Cocoa mass, cocoa butter, skimmed milk powder, milk powder, sugar, lactose, butter fat, emulsifier, malt extract (barley), flavouring (vanillin).

NZ-1 DC (70% cocoa solids): Cocoa mass, cocoa powder, cocoa butter, milk solid, sugar, flavour.

NZ-2 DC: Cocoa mass (72%), sugar, emulsifier (soya lecithin), flavour.

Swiss DC (70% cocoa): Cocoa mass, cocoa butter, sugar, natural Bourbon vanilla pods.

4.4.1.1 Experimental Method

The preparation and analysis of chocolate was the same for all samples. Three replicate 22 g samples of each chocolate brand were placed in clean 1L Schott glass bottles and sealed with a silicon rubber septum. All chocolate samples (including three blank bottles) were incubated at 65°C for at least half an hour and a bottle removed from the incubator just before SIFT-MS analysis.

4.4.1.2 Experimental Analysis

A VOICE200® SIFT-MS selected ion mode (SIM) analysis was performed on all chocolate headspace samples. Compounds were selected from Table 4.1 for analysis. To draw out the sample, a hot passivated needle attached to the instrument inlet was used to pierce the septum. At the onset of analysis, three blank replicates were measured then three chocolate samples in succession. An additional SIM scan of laboratory air was performed between chocolate samples to minimize any carryover of concentration from the previous sample. A SIM scan took 2 min. to complete, and following that a 1½ min. full mass scan (MS) 15 – 250 *m/z* was run for each bottle. The concentration of analyte compounds was calculated as the average of three scans minus the average of three blank scans.

4.4.2 SIFT-MS Measurements and Discussion

The SIFT-MS measured concentration of compounds is not absolute in the analysis because the vapour pressure and partition co-efficient value for each compound was not ascertained. However Frauendorfer & Schieberle (2008) suggested differences in the aroma profiles of unroasted and roasted Criollo beans create a quantitative change of quite a small set of key aroma compounds. In a similar sense differences in the relative amounts of selected aroma compounds measured in the headspace of MC and DC are presented and discussed here.

4.4.2.1 Pyrazines

The concentrations of 2,5-dimethylpyrazine and C4-alkylpyrazines indicate a similar intensity of '*cocoa-chocolate*' aroma present in MC (see Figure 28). It also appears the '*cocoa-chocolate*' intensity is greater in NZ-2 and Swiss DCs than NZ-1 DC because of higher concentration of these compounds, particularly C4-alkylpyrazines.

Among the MCs, three times the amount of 2-isopropyl-3-methoxypyrazine was measured in NZ-2 MC suggesting it may contribute an unfavourable '*musty bean*' note to the chocolate. On the other hand it appears 2-isopropyl-3-methoxypyrazine is a characteristic aroma compound of DC as greater amounts of the compound were present in NZ-1 DC and Swiss DC.

Relatively little (or none) 2,3-diethyl-5-methylpyrazine was measured. It is a characteristic compound of NZ MC and some was measured for Swiss DC. The relative importance of this compound is uncertain but its contribution to chocolate aroma is probably moderated by the conching process (Afoakwa et al. 2008).

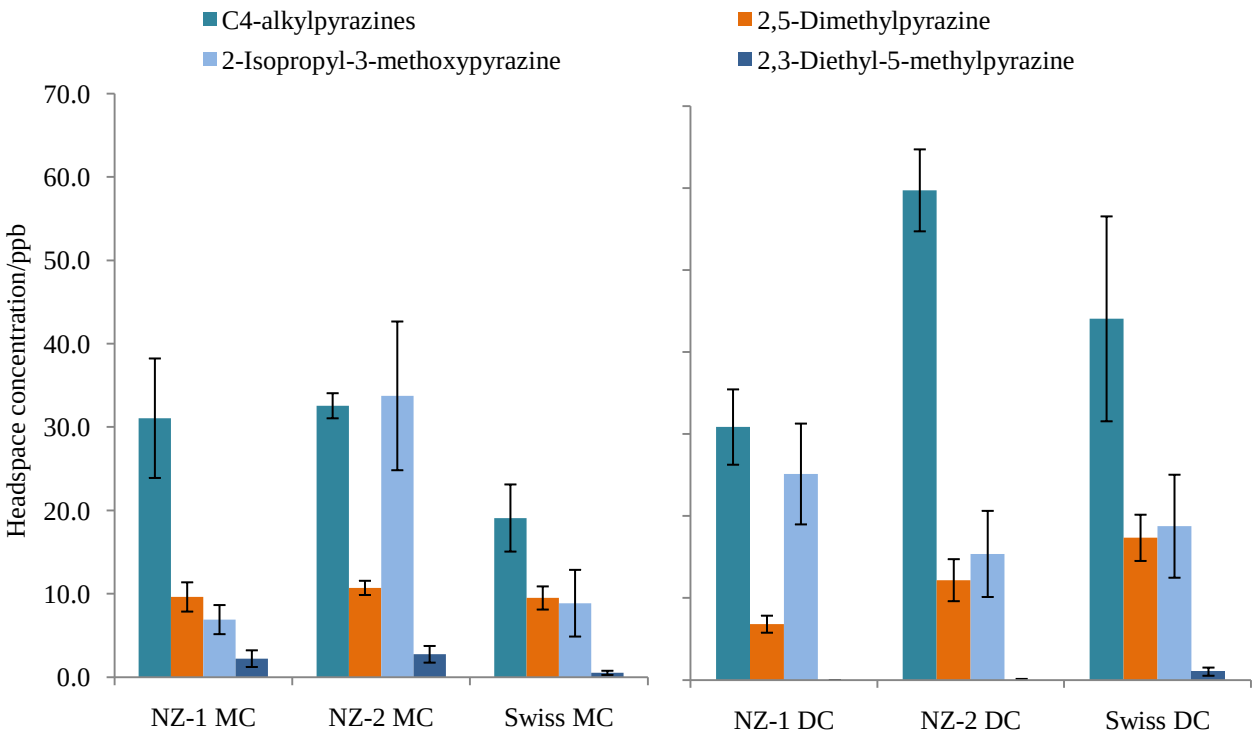

Figure 28: SIFT-MS analysis of selected pyrazines in chocolate headspace. In the figure C4-alkylpyrazines includes tetramethylpyrazine, 3(or 5)-dimethyl-3(or 2)-ethylpyrazine. Also 2,5- and 2,3-Dimethylpyrazine, and ethylpyrazine are reported together. (The error bars are 1 standard deviation (SD) of the average concentration)

4.4.2.2 Aldehydes

Based on the established importance of 3-methylbutanal to chocolate aroma and the concentration measured, it appears Swiss MC has a stronger '*chocolate*' intensity compared to the other MCs examined (see Figure 29). Incidentally Keeney (1972) correlated high concentrations of 3-methylbutanal with good quality roasted cocoa beans that may suggest better quality beans used in the manufacture of Swiss MC. More 2-methylpropanal was measured in MC overall, but for DC it is probably lost by the conching process (Counet et al. 2002). The same relative balance of 3-methylbutanal 2-methylpropanal and phenylacetaldehyde contributes to chocolate aroma in all DCs.

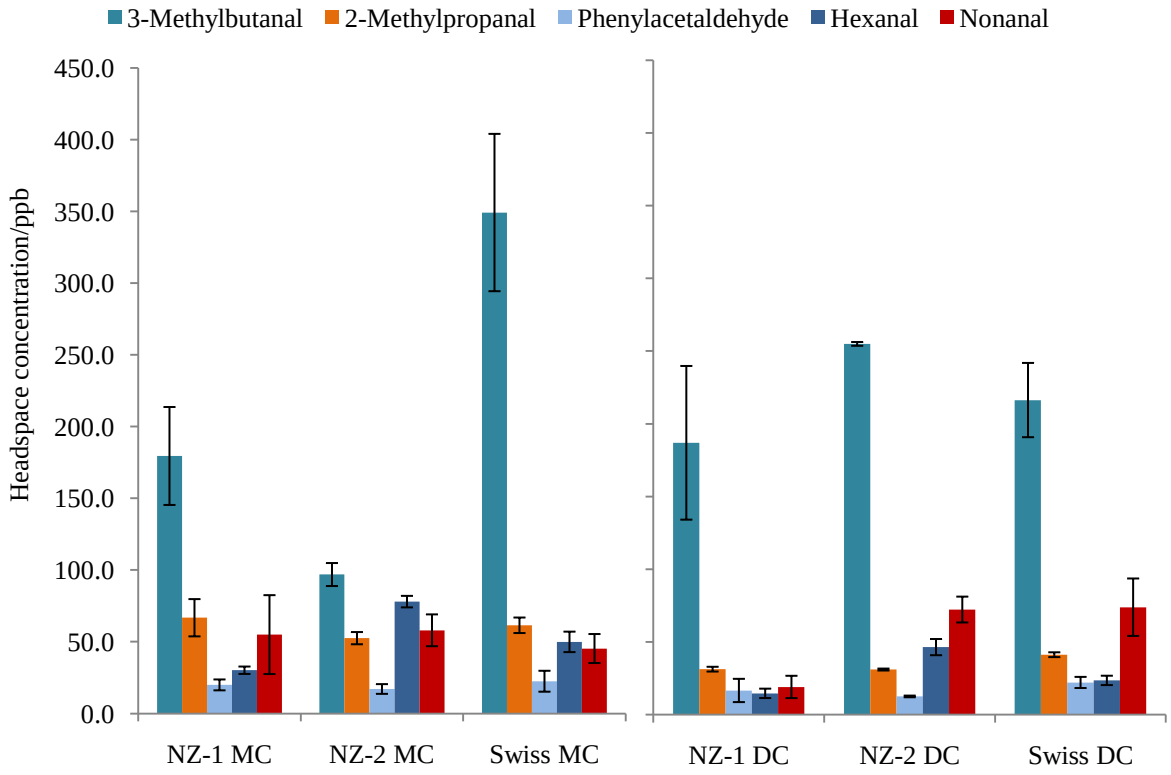

Figure 29: SIFT-MS analysis of selected aldehydes in chocolate headspace. In the analysis 2- and 3-methylbutanal are reported together. (The error bars are 1SD of the average concentration)

	(E)-2-Heptenal		(E)-2-Nonenal		(E)-2-Octenal	
NZ-1 MC	6	*(5)*	2	*(0)*	3	*(1)*
NZ-2 MC	5	*(2)*	3	*(1)*	3	*(0)*
Swiss MC	0	*(3)*	1	*(0)*	2	*(0)*
NZ-1 DC	0	*(2)*	2	*(0)*	2	*(0)*
NZ-2 DC	11	*(5)*	4	*(0)*	2	*(2)*
Swiss DC	3	*(4)*	1	*(1)*	2	*(0)*

Table 13: SIFT-MS analysis of selected unsaturated aldehydes (2-enals) in chocolate headspace. Values are recorded as ppb. (The numbers in brackets are 1sd of the average concentration).

As expected, low concentrations of (E)-2-alkenals were measured (see Table 13). The contribution these compounds make to chocolate aroma is uncertain, but a characteristic amount is present in both MC and DC. Except for NZ-2 DC that is, where a relatively high amount of (E)-2-heptanal was measured. High concentrations of (E)-2-nals have been associated with mouldy beans (Dimick & Hoskin 1999), which suggests a poorer quality chocolate and an unfavourable '*fatty, bitter almond*' note to the chocolate.

4.4.2.3 Pyrones and Furanone

There is a difference in the balance of furaneol, sotolon, and maltol between NZ MC and DC (see Figure 30). In saying that, relatively high concentrations of furaneol, sotolon and maltol were measured for NZ-1 MC that indicates strong '*caramel-like*' odour intensity by additive effects. Incidentally this chocolate is made with full cream milk and is also well known for its sweet caramel flavour that is typically associated with milk crumb ingredient (Haylock & Dodds 1999).

Swiss chocolate on the other hand is not typically known for caramel or sweet chocolate flavour with the difference apparently due to the blend of milk powder and the addition of lactose in Swiss chocolate to replace the sweetness of sucrose. This difference allows a clean milk flavour to be recognised in the chocolate (Haylock & Dodds 1999, Bolenz et al. 2003).

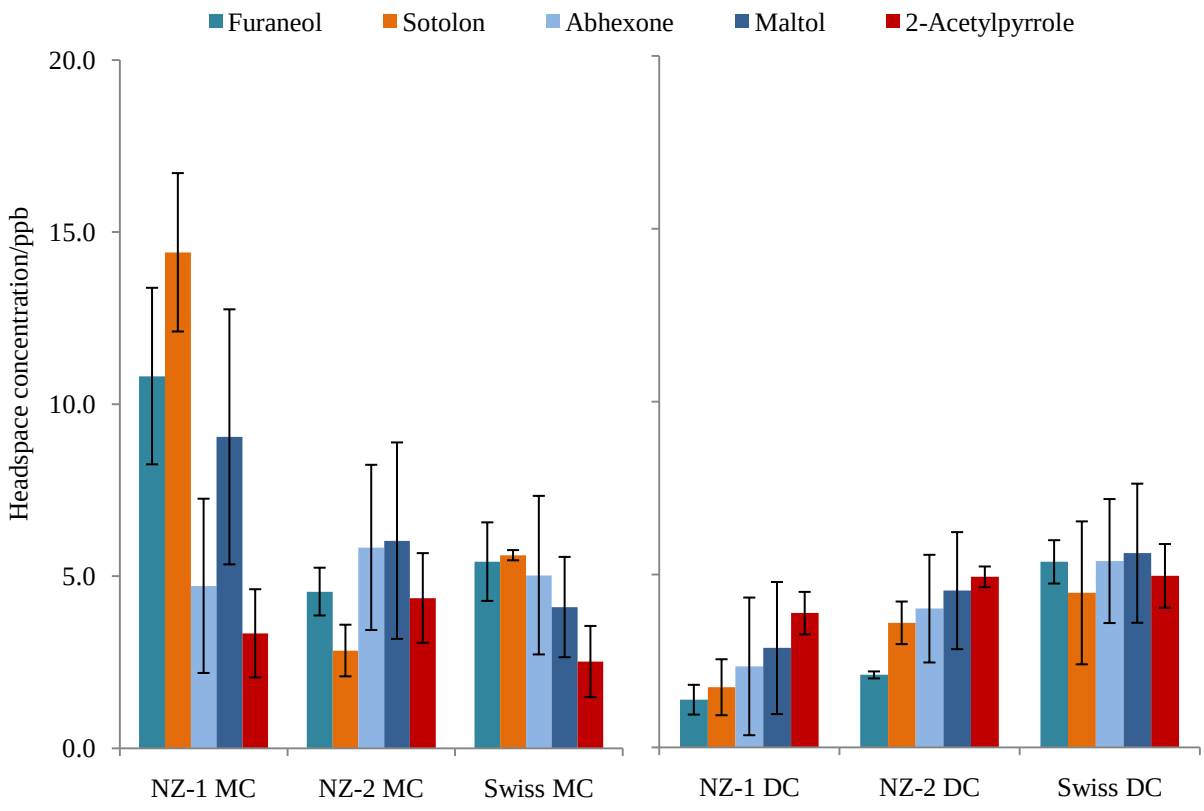

Figure 30: SIFT-MS analysis of selected furanones, pyranones, and 2-acetylpyrrole in chocolate headspace. (The error bars are 1SD of the average concentration)

4.4.2.4 Volatile fatty acids

A significant amount of acetic acid is still present in chocolate headspace (see Table 14). The highest amount of acetic acid was measured for Swiss DC however this chocolate is described as having a "well balanced sourness" by the manufacturer. Comparatively moderate amounts of butanoic acid were measured and considering all the acids monitored, Swiss chocolate appears to be slightly more acidic than the other chocolates.

3-Methylbutanoic acid content varies widely among chocolates. Its amount is determined by cocoa bean composition and the generation of amino acids during fermentation (Camu et al. 2008, Rohsius et al. 2006). By comparison a significant amount of 3-methylbutanoic acid was measured in NZ-2 chocolate. Unlike the other chocolates in the analysis, this chocolate is made from one bean type (Ghana beans) rather than a bean blend which is probably the reason for the higher concentrations of 3-methylbutanoic acid.

	Acetic acid		Butanoic acid		3-Methylbutanoic acid*	
NZ-1 MC	4070	*(798)*	259	*(51)*	166	*(26)*
NZ-2 MC	6243	*(741)*	190	*(19)*	968	*(94)*
Swiss MC	5563	*(764)*	335	*(44)*	232	*(37)*
NZ-1 DC	5946	*(1773)*	116	*(20)*	73	*(11)*
NZ-2 DC	7477	*(138)*	203	*(2)*	583	*(17)*
Swiss DC	11355	*(1408)*	246	*(58)*	240	*(30)*

*In this analysis, 2- and 3-methylbutanoic acid cannot be differentiated and are reported as 3-methylbutanoic acid.

Table 14: SIFT-MS analysis of select volatile fatty acids in chocolate headspace. (The numbers in brackets are 1SD deviation of the average concentration)

4.4.2.5 Sulfur-containing compounds

Similar amounts of methional were measured for NZ and Swiss chocolates (see Figure 31). It appears NZ-1 MC has an uncharacteristicly high concentration of DMTS that may be due to interference from furaneol or maltol (see §4.4.2.3). The difference in DMTS concentration among NZ and Swiss chocolates may be explained by the methionine content

of the cocoa bean (Rohsius et al. 2006, Bonheví 2005). An alternative and possibly more likely explanation may be that DMTS is generated during conching (Counet et al. 2002).

The measured levels of 2-methyl-3-(methyldithio)furan are low in chocolate. This compound has been identified as a high impact odorant of milk chocolate, but as it has also been described as having the distinctive odour of '*cooked-meat*' (Schnermann & Schieberle 1997), then a low concentration might be expected as were observed.

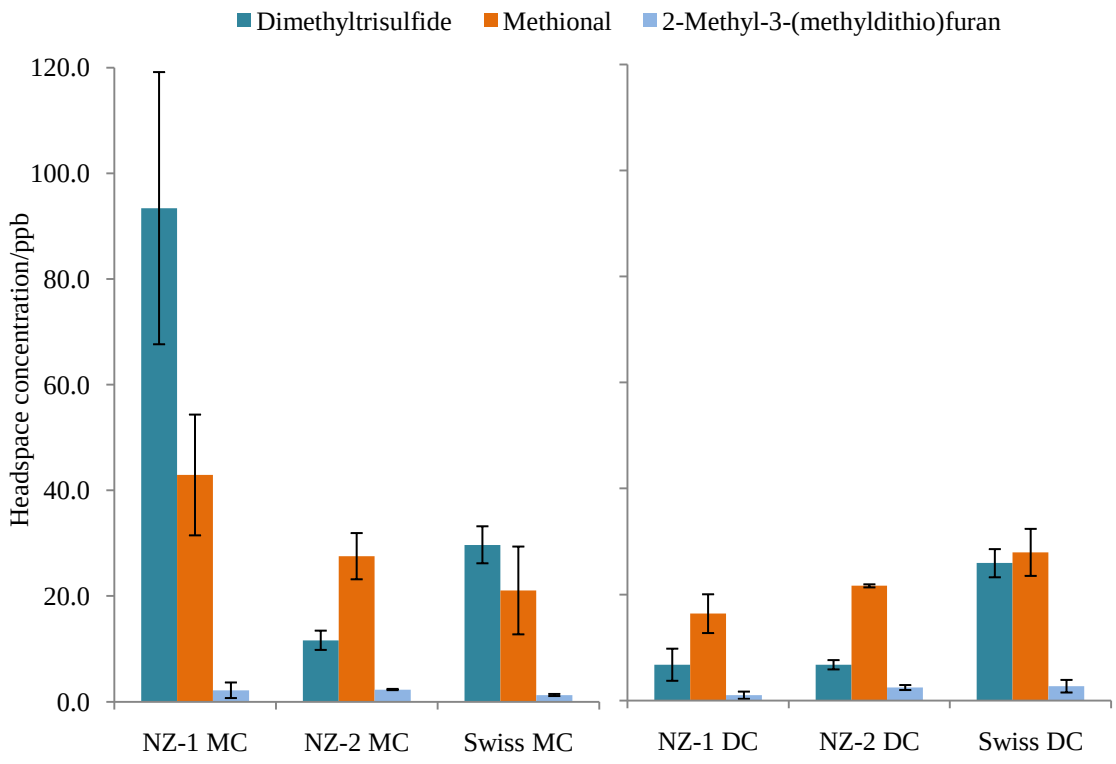

Figure 31: SIFT-MS analysis of selected sulfur compounds in chocolate headspace. (The numbers in brackets are 1SD deviation of the average concentration)

4.4.2.6 Ketones and Alcohols

2,3-Butanedione appears to contribute more to the aroma of MC (see Figure 32) especially Swiss MC, where the difference in amount between NZ and Swiss MCs may be due to the milk powder content and/or malt extract (Coghe 2005).

Similar amounts of 2-phenylethanol were measured for all chocolates. Linalool was found to be relatively low in DC, except for Swiss DC, and a greater amount measured for MCs. Additive effects would indicate these two compounds contribute a *flowery* odour note to MC and Swiss DC.

1-Octen-3-one showed slightly higher concentrations in NZ MCs than NZ DCs that suggests the difference is due to milk content. However for Swiss chocolate there is no difference in 1-octen-3-one content between its MC and DC.

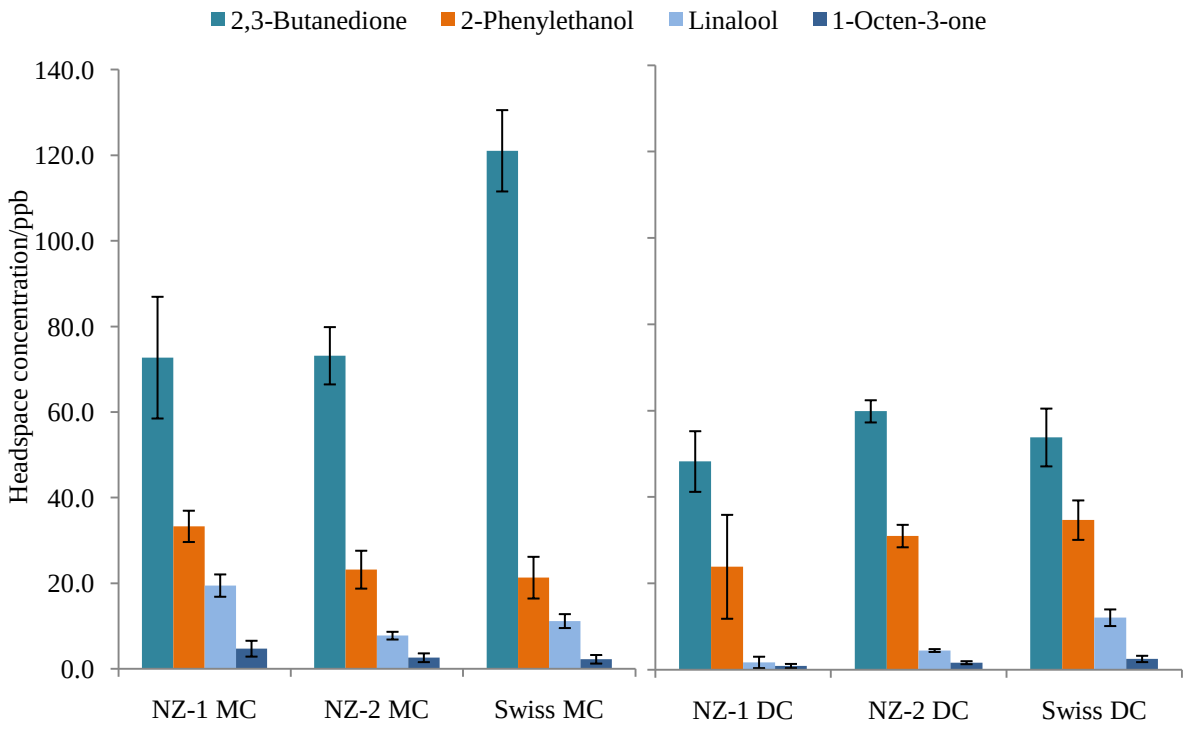

Figure 32: SIFT-MS analysis of selected alcohols and ketones in chocolate headspace. (The numbers in brackets are 1SD deviation of the average concentration)

4.4.2.7 Esters and Vanillin

The '*fruity*' ester contribution to aroma appears to be similar for all MCs (see Figure 33). For DC, the ester aroma intensity varies with the greatest '*fruity*' contribution to Swiss DC and which is apparently characteristic of this chocolate.

A significant amount of vanillin was measured in Swiss MC. Presumably the Swiss chocolate manufacturer has added comparatively larger amounts of vanillin to their chocolate to enhance the creamy notes of the chocolate. On the other hand a relatively small amount of vanillin was measured in NZ-1 MC and evidently only makes a subtle contribution to aroma. Vanillin appears to make a similar contribution to DC flavour between brands.

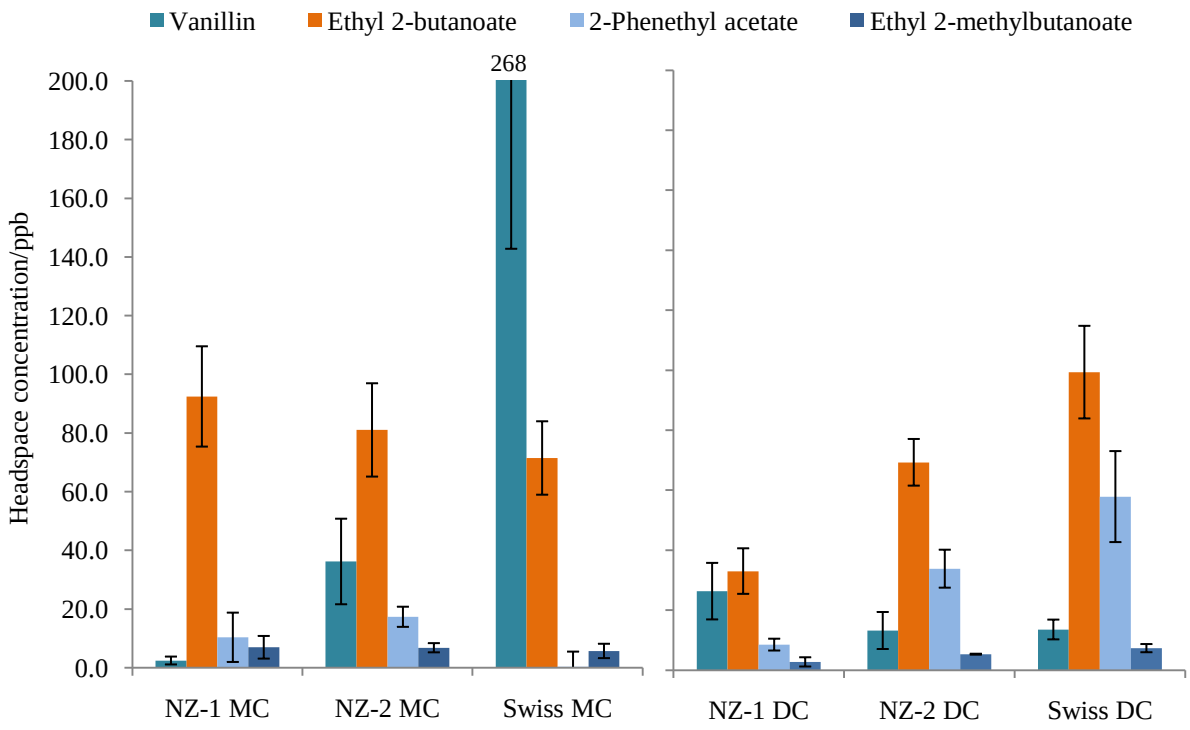

Figure 33: SIFT-MS analysis of selected esters and vanillin in chocolate headspace. (The numbers in brackets are 1SD deviation of the average concentration)

4.5 Conclusion

A comparison of aroma character between MC and DC by the SIFT-MS technique has been performed. Even though interpretation of the differences in the volatile organic compound (VOC) concentration is complicated as many variables arise from differences in bean type, fermentation and drying methods, bean roasting and subsequent chocolate

production steps, some notable similarities and differences in concentration of selected compounds have been observed.

For example, MC is characterized by greater amounts of 3-methylbutanal and 2-methylpropanal, 2,3 butanedione and 1-octen-3-one compared to DC. The first two compounds are potent odourants of chocolate flavour and the other compounds are associated with milk content. On the other hand, DC is characterized by higher concentrations of C4-alkylpyrazines and 2-isopropyl-3-methoxypyrazine that contribute to the stronger cocoa flavour of DC.

General information provided by the manufacturers about the beans used for the chocolate provides further insight into the VOC profiles obtained: (1) The NZ-1 chocolate is produced with a blend of South East Asia and West African cocoa beans. (2) The NZ-2 chocolate is produced with the Ghana cocoa bean of West Africa. (3) The Swiss chocolate is produced with a blend of South and Central American and West African cocoa beans (Afoakwa et al 2008, Counet et al. 2004). Swiss MC was found to have a relatively high amount of 3-methylbutanal suggesting the use of higher quality beans in manufacture. By comparison a significant amount of 3-methylbutanoic acid was measured in NZ-2 chocolate that is perhaps indicative of lower quality beans.

A significant amount of vanillin was measured for Swiss MC, and attributed here to the manufacturer's recipe. Another example of what can be determined by SIFT-MS analysis is the relatively high concentration of 2,3-butanedione for Swiss MC that can also be attributed to the milk powder determined by the manufacturer's recipe.

4.6 References

Afoakwa, E. O.; Paterson, A.; Fowler, M.; Ryan, A. Matrix effects on flavour volatiles release in dark chocolates varying in particle size distribution and fat content using GC – mass spectrometry and GC – olfactometry. *Food Chemistry*, **2009**, 113,0 208–215.

Afoakwa, E. O.; Paterson, A.; Fowler, M.; Ryan, A. Flavor Formation and Character in Cocoa and Chocolate: A Critical Review. *Crit. Rev. in Food Sci. and Nutr*. **2008**, 48, 840–857.

Afoakwa, E. O.; Paterson, A.; Fowler, M. Factors influencing rheological and textural qualities in chocolate - a review. *Trends in Food Science & Tech.* **2007**, 18, 290 – 298.

Beckett, S. T. *The science of chocolate*. Royal Society of Chemistry Paperbacks, **2000.**

Beckett, S. T. Conching. In *Industrial Chocolate manufacture and use.* (3rd edition), S. T. Beckett., Blackwell Science, Oxford, 153 – 181, **1999**.

Belitz, H. –D.; Grosch, W.; Schieberle, P. *Food Chemistry (3rd Revised Edition)*, Translation by Burghagen, B. B., Springer-Verlag Berlin Heidelberg, **2004**.

Bolenz, S.;Thiessenhusen, T.; Schäpe, R. Fast conching for milk chocolate. *Eur Food Res Technol*, **2003**, 218, 62–67.

Bonvehí. J. S. Investigation of aromatic compounds in roasted cocoa powder. *Eur Food Res Technol*. **2005**, 221, 19–29.

Camu, N.; de Winter, T.; Addo, S. K.; Takrama, J. S.; Bernaert, H.; de Vuyst, L. Fermentation of cocoa beans: influence of microbial activities and polyphenol concentrations on the flavour of chocolate. *J Sci Food Agric*, **2008**, 88, 288–2297.

Chevalley, J. (1999). Chocolate flow properties. In *Industrial chocolate manufacture and use* (3rd Edition), S. T. Beckett., Blackwell Science, Oxford, 182 – 199, **1999**.

Counet,C.;Ouwerx. C.; Rosoux, D.; Collin, S. Relationship between Procyanidin and Flavor Contents of Cocoa Liquors from Different Origins *J. Agric. Food Chem.* **2004,** 52, (20):6243 – 6249.

Counet, C.; Callemien, D.; Ouwerx, C.; Collin, S. Use of Gas Chromatography-Olfactometry To Identify Key Odorant Compounds in Dark Chocolate. Comparison of Samples before and after Conching. *J. Agric. Food Chem.* **2002**, 50, 2385 – 2391.

Cogh, S.; D'Hollander, H.; Verachtert, H.; Delvaux, F. R.; Impact of Dark Specialty Malts on Extract Composition and Wort Fermentation. *J. Inst. Brew.* 111, 1:51–60, **2005.**

Dimick, P. S.; Hoskin, J. C. The Chemistry of Flavour Development in Chocolate. In *Industrial Chocolate manufacture and use.* (3rd edition). S. T. Beckett., Blackwell Science, Oxford, 137–151, **1999**.

Frauendorfer, F.; Schieberle, P. Changes in Key Aroma Compounds of Criollo Cocoa Beans During Roasting. *J. Agric. Food Chem.* **2008**, *56*, 10244–10251.

Haylock, S. J.; Dodds, T. M. Ingredients from Milk. In *Industrial Chocolate manufacture and use*. (3rd edition), S. T. Beckett., Blackwell Science, Oxford, 57 – 76, **1999**.

Heemskerk, R. F. M. Cleaning, Roasting and Winnowing. *Industrial Chocolate manufacture and use. (3rd edition*), S. T. Beckett., Blackwell Science, Oxford, 78 – 99, **1999**.

Hoskin, J. C. Sensory properties of chocolate and their development. *Am J Clin. Nutr.* ***1*994**, 60 (suppl), 1068S - 1070S.

Hoskin, J.; Dimick, P. Role of sulfur compounds in the development of chocolate flavours - A review. *Proc. Biochem.* **1984**, 19, 150–156.

Hoskin, J.; Dimick, P. Role of non-enzymatic browning during the processing of chocolates - A review. *Proc. Biochem.* **1983,** 11, 92–104.

Jackson, K. Recipes. *Industrial Chocolate manufacture and use. (3rd edition*), S. T. Beckett., Blackwell Science, Oxford, 323 – 345, **1999**.

Keeney, P. G. Various interactions in chocolate flavor. *J. Am.Oil Chem. Soc.* **1972**, *49*, 567–572.

Lopez, A.; Quesnel, V. The contribution of sulphur compounds to chocolate aroma. In *Proceedings of the 1st International Congress on Cocoa and Chocolate Research*; Inst. Lebensmitteltechnologie Verpack: Germany, **1974**, 92-104.

Luna, F.; Crouzillat, D.; Cirou, L.; Bucheli, P. Chemical Composition and Flavor of Ecuadorian Cocoa Liquor. *J. Agric. Food Chem.* **2002,** *50*, 3527-3532.

Maarse, H. *Volatile Compounds in Food and Beverages (1st Edition*). Food Science and Technology (Marcel Dekker Inc.), **1991.**

Mongia, G. *Particle size distribution affects the rheology and sensory attributes of milk chocolate.* PhD. Thesis. Pennsylvania State University, **1997.**

Nebesny, E.; Żyżelewicz. D. Effect of lecithin concentration of properties of sucrose-free chocolate masses sweetened with isomalt. *Eu. Food. Res. Tech.*, **2005**, 22, 2:131 – 135.

Perego, P.; Fabiano, B,; Cavicchioli, M.; del Borghi, M. COCOA QUALITY AND PROCESSING. A Study by Solid-phase Microextraction and Gas Chromatography Analysis of Methylpyrazines. *Food and Bioproducts Processing*, **2004**, 84, 291–297.

Reineccius, G. A. *Flavour Chemistry and Technology (Second Edition)*, Taylor & Francis Group, **2006**.

Reineccius, G. A.; Andersen, D. A.; Kavanagh, T. E.; Keeney, P. G. Identification and Quantification of the Free Sugars in Cocoa Beans. *J. Agr. Food Chem*, 20, **1972**, (2):199 – 202.

Rohsius, C.; Matissek, R.; Lieberei, R. Free amino acid amounts in raw cocoas from different origins. *Eur Food Res Technol*. **2006**, 222, 432–438.

Sanagi, M. M.; Hung, W. P.; Yasir, S. M. Supercritical fluid extraction of pyrazines in roasted cocoa beans Effect of pod storage period. *Journal of Chromatography A*, **1997**, 785, 361-367.

Schieberle, P.; Pfner P. *Flavour Chemistry: 30 Years of Progress*, Edited by Teranishi et al., **1999**, 147 – 153.

Schnermann, P.; Schieberle, P. Evaluation of Key Odorants in Milk Chocolate and Cocoa Mass by Aroma Extract Dilution Analyses. *J. Agric. Food Chem.* **1997**, 45, (3):867 – 872.

Schwan, R. F.; Wheals, A. E. The Microbiology of Cocoa Fermentation and its Role in Chocolate Quality. *Crit. Rev. Food Sci. Nutr.* **2004**, 44, 205 – 221.

Smit, B. A.; Engels, W. J. M.; Smit, G. Branched chain aldehydes: production and breakdown pathways and relevance for flavour in foods. *Appl Microbiol Biotechnol*. **2008**, 81, 987–999.

Talbot, G. Chocolate Temper. In *Industrial Chocolate manufacture and use.* (3rd edition), S. T. Beckett., Blackwell Science, Oxford, 218 – 230, **1999**.

Vandamme, E. J. Bioflavours and fragrances via fungi and their enzymes. *Fungal Diversity*, **2003**, 13, 153-166.

World Cocoa Foundation Market Update **July 2009**. http://www.worldcocoafoundation.org (accessed Oct, 2009).

Ziegler, G.; Hogg, R. Particle size reduction. In *Industrial chocolate manufacture and use*. *(3rd Edition)*. S. T. Beckett., Blackwell Science, Oxford, 115 – 135, **1999**.

.

CHAPTER FIVE

Concluding Comments and Suggestions for Future Work

The following comments include a brief description of the new generation SIFT-MS instrument VOICE200® and, some suggestions for future work that may develop on and/or strengthen the conclusions presented in the preceding chapters.

5.1 The Development of SIFT-MS

Many SIFT-MS applications demand high sensitivity to low concentrations of analyte (Prince et al. 2010). Where the sensitivity of trace gas analysis is increased, attention must be paid to the accuracy of data. One important requirement of an accurate analysis is the sample must be able to be transferred to the flow tube for analysis in a quantitative manner. For this reason, characterisation of a new passivated inlet was undertaken with known "sticky" compounds (see Chapter 2).

From the onset it was thought a passivated inlet would reduce the problem of "sticky" compound adsorption to the inlet system of SIFT-MS. From the work undertaken in this study, it was apparent the passivated inlet at elevated temperature does perform better than the unpassivated inlet. In 2007 the new generation VOICE200® instrument was launched and a high performance passivated inlet installed as a consequence of the work developed on the prototype inlet in Chapter 2.

The high performance inlet of the VOICE200® instrument contains no solenoid valves and may be operated at 160 - 200°C depending on the sample. This inlet has also been retrofitted to the VOICE100™ instrument used in the laboratory of SYFT for food flavour

analyses. Previously, multiple valves were implemented for the VOICE100™ inlet system (Francis 2007). The rubber seals of these valves placed a restriction on the inlet temperature that could be used, and although chemically inert, adsorption by certain compounds to the rubber caused sample contamination. In contrast the new passivated inlet should prove to be a great improvement to the analysis technique.

5.2 Flavour Research

SIFT-MS analysis of food aroma can serve as an objective method for assessing food quality. Direct analysis of equilibrium headspace is relatively easy using the VOICE200® instrument and the amount measured is reflective of what is present in the bulk food. However no one analytical method can accurately account for all aroma compounds in the food, because the volatility of aroma compounds in the gaseous phase and their partition co-efficient influence the amount present in headspace (Reineccius 2006). However if there is a good correlation between flavour quality and the compounds being measured, the goal of quality control has been accomplished (Belitz et al. 2004).

5.2.1 Food Aroma Analysis

The application of SIFT-MS analysis of food aroma compounds has great potential as it provides a simple probe into assessing and quantifying different classes of foods and manufacturers of food (see Chapters 3 and 4) without the need for complex sample pre-treatment.

- The objective of cheese aroma analysis was to relate differences in the amount of key odourants to the manner in which the cheese was made. A primary result of Parmesan analysis was certain odourants related to the use of raw milk in cheese production was partly responsible for the differences between Italian Parmesan and some of the New Zealand cheeses.

- A similar analysis was made for chocolate aroma, where the objective was to develop an aroma profile for milk chocolate and dark chocolate. This was a difficult analysis, one reason being the great number of parameters combining to influence chocolate flavour. A true aroma profile was not obtainable by this method. However a primary result of chocolate analysis using SIFT-MS was the recognition that certain odourants were related to the cocoa bean variety, fermentation, roasting and subsequent chocolate manufacture. It is also possible to detect additions added by different manufacturers to their chocolate products.

The analysis carried out in this thesis was preliminary in nature and it is now necessary to establish norms for selected food varieties. Then any deviation from what is established as the norm may be investigated further. In addition the vapour pressure (volatility) and partition coefficients of key odourants would benefit the further study of cheeses as much effort was put into relating relative amounts of odourants in the headspace to flavour.

More work could also be done in the area of data analysis. The next section presents the results of multivariate statistical analysis applied by another member of the SYFT Technologies research team to the SIM data of Parmesan cheese (Langford et al. 2009).

5.2.2 Multivariate Statistical Analysis of Parmesan cheese

Principal component analysis (PCA) is a multivariate statistical technique that can assist in identifying the key differences between Parmesan cheeses of differing country and manufacturer. Soft independent modeling of class analogy (SIMCA) is a sophisticated implementation of PCA (Wold 1976) that was applied to SIM data obtained from SIFT-MS analysis of key aroma compounds in Chapter 3. The objective was to determine the ability of SIFT-MS to discriminate (i) between each of the cheeses regardless of the country of origin (that is, by manufacturer), and (ii) between cheeses by their country of origin.

Code	Country of Origin; Type	Manufacturer
GPA	Italy; 'Grana Padano'	Italian-A
GPC	Italy; 'Grana Padano'	Italian-B
PRA	Italy; 'Parmigiano Reggiano'	Italian-A
PRC	Italy; 'Parmigiano Reggiano'	Italian-B
NZF	New Zealand; 'Parmesan'	NZ-A
NZG	New Zealand; 'Parmesan'	NZ-B
NZK	New Zealand; 'Parmesan'	NZ-C
NZP	New Zealand; 'Parmesan'	NZ-D

Table 15: The descriptor (code) given to the cheeses analysed.

In Figure 34, the three largest principal component axes (PC1, PC2, PC3) are linear combinations of the analysed compounds (variables). Coloured dots represent the projections of the individual Parmesan cheeses grouped according to manufacturer. The shading represents the multidimensional space over which a particular product varies. We see the statistical analysis of SIM data is sufficient to enable distinction between different manufacturers of cheese using key aroma compounds

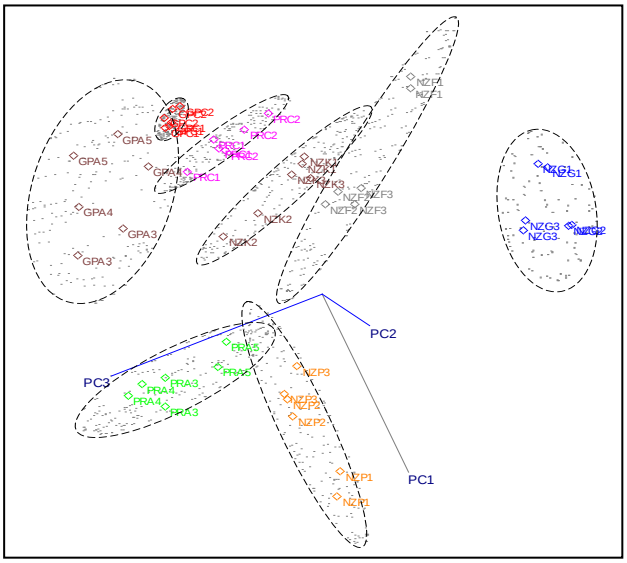

Figure 34: SIMCA class projections of individual Parmesan cheeses generated using data from SIFT-MS analysis of key aroma compounds.

Table 16 shows another metric derived from the SIMCA algorithm – class separation. It is generally accepted that a value of 3 indicates separability (Kvalhelm & Karstang 1992).

	GPA	GPC	PRA	PRC	NZG	NZP	NZF
GPC	35						
PRA	54	137					
PRC	17	28	99				
NZG	100	213	94	102			
NZP	53	72	107	80	127		
NZF	45	151	60	53	84	124	
NZK	22	40	48	28	54	52	67

Table 16: Interclass differences between the cheese samples grouped by individual manufacturer.

Grouping the cheeses by individual manufacturer results in larger interclass distances than grouping according to country of origin suggesting significant factory variations exist. Future work needs to better characterize the products from individual factories rather than taking individual samples of unknown origin from supermarkets. This would enable a useful database of product variability from particular factories to be established (Barbieri et al. 1994).

5.3 References

Barbieri, G.; Bolzoni, L.; Careri, M.; Mangia, A.; Parolari, G.; Spagnoli, S.; Virgili, R. Study of the Volatile Fraction of Parmesan Cheese. *J. Agric. Food Chem.*, **1994**, 42, 1170-1176.

Belitz, H. –D.; Grosch, W.; Schieberle, P. *Food Chemistry (3rd Revised Edition)*, Translation by Burghagen, B. B., Springer-Verlag Berlin Heidelberg, **2004**.

Francis, G. J. *SIFT-MS: Development of instrumentation and applications*, Ph.D. Thesis (Chapter 2), University of Canterbury, **2007**.

Kvalheim, O. M.; Karstang, T.V. "SIMCA - Classification by Means of Disjoint Cross Validated Principal Components Models." in R.G. Brereton, Ed., *Multivariate pattern recognition in chemometrics, illustrated by case studies* (Elsevier: Amsterdam, **1992**), p. 237ff.

Langford, V. S.; Reed, C. J.; Milligan, D. B.; McEwan, M. J.; Barringer, S.; Harper, W. J. Headspace Analysis of Italian and New Zealand Parmesan Cheeses, using SIFT-MS. Poster presented at *Institute of Food Technologists Conference and Exhibition (IFT09)*, **2009**, June 7 – 9, California.

Prince, B. J.; Milligan, D. B.; McEwan, M. J. Application of SIFT-MS to Real-time Atmospheric Monitoring. (*Rap. Comm. Mass Spect.* **2010** (In Press)).

Reineccius, G. *Flavour Chemistry and Technology (Second Edition)*, Taylor & Francis Group, **2006**.

Wold, S. Pattern Recognition by Means of Disjoint Principal Components Models. *Pattern Recognition*, **1976**, 8, 127-139.